The Na^+/I^- Symporter (NIS): Mechanism and Medical Impact

Carla Portulano,* Monika Paroder-Belenitsky,* and Nancy Carrasco

Department of Molecular and Cellular Physiology (C.P., N.C.), Yale University School of Medicine, New Haven, Connecticut 06510; and Department of Molecular Pharmacology (M.P.-B.), Albert Einstein College of Medicine, Bronx, New York 10469

The Na^+/I^- symporter (NIS) is the plasma membrane glycoprotein that mediates active I^- transport in the thyroid and other tissues, such as salivary glands, stomach, lactating breast, and small intestine. In the thyroid, NIS-mediated I^- uptake plays a key role as the first step in the biosynthesis of the thyroid hormones, of which iodine is an essential constituent. These hormones are crucial for the development of the central nervous system and the lungs in the fetus and the newborn and for intermediary metabolism at all ages. Since the cloning of NIS in 1996, NIS research has become a major field of inquiry, with considerable impact on many basic and translational areas. In this article, we review the most recent findings on NIS, I^- homeostasis, and related topics and place them in historical context. Among many other issues, we discuss the current outlook on iodide deficiency disorders, the present stage of understanding of the structure/function properties of NIS, information gleaned from the characterization of I^- transport deficiency-causing NIS mutations, insights derived from the newly reported crystal structures of prokaryotic transporters and 3-dimensional homology modeling, and the novel discovery that NIS transports different substrates with different stoichiometries. A review of NIS regulatory mechanisms is provided, including a newly discovered one involving a K^+ channel that is required for NIS function in the thyroid. We also cover current and potential clinical applications of NIS, such as its central role in the treatment of thyroid cancer, its promising use as a reporter gene in imaging and diagnostic procedures, and the latest studies on NIS gene transfer aimed at extending radioiodide treatment to extrathyroidal cancers, including those involving specially engineered NIS molecules. **(*Endocrine Reviews* 35: 106–149, 2014)**

I. Introduction
II. A Historical Perspective on I^- Deficiency
  A. I^- is an essential micronutrient and its lack causes ID disorders
  B. The elusive thyroid I^- trapping system
III. From I^- to THs
  A. Candidate proteins as possible mediators of apical I^- efflux
  B. The complex machinery responsible for I^- organification
IV. I^- and THs: From Phytoplankton to Humans
  A. THs in human development
  B. Maternal thyroxinemia has a profound effect on fetal development
V. NIS, the Mediator of Active I^- Uptake in the Thyroid and Beyond
  A. Molecular identification of NIS
  B. NIS substrates
  C. New developments concerning NIS stoichiometry: NIS transports I^- electrogenically but ClO_4^- and ReO_4^- electroneutrally
VI. Recent Advances in Structure/Function of NIS
  A. CH-causing NIS mutations have been a rich source of structure/function information on NIS
  B. Identification of transmembrane segment IX amino acids key for Na^+ binding and/or translocation
  C. A crucial structure/function insight from the analysis of NIS mutants: seemingly unrelated transporters may exhibit a common fold and other shared characteristics
  D. Position 93 is critical for NIS substrate specificity and stoichiometry

ISSN Print 0163-769X ISSN Online 1945-7189
Printed in U.S.A.
Copyright © 2014 by the Endocrine Society
Received June 4, 2012. Accepted October 11, 2013.
First Published Online December 5, 2013

* C.P. and M.P.-B. contributed equally to this work.

Abbreviations: Ad, adenoviral; AEC, airway epithelia culture; AFP, α-fetoprotein; ASL, airway surface liquid; BetP, Na^+/betaine symporter; C293B, [3R,4S]-chromanol 293B; CF, cystic fibrosis; CFTR, CF transmembrane conductance regulator; CG, chorionic gonadotropin; CH, congenital hypothyroidism; CMV, human endothelial progenitor cell; CNS, central nervous system; Dehal1, iodotyrosine dehydrogenase; DIT, 3,5-di-iodotyrosine; Duox2, dual oxidase 2; EC, endothelial cell; HIF, hypoxia-inducible factor; hNIS, human NIS; ID, I^- deficiency; IDD, ID disorder; ITD, I^- transport defect; KCNQ1, potassium voltage-gated channel, KQT-like subfamily member 1; KO, knockout; LPO, lactoperoxidase; MEK, MAPK kinase; Mhp1, benzyl-hydantoin transporter; MIT, 3-mono-iodotyrosine; MMI, methimazole; MV, measles virus; NIS, Na^+/I^- symporter; PET, positron emission tomography; PTC, papillary thyroid cancer; $OSCN^-$, hypothiocyanite; RIT, radioiodide therapy; rNIS, rat NIS; ROS, reactive oxygen species; RRA, radioiodide remnant ablation; SCN^-, thiocyanate; $SeCN^-$, selenium cyanate; SGLT, Na^+/glucose transporter; SMCT, Na^+/monocarboxylate transporter; SMVT, Na^+/multivitamin transporter; Tg, thyroglobulin; TH, thyroid hormone; TMS, transmembrane segment; TPO, thyroperoxidase; UI, urinary I^-; vSGLT, *Vibrio parahaemolyticus* SGLT; WT, wild-type.

Downloaded from https://academic.oup.com/edrv/article/35/1/106/2354709 by guest on 09 April 2024

E. The study of the ITD-causing NIS mutation Δ439–443 provided novel information on helix capping
VII. Functional Expression of NIS in Extrathyroidal Tissues
A. Salivary glands
B. Stomach
C. Small intestine
D. Lactating breast
E. Kidney
F. Placenta
G. Airway mucosal surface host defense: a new role for NIS?
VIII. Regulation of NIS in the Thyroid and Extrathyroidal Tissues
A. By TSH
B. By I^-
C. By a novel mechanism involving a K^+ channel
D. By lactogenic hormones
IX. Clinical Applications of NIS
A. Hyperthyroid states
B. Thyroid cancer
C. Emerging roles of NIS in extrathyroidal pathologies: endogenous NIS expression and exogenous NIS expression by gene transfer
D. Downregulation of thyroid function is required for NIS-mediated $^{131}I^-$ therapy of extrathyroidal tumors
E. Another NIS substrate potentially useful for therapy: $^{188}ReO_4^-$
F. Additional considerations pertaining to NIS gene transfer
X. Concluding Remarks

I. Introduction

The significance of the thyroid gland for human health is difficult to overstate, given the wide-ranging effects of the thyroid hormones (THs) on prenatal and early development as well as on intermediary metabolism at all stages of life. Thyroid function, in turn, depends on an adequate supply of iodide (I^-), an essential constituent of the THs. I^- reaches the thyroid via a highly specialized I^--concentrating system, the Na^+/I^- symporter (NIS), the key plasma membrane transport protein located on the basolateral surface of thyrocytes. The thyroid's ability to concentrate I^- was first identified in 1896 by Baumann (1, 2). Fifty years later, in 1946, this ability of the thyroid began to be successfully exploited for the treatment of thyroid disease, including thyroid cancer (3). Another 50 years passed before the molecule involved, NIS, was finally cloned in 1996 (4, 5). Since then, NIS research has become a field of inquiry in its own right. Discoveries in this field have had a remarkable impact on numerous basic and translational areas, ranging from thyroid pathophysiology to the structure/function properties of other plasma membrane transporters, as well as on gene transfer, breast cancer, and even public health and environmental pollutants, to name but a few. The characterization of NIS has reached a particularly exciting point in the last few years, partly as a result of the recent elucidation of the crystal structures of bacterial analogs of various Na^+-driven transporters. In this article, we discuss the latest research on NIS and related fields, showing clearly that the more mechanistic information we obtain on NIS, the better equipped we are to identify, implement, and extend clinical applications for this remarkable molecule.

II. A Historical Perspective on I^- Deficiency

I^- deficiency (ID) and goiter, its most visible manifestation, have been observed throughout human history. Although goiter had already been described in ancient times as an "enlargement of the cervical gland" (Hippocrates, fifth century BCE), and besides descriptions just of "guttur tumidum" by the medical scholars of the Scuola di Salerno, goiter was first recognized as an enlargement of the thyroid gland by Albrecht von Haller in the 18th century (6).

Mountainous regions and areas far away from the sea have traditionally been plagued by endemic goiter and cretinism, both direct consequences of ID. Switzerland was one of the areas most afflicted by cretinism, and I^- supplementation for humans and cattle was introduced in that country as early as 1922 (7). This was the first mass nutritional intervention ever recorded. Pockets of endemic ID were also present in the United States, in the Great Lakes area and Northwestern states.

Evidence of a direct link between ID and cretinism came as late as 1966, from a controlled trial carried out in Papua New Guinea, in which half the families received injections of iodized oil and half received injections of saline (8), dramatically reducing the incidence of cretinism and goiter in the treated group as compared with the control group, and only when I^- supplementation was provided before the onset of pregnancy.

A. I^- is an essential micronutrient and its lack causes ID disorders

Inadequate dietary I^- intake results in hypothyroidism and goiter at all ages. Mild ID also has a significant impact on reproductive health, increasing miscarriages and stillbirths, and is the most common cause of reproductive failure worldwide (9). In addition, it is associated with increased perinatal mortality in the population (9, 10).

Insufficient I^- intake in critical windows of development during fetal life and childhood results in the most dramatic manifestation of ID disorders (IDDs), ie, neurological cretinism, characterized by severe and permanent growth and cognitive impairment. The TH T_4, which in-

Downloaded from https://academic.oup.com/edrv/article/35/1/106/2354709 by guest on 09 April 2024

cludes 4 iodine atoms in its structure (Figure 1 and *Section III.B.*), has a profound effect on brain development; it is required for myelination, somatogenesis, neuronal differentiation, and formation of neural processes, and its function is critical for proper development of the cerebral cortex, cochlea, and basal ganglia during the first trimester of gestation and for brain growth and differentiation in the third trimester (9).

IDDs form a spectrum and can result in wide variability in the severity of physical and cognitive symptoms. More subtly, suboptimal I^- intake is a cause of reduced mental ability, lower school and work performance, and loss of an estimated 13.5 intelligence quotient (IQ) points at a population level (11) and intellectual potential (for a brief overview, see Refs. 11–13). The urinary I^- (UI) concentration (normal value >100 μg/L) is a significant indicator of thyroid function and the most useful measure of I^- status of a given population. Even in I^--sufficient countries, suboptimal I^- intake still affects a significant number of people. In the United States, ~8% of the population has a UI <50 μg/L. This percentage increases in women of reproductive age to 14.8%, and ~11% of pregnant women have also been reported to have a UI <50 μg/L, both numbers higher than in previous years (14, 15). Strikingly, ID is still the most common cause of preventable brain damage after starvation.

Resolutions were passed by international organizations, such as the United Nations, the World Health Organization (WHO), the United Nations Children's Fund (UNICEF), and the Food and Agriculture Organization (FAO), with the aim of eradicating IDDs by 2000, a goal that was later delayed to 2005. As a result of these efforts, currently 68% of the world's households have access to iodized salt, compared with 20% in 1990, and since 2003,

Figure 1.

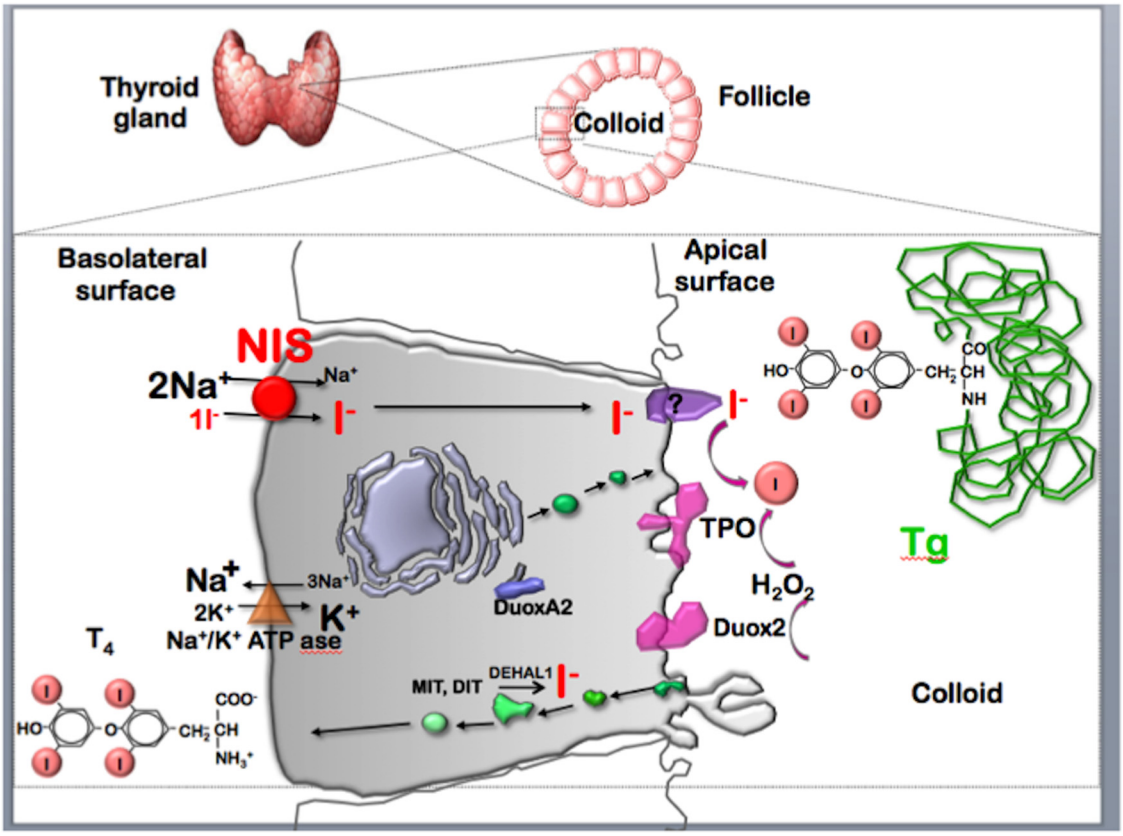

Figure 1. Schematic representation of TH biogenesis in polarized thyroid epithelial cells. The thyroid gland (upper left) is composed of follicles (upper right), each of which consists of a single layer of epithelial cells (main panel). NIS (red circle), located on the basolateral surface of the thyrocyte, mediates Na^+/I^- symport with a 2:1 stoichiometry. The driving force for this process is the Na^+ electrochemical gradient generated by the basolateral Na^+/K^+ ATPase (brown triangle). I^- crosses the apical membrane via an unidentified carrier or carriers (purple structure with question mark) and is then oxidized and incorporated into Tg (green wire in the colloid) via an enzymatic oxidation carried out by TPO (pink), with the H_2O_2 generated by Duox2 (also pink). Duox2A, an endoplasmic reticulum chaperone required for Duox2 maturation and function, is represented as a blue structure in the endoplasmic reticulum. Iodinated Tg is endocytosed and proteolyzed in the endocytic/lysosomal compartment (green intracellular vesicles), and THs are released into the bloodstream. I^- incorporated into MIT and DIT is recycled through a deiodination reaction by the iodotyrosine dehalogenase Dehal1.

Downloaded from https://academic.oup.com/edrv/article/35/1/106/2354709 by guest on 09 April 2024

the prevalence of insufficient I^- intake has decreased globally by 5% (16). However, according to the WHO, as of 2007, over 30% of the world population (2 billion people), including 270 million school-age children, still have inadequate I^- intake (UI <100 μg/L) and are at risk of developing IDDs (16). Recent data indicate that the most affected areas in the world are South Asia, Central and Eastern Europe, and Africa (16, 17).

B. The elusive thyroid I^- trapping system

Only 7 years after its discovery in 1812 by Courtois, iodine was used for the treatment of goiter (18). The ability of the thyroid to concentrate I^- was formally demonstrated as early as 1896 (2, 18) and has provided the basis for the diagnosis and treatment of thyroid disease, including the highly successful treatment of thyroid cancer with radioiodide after thyroidectomy (19, 20). However, the molecular basis for I^- accumulation was not elucidated until a century later (5). I^- is a scarce element in the environment and can be acquired only through the diet. As the reported concentration of free I^- in mammalian plasma is only 50nM to 300nM (21), the thyroid evolved an extremely efficient mechanism to actively accumulate I^- from the blood. The nature of the I^- conduit was a subject of debate for many decades. At one point, even phospholipids were proposed to act as I^- carriers through complexing anions and making them lipid-soluble (22, 23). Ultimately, the molecule responsible for active transport of I^- in the thyroid was finally identified as NIS (5) (Figure 2), which is located on the basolateral membrane of thyroid epithelial cells (Figure 1; for details on the cloning and characterization of NIS, see *Section V*).

III. From I^- to THs

Iodine (I), the oxidized form of I^-, is an essential constituent of the THs, which are phenolic rings joined by an ether link and iodinated at 3 positions (3,5,3′-tri-iodo-L-thyronine, or T_3) or 4 positions (3,5,3′,5′-tetra-iodo-L-thyronine, or T_4). As indicated above, THs are required for the development and maturation of the central nervous system (CNS), lungs, and skeleton (21, 24–26). They are master regulators of cell metabolism (lipid, protein, and carbohydrate anabolism and catabolism). Thus, their deficiency or excess perturbs homeostasis and leads to disease.

Anatomically, the thyroid is located anterolaterally to the trachea and larynx and consists of 2 lobes connected by an isthmus. The functional units of the mature thyroid gland are the thyroid follicles, which are enclosed by a basement membrane. Histologically, the spherical follicles are lined by a monolayer of polarized epithelial cells, with the basolateral surface facing the bloodstream and the apical surface the follicular lumen (Figure 1). The lumen is filled with colloid, which is mainly composed of thyroglobulin (Tg), a protein present at a very high concentration (~100–750 mg/mL) (27) that serves as the backbone for the THs. I^- is covalently incorporated into Tg, a process called I^- organification; iodinated Tg is the precursor and storage form of the THs, which are released into the bloodstream upon stimulation by TSH (see *Section III.B.* for more details). The thyroid is unique among endocrine glands in that its hormonal products are stored extracellularly in the colloid.

A. Candidate proteins as possible mediators of apical I^- efflux

Although the role of NIS in the first transport step of I^- from the bloodstream across the basolateral surface of the thyroid cell has been unequivocally shown, the pathway for I^- across the apical surface is less certain. One candidate to be an apical I^- transporter is pendrin, originally identified as an anion exchanger that is mutated in Pendred's syndrome, a condition characterized by sensorineural hearing loss, a partial organification defect, and a positive perchlorate (ClO_4^-) discharge test (28, 29). In this test, ClO_4^-, a competitive inhibitor of NIS, is administered to patients after radiolabeled I^- has been taken up, thereby inhibiting I^- reuptake by the thyroid and causing a leak of nonorganified I^- from thyrocytes into the bloodstream. This I^- leak is higher in subjects with impaired I^- efflux or I^- organification. Although pendrin's role in anion balance in the inner ear and in renal reabsorption/secretion of Cl^- and bicarbonate (HCO_3^-) has been extensively studied (28), pendrin-mediated I^- efflux in the thyroid has not been thoroughly characterized. In addition, the development of goiter or hypothyroidism in patients with Pendred's syndrome may depend on dietary I^- intake (28), suggesting that pendrin's role is limiting only when I^- intake is low and that other carriers are therefore involved in apical I^- efflux in the thyroid. Of note, pendrin knockout (KO) mice do not exhibit any thyroid phenotype, either under I^--sufficient (30) or under low-I^- conditions (31).

Chloride (Cl^-) channels are also permeable to I^- and are potential candidates for mediating I^- efflux at the apical membrane of thyrocytes. The cystic fibrosis (CF) transmembrane conductance regulator (CFTR), which is permeable to I^-, is expressed in the thyroid, where currents carrying the biophysical signature of CFTR have been measured (32), so it may be involved, at least in part, in apical I^- efflux. It has been reported that CF patients may be more likely to develop subclinical hypothyroidism (33, 34), although the mechanism of reduced serum TH concentrations in CF has not yet been elucidated (32).

Downloaded from https://academic.oup.com/edrv/article/35/1/106/2354709 by guest on 09 April 2024

Figure 2.

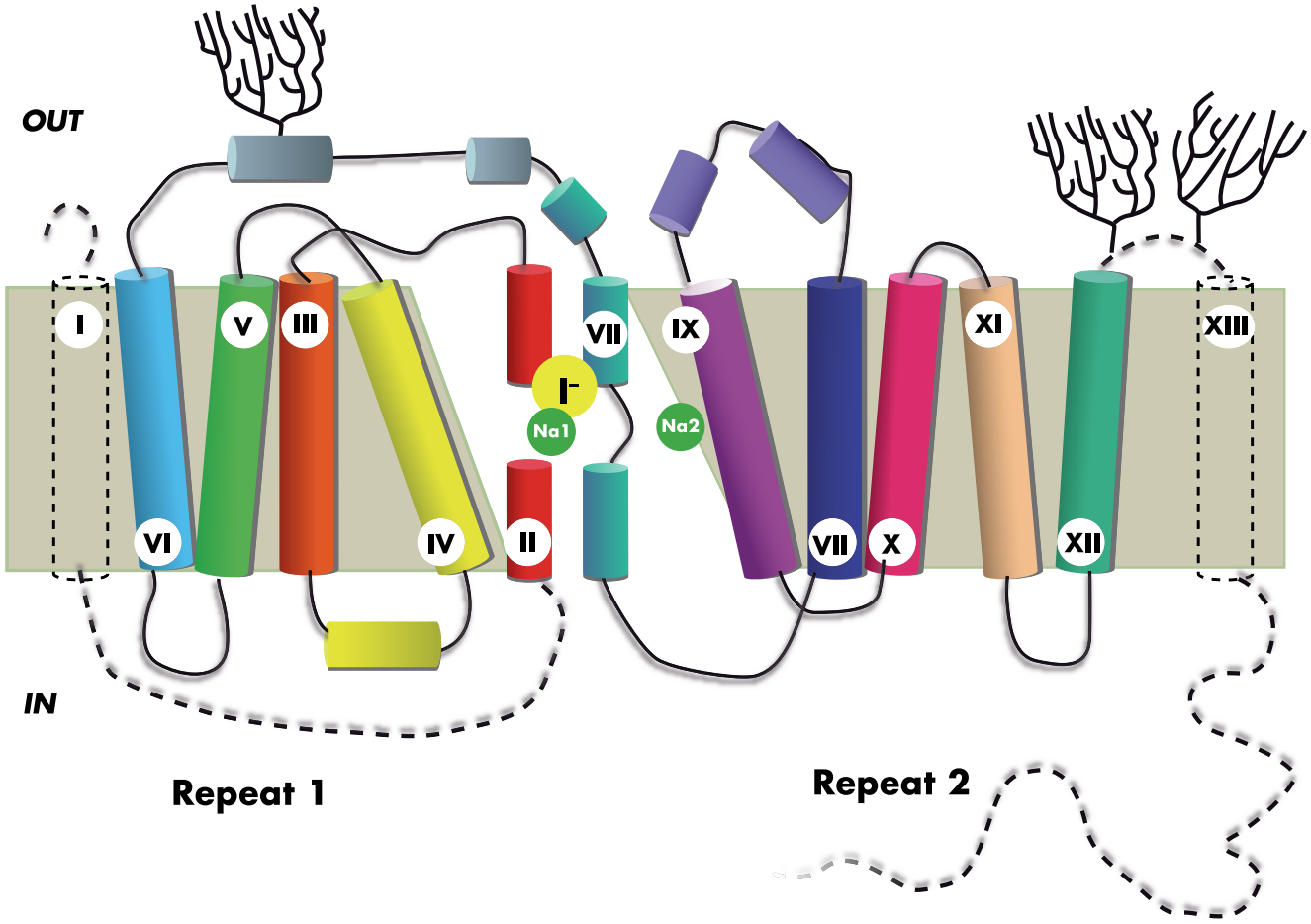

Figure 2. Secondary structure of NIS. The secondary structure model for NIS was constructed on the basis of biochemical data and the protein's structural homology with transporters whose 3-dimensional structures are known (for details, see *Section VI*). NIS is a 13-TMS protein, with the amino terminus facing the extracellular milieu and an intracellular carboxy terminus. TMSs I and XIII, and the loops between TMSs I and II and XII and XIII, are represented by dotted lines; their position relative to the other TMSs in the secondary structure could not be defined by homology modeling. Ten helical TMSs form an internal inverted topology repeat consisting of 5 transmembrane helical bundles (repeat 1, comprising TMSs II–VI, and repeat 2, comprising TMSs VII–XI), related to each other by a 2-fold pseudosymmetry axis running parallel to the membrane plane through the center. There are 3 glycomoieties (black trees), 1 between TMSs VI and VII and 2 between TMSs XII and XIII. Based on the crystal structures of several prokaryotic transporters (134–136, 178), unwound regions in the helices are predicted to provide flexibility and expose side- and main-chain contacts critical for substrate coordination. TMSs II and VII are proposed to define the substrate cavity accommodating both the anion and Na1, and TMS IX contributes to coordination of Na2 (as discussed in *Sections VI.D.* and *VI.B.* respectively).

ClC-5, a H^+/Cl^- antiporter with a high permeability to I^- (~70% that of Cl^-) (35), was found to be important for pendrin expression; in ClC-5 KO mice, which develop a euthyroid goiter, pendrin mRNA and protein expression are reduced by 60% (36). However, the role of ClC-5 itself in thyroid I^- efflux awaits further investigation.

The Na^+/monocarboxylate transporter (SMCT), a protein formerly known as AIT (for apical I^- transporter), was cloned by using degenerate primers based on the NIS sequence and was thought to be the apical I^- transporter owing to its striking homology with NIS (46% identity and 70% similarity) and its apical localization in thyroid cells (37). However, it was later shown that SMCT does not transport I^-; instead, it transports a variety of monocarboxylates, including lactate, pyruvate, butyrate, and nicotinate, which is its most specific substrate (38). The function of SMCT and its physiological substrates in the thyroid remain unknown. Interestingly, aside from its presence in the thyroid, the promoter of SMCT is hypermethylated in colon cancer (39), and a correlation between SMCT expression in human colon cancer and patient survival has been shown (40). The most relevant phenotype of the SMCT KO mouse is lactaturia. Intestinal cancer incidence was not increased in these animals, even when they were challenged with oncogenic chemicals or crossed with transgenic mice with mutant

Downloaded from https://academic.oup.com/edrv/article/35/1/106/2354709 by guest on 09 April 2024

tumor suppressors such as adenomatous polyposis coli (APC^{min}) (41).

In conclusion, although various candidate proteins that may mediate I^- translocation across the apical membrane of thyrocytes have been proposed, at the present time, the identity of the I^- apical translocation pathway remains poorly understood.

B. The complex machinery responsible for I^- organification

After its translocation into the follicular lumen, I^- is first oxidized to iodine (I_2) and then covalently incorporated into tyrosyl residues on Tg. Iodinated tyrosyl residues are coupled on Tg to form THs, which are stored in the colloid covalently linked to the Tg backbone (Figure 1). This 3-step process is catalyzed by thyroperoxidase (TPO), an apical monotopic membrane protein with a heme catalytic domain, which shares 44% similarity with leukocyte myeloperoxidase and faces the follicular lumen. Iodine is covalently bound on 3 or 4 positions of tyrosyl residues on Tg. 3-Mono-iodotyrosine (MIT) and 3,5-diiodotyrosine (DIT), the iodinated TH intermediates bound to Tg, are then coupled by TPO via an ether bond to form T_3 and T_4. After the iodophenol moiety of the Tg donor site is bound on the tyrosyl residue of the acceptor site, a dehydroalanine remains in the Tg backbone and quickly reacts with H_2O to yield a serine (42, 43).

The oxidative power for I^- organification is provided by H_2O_2 generated by dual oxidase 2 (Duox2), a multispanning membrane protein belonging to the family of the nicotinamide adenine dinucleotide phosphate-dependent flavin adenine dinucleotide oxidases. The name dual oxidase stems from the presence of a lumen-facing domain that exhibits >45% amino acid similarity with TPO, with putative and controversial peroxidase activity (44–46). Interestingly, Duox2 shares 47% amino acid similarity to $gp91^{phox}$ (Nox2), which is responsible for the respiratory burst and the production of reactive oxygen species (ROS) in neutrophils (45). In contrast to most of the proteins involved in TH biosynthesis, Duox2 expression and activity do not appear to be regulated by TSH (47–49). On the other hand, Duox2 activity is enhanced by a rise in the intracellular Ca^{2+} concentration. Mutations in *DUOX2* and in *DUOXA2,* its maturation factor and chaperone, have been identified as causes of congenital hypothyroidism (CH) (50, 51). Because in some cases transient hypothyroidism occurs (TH biosynthesis is restored to a level where pharmacological supplementation is no longer needed, usually during late childhood or adolescence) (52), it was postulated that permanent hypothyroidism was caused by biallelic *DUOX2* mutations and transient hypothyroidism by heterozygous mutations. However, recent evidence suggests that other mechanisms are in place, as transient hypothyroidism has also been observed in patients with homozygous mutations (briefly summarized in Ref. 53). Because H_2O_2 generation is absolutely required for TH biosynthesis, it is possible that Duox1, which is functionally identical to Duox2 but has a different tissue distribution pattern and regulation, is upregulated to compensate for the loss of Duox2.

Tg is a highly glycosylated 660-kDa homodimer with 132 Tyr residues. Strikingly, each Tg molecule contains on average only 5 MIT, 5 DIT, 2.5 T_4, and 0.7 T_3 moieties, distributed on only one-third of all Tyr residues, with some hormonogenic positions that are preferentially iodinated (43). Iodinated Tg is stored in the follicular lumen in a colloidal form, including insoluble microglobules of protein, highly cross-linked with disulfide, dityrosine, and glutamyl-lysine bonds (27). Tg is internalized via endocytosis or micropinocytosis under basal conditions. When TSH serum levels increase, all steps of TH biosynthesis and release are stimulated, including Tg internalization. Pseudopod formation and Tg macropinocytosis occur within minutes of TSH stimulation; internalized Tg undergoes proteolytic cleavage in lysosomes, and T_3 and T_4 are then released into the bloodstream (43). In this process, MIT and DIT from partial or incomplete TH synthesis are also released. Interestingly, it was discovered over 50 years ago that MIT and DIT produced during Tg proteolysis, and accounting for 70% of Tg iodine content, are metabolized in the thyroid to I^- and Tyr by a nicotinamide adenine dinucleotide phosphate-dependent flavin mononucleotide (FMN) iodotyrosine dehydrogenase (Dehal1) (52, 54–56). The Dehal1 gene (*IYD*) and its CH-causing mutations were identified only recently (57). I^- recovered from MIT and DIT can reenter the cycle of organification. Dehal1 activity is critical for the synthesis of adequate amounts of THs because it ensures recycling of the intrathyroidal I^- pool from partially iodinated TH intermediates. Surprisingly, 3 to 5 times more I^- is recycled from partially iodinated Tg than enters the thyroid from the dietary pool (58). Defects in Dehal1, which can be treated successfully by administering large amounts of I^-, cause CH, goiter, increased MIT and DIT serum levels, and severe urinary loss of organic I^- (59). Variable mental deficits can result, depending on the age of the patient when hypothyroidism is recognized and/or when hypothyroidism occurs during development, possibly varying with I^- availability in the diet. Dehal1 activity underscores the importance of the I^- recycling process and highlights the avidity with which I^- is conserved and reused.

Downloaded from https://academic.oup.com/edrv/article/35/1/106/2354709 by guest on 09 April 2024

IV. I^- and THs: From Phytoplankton to Humans

TH synthesis, and thus proper development and function of the body, relies entirely on the availability and adequate dietary intake of I^-, raising provocative questions about the evolution of the TH pathway and why it has been selected for, and conserved, during evolution, despite the need for a continuous source of I^- and the high cost of ID for health and reproductive success. Strikingly, although they may lack thyroid-like structures per se, TH-like compounds are essential for organisms from various phyla of the animal kingdom (Figure 3).

Chordata [Craniata, which includes vertebrates, and the closely related invertebrates Urochordata (tunicates) and Cephalochordata (amphioxus)] evolved a specific organ for accumulating I^-, producing THs and storing them until needed (Figure 3A). Putative ortholog proteins for TH biosynthesis (TPO and Tg), a putative TH receptor, and thyroid development proteins (thyroid transcription factor-1 Foxe-1 and Pax8) have all been identified in the endostyle, a specific organ used for feeding, in the most basal, nonvertebrate chordates, namely urochordates (such as *Ciona intestinalis*) and cephalochordates (eg, amphioxus) (60, 61). In the parasitic lamprey, a basal vertebrate, a thyroid-like structure with a follicular organization develops after metamorphosis in addition to the endostyle (62).

Although they lack a thyroid-like organ, invertebrate development is also affected by THs (Figure 3B). In echi-

Figure 3.

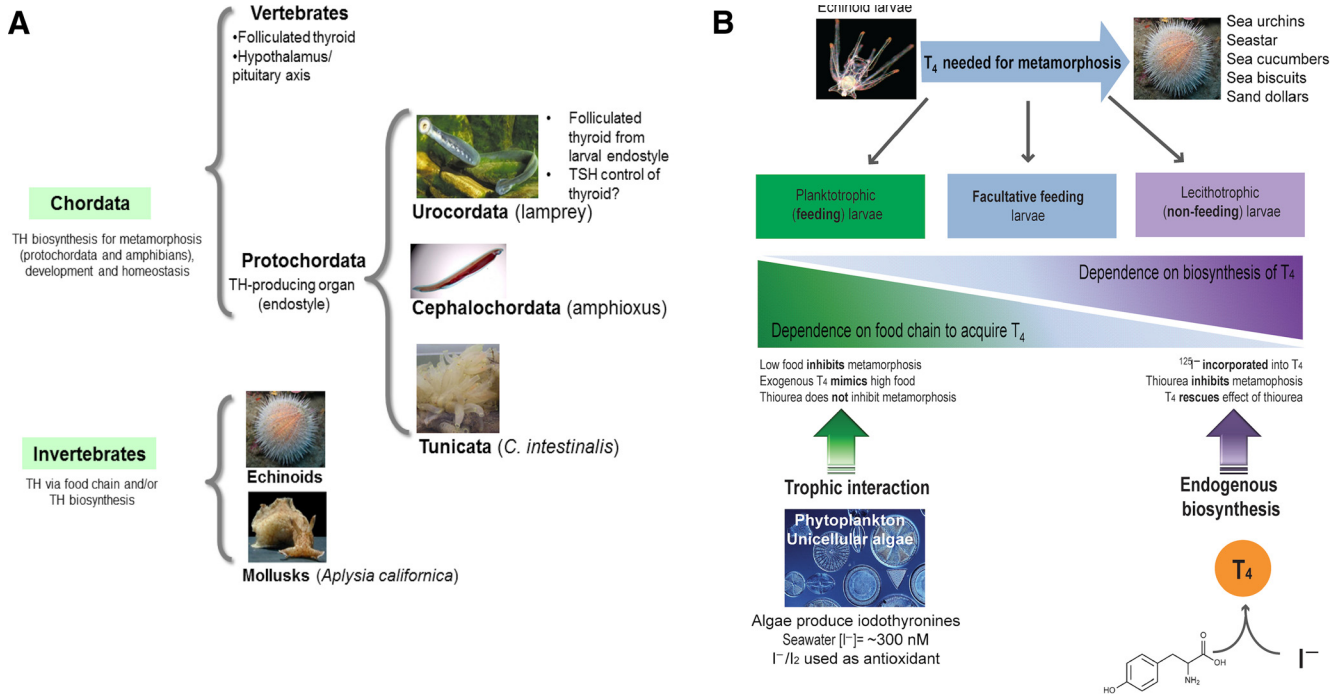

Figure 3. Evolution of THs: from unicellular algae to mammals. A, In the phylum Chordata, TH biosynthesis is required to signal for metamorphosis (in Protochordata and amphibians) and for development and homeostasis (in vertebrates). In the subphylum Protochordata, which includes Tunicata and *Amphioxus*, THs are produced in the endostyle, an exocrine gland associated with the pharynx and used for feeding, and end up in the esophagus together with food. In the parasitic lamprey, the endostyle is present during the larval stage, but after metamorphosis, it is replaced by a thyroid. Control of thyroid function by TSH has never been demonstrated in jawless fish, and pituitary modulation of TH synthesis is a characteristic of higher vertebrates. B, Unicellular algae, which use I^-/I_2 as an antioxidant system, synthesize iodothyronines from marine components. Echinoid larvae feeding on phytoplankton (green box) evolved to sense algal T_4 as a cue to the amount of energy available for their development, in a process called cross-kingdom cross-talk. Lecithotrophic larvae, which evolved from echinoids with planktotrophic larvae (purple box), are not exposed to environmental iodothyronines; however, TH signaling became essential for their metamorphosis earlier in evolution, and rather than losing THs as a development-inducing signal, these larvae evolved the ability to synthesize their own iodothyronines. Facultative feeding larvae (blue box) acquire T_4 from the plankton they feed on but also synthesize endogenous T_4, which in some cases can be enough to trigger metamorphosis in the absence of food. In larvae that depend on food to undergo metamorphosis, exogenous administration of T_4 rescues the effect of food withdrawal (ie, inhibition of metamorphosis), whereas the TH synthesis inhibitor thiourea does not, demonstrating that T_4 is both necessary and sufficient for metamorphosis and indicating that endogenous TH biosynthesis does not occur in these organisms. In contrast, thiourea inhibits metamorphosis in nonfeeding larvae, and these larvae also incorporate $^{125}I^-$ into THs. This indicates that endogenous TH biosynthesis occurs in nonfeeding larvae and that it triggers a developmental step in these organisms.

Downloaded from https://academic.oup.com/edrv/article/35/1/106/2354709 by guest on 09 April 2024

noids (sea urchins, sea biscuits, sand dollars, and sea cucumbers), larval and juvenile morphogenesis, as well as metamorphosis, are influenced by exogenous T_4. Echinoderms can develop from nonfeeding larvae, feeding larvae, or nonobligatorily feeding larvae. Intriguingly, exogenous T_4 produces the same effects in feeding larvae as exposure to algae (ie, to a food-rich environment), in contrast to the morphologic effects of a low-food environment (development of larval structures instead of juvenile structures and delay in reaching metamorphosis) (Figure 3B, left). The remarkable similarity of the effect of T_4 to that of food abundance suggests that the developmental cue in food that echinoid larvae respond to is actually T_4. Interestingly, larvae that develop without feeding (63), and therefore cannot acquire algal T_4, have been found to synthesize T_4 (Figure 3B, right) via a mechanism sensitive to thiourea (a TPO inhibitor). In nonfeeding larvae, exposure to thiourea favors the development of larval structures at the expense of juvenile structures and also delays the acquisition of metamorphic competence. In addition, exposure to T_4 favors the development of juvenile structures in a dose-dependent manner and can rescue the developmental effects of thiourea-treated larvae (Figure 3B, right). The prediction was that facultative feeding larvae were more dependent on endogenous T_4 biosynthesis than feeding larvae (Figure 3B, middle). This was confirmed in 2 sea biscuit larvae, *Dendraster excentricus* (which develops from an obligatorily feeding larva) and *Clypeaster rosaceus* (which develops from a facultative planktotrophic larva) (64, 65). The latter can also synthesize endogenous T_4 in a thiourea-dependent fashion, but not enough to trigger metamorphosis in the absence of food. An example of the dramatic developmental dependence of these organisms on T_4 is that, in a sand dollar (*Leodia sexiesperforata*), the availability of exogenous T_4 induces a switch in developmental mode from obligatorily feeding to facultative feeding larvae, which can undergo complete metamorphosis in the absence of food (65).

Why did invertebrates evolve a TH-dependent plasticity pathway? The hypothesis is that phytoplankton is a source of hormone or prehormone to echinoderm larvae via the food chain (trophic interaction) (66). T_4, and T_3 in smaller amounts, has been found so far in 3 unicellular algae (*Dunaliella tertiolecta, Isochrysis aff. Galbana,* and *Rhodomonas lens*) (67) and a diatom (*Chaetoceras gracilis*) (68). Notably, T_4 is one order of magnitude more potent than T_3 in feeding sea urchin larvae (68). The building blocks of TH are all present in the marine environment as follows (67): iodine species that are found in seawater at a concentration of 0.5μM, mainly in the form of iodate (IO_3^-) and I^-; micro- and macroalgae that can contain up to 1% iodine in organic or inorganic forms; and tyrosine that can be either transferred from symbiotic algae or acquired from the water-dissolved organic matter. It is possible that algal biosynthesis of iodotyrosines via haloperoxidases evolved as a detoxification reaction to protect against ROS (69). Organisms feeding on algae later evolved a system to detect iodotyrosines as an energy-related plasticity cue, in an evolutionary mechanism called cross-kingdom cross-talk (62, 66, 67) (Figure 3B). A classic and well-studied example of this phenomenon is the interaction between plants and arthropods. All arthropods lack sterol synthesis, but the synthesis of ecdysteroids (arthropod hormones) requires sterols, which arthropods obtain via trophic interactions with autotrophs. The hypothesis is that autotrophs evolved to produce compounds (for example, phytosterols) to deter excessive predation, and arthropods coevolved to tolerate high concentrations of these compounds by metabolizing them and eventually evolved to use them as developmental signals (66).

Iodotyrosine signaling in invertebrates may have evolved from cross-reaction with nuclear receptors; however, the invertebrate TH receptor–like proteins that have been characterized so far do not show high affinity for TH or bind DNA. It is conceivable that, in invertebrates, THs act through a different mechanism, such as plasma membrane receptors. This phenomenon is also observed in the arthropod-plant coevolution; arthropod ecdysteroid hormones signal through a nuclear receptor, whereas plant gibberellins act via different plasma membrane mechanisms (66).

The mechanism of I^- transport in invertebrates is not known. In the nonfeeding sand dollar *Peronella japonica*, thiourea and ClO_4^- both delay metamorphosis (63). In *C. rosaceus* (64), treatment with thiourea also decreases free $^{125}I^-$ content, suggesting, according to the authors, a mechanism of I^- transport different from a NIS-like molecule, as NIS is not sensitive to thiourea in vertebrates. However, there is also the possibility that when I^- organification is blocked by thiourea, I^- leaks out of the cells. Likewise, in the obligatorily feeding sea urchin *Lytechinus variegatus*, ClO_4^- does not affect I^- accumulation (64). However, it is entirely possible that, if a NIS homolog exists in invertebrates (70), the anion binding pocket is different and allows binding and transport of I^-, but not of ClO_4^-. In support of this hypothesis, Paroder-Belenitsky et al (71) reported that placing different amino acid side chains at position 93 of NIS, which faces the anion/Na^+ binding cavity, modifies the transporter anion selectivity, even abolishing the ability of NIS to transport I^-, but not ClO_4^- and perrhenate (ReO_4^-) in some cases (discussed in more detail in *Section VI.D.*).

Downloaded from https://academic.oup.com/edrv/article/35/1/106/2354709 by guest on 09 April 2024

Once animals acquired TH-mediated developmental signals via cross-kingdom cross-talk (Figure 3B), they evolved strategies to cope with a temporary shortage of I^- supply, such as TSH regulation of TH synthesis, a follicular thyroid structure that allows THs to be stored (Figure 3A), mechanisms to recycle I^- from the thyroid (iodotyrosine dehalogenases, such as Dehal1), and the body pool (peripheral deiodinases and NIS expression in salivary glands and stomach). It is also possible that a positive selection was in place to keep useful, non-TH–related roles of I^- accumulation in the body, such as the antimicrobial role in the mucosal surface host defense system (72) (*Section VII*).

A. THs in human development

In mammals, the first glandular tissue to develop is the thyroid gland. The thyroid begins to take up I^- and secrete THs as early as 10 to 12 weeks of gestation in humans (73). Before this, maternal TH is critical for fetal development and is provided via placental vessels. Thyroid follicular cells arise from the embryonic endoderm. The anlagen, a thickening in the floor of the primitive pharynx between the first and second brachial arches, becomes apparent at gestational day 17. The anlagen proliferates ventrally and laterally to form the characteristic bilobed structure of the thyroid gland (43).

In humans, thyroid morphogenesis is completed by gestation week 7, when the gland descends to its permanent pretracheal position. At this point, thyrocyte precursors are still undifferentiated but begin to express thyroid-specific and thyroid-related genes (TSH receptor [*TSHR*] and *DUOX2* followed by *TG*, *TPO*, and pendrin [*SLC26A4*]) (74). NIS expression is the limiting step in the terminal differentiation and onset of thyroid function, being the last to appear at gestation week 10, just before the beginning of hormonogenesis. At this stage, although the NIS protein is mainly found in perinuclear compartments, basolateral localization is observed in very few thyrocytes, but it is enough to initiate fetal I^- accumulation (74). The thyroid gland is considered terminally differentiated at gestation week 11, once thyrocytes have fully polarized, formed follicles, and fetal TH synthesis begins (74).

THs play a critical role in the development of the CNS of the fetus and newborn, affecting neuronal migration, differentiation, myelination, and synaptogenesis (Figure 4A) (75–81). The importance of T_3 and T_4 in the CNS is underscored by the fact that at week 12 of gestation, both hormones can be detected in the cortex but not in other tissues or in serum (80). TH insufficiency can cause severe neurodevelopmental defects, cretinism being the gravest. In fact, even a slight reduction in maternal T_4 production (hypothyroxenemia) during gestation can impair cognitive development in the newborn and result in decreased IQ (82, 83). At birth, maternal T_4 accounts for 20% to 50% of the T_4 measured in cord blood (Figure 4A) (81, 84). Interestingly, symptoms of CH in babies born to euthyroid mothers do not manifest at birth. On the other hand, insufficient maternal thyroid function may influence the thyroid status of the fetus, even after it gains the ability to produce its own THs, and so should be monitored closely (85). Consistent with the increased demand for TH in pregnancy, human chorionic gonadotropin (CG) has been shown to increase I^- transport and NIS expression in the highly functional rat thyroid-derived FRTL-5 cells in a dose-dependent manner (86–88).

B. Maternal thyroxinemia has a profound effect on fetal development

Maternal I^- insufficiency can result in a wide spectrum of growth and mental impairment in the newborn. Pregnant women are at a higher risk of I^- insufficiency, as their daily requirement is higher than that of the general population (250 vs 150 μg/d) (International Council for the Control of Iodine Deficiency Disorders) (89, 90). The contribution of maternal THs, the sensitivity of the fetus to THs, and consequently the absolute requirement for an adequate supply of I^- during pregnancy have been a subject of debate. As late as 1971, the hypotheses concerning the effect of ID on fetal brain development were several: 1) that I^- had an effect per se on brain function, 2) that fetal hypothyroidism had the most relevant impact, and 3) that maternal hypothyroidism had the most relevant impact (91).

The importance of maternal thyroid health was first recognized at the beginning of the 20th century by physicians aware of severe endemic goiter and cretinism in regions such as the Swiss Alps and the Himalayas (10, 92). Studies performed in the 1960s found that women in areas where ID was common had low levels of serum protein-bound I^- (a measure of T_4), which physiologically increases at the onset of pregnancy (93). The maternal T_4 surge is mainly caused by the high circulating levels of CG produced by the embryo. CG, a glycopeptide hormone of the same family as TSH, cross-reacts with the TSH receptor and causes an increase in TH synthesis, to such an extent that maternal TSH is generally suppressed. This is a mechanism by which embryos ensure that they receive enough THs independently of the maternal thyroid status (94). It also became evident that elimination of neurological cretinism, characterized by a deaf-mutism and neuromuscular impairment phenotype, required a preventive intervention by correcting ID in the prenatal period, mainly in the first 2 trimesters of pregnancy, corroborating the observation that maternal THs are needed for the

Downloaded from https://academic.oup.com/edrv/article/35/1/106/2354709 by guest on 09 April 2024

Figure 4.

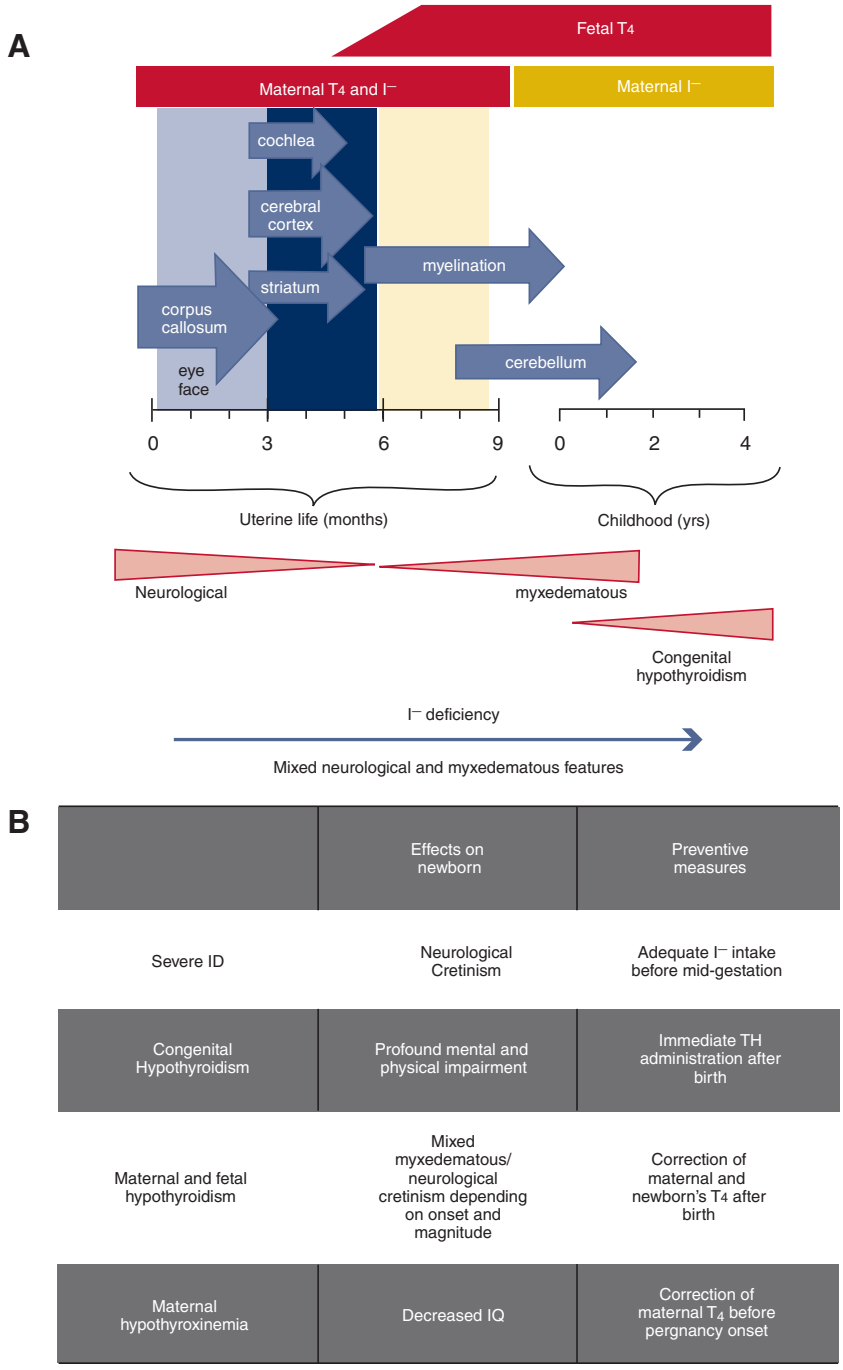

Figure 4. THs in human development and effects of ID and maternal hypothyroidism on fetal development. A, Maternal dietary I^- and T_4 are critical over the entire course of gestation. The fetus's thyroid starts producing THs at ~20 weeks, but the mother's T_4 contribution is still crucial. After birth, maternal I^-, which is transferred by NIS into the milk, is key for the newborn's development. Light blue arrows indicate the time of development of specific brain areas and body features that depend on adequate T_4 levels and can be affected by low T_4 at the indicated time of gestation. Neurological or myxedematous cretinism features occur depending on the onset and levels of maternal hypothyroxinemia or hypothyroidism. Congenital hypothyroidism due to fetal mutations in TH synthesis genes have a negative impact after birth, when the supply of maternal T_4 is interrupted. B, Effects of maternal thyroid conditions on fetal development and preventive measures.

child's CNS development. However, in the second half of the 20th century, these findings were disregarded, and the view that maternal T_4 transfer was blocked by the placental barrier and the child becomes sensitive to T_4 only after birth became predominant. The confusion was generated by the observation that athyroid newborns affected by CH could be effectively treated by prompt administration of T_4, suggesting that the fetus is insensitive to THs until after birth, and that neurological cretinism is not observed in children from hypothyroid mothers, reinforcing the hypothesis that maternal THs are not important for fetal growth (Figure 4B). The confusion was further exacerbated by the fact that the general living condition improvements in many regions had decreased the incidence of cretinism without I^- supplementation (95).

Questions about the physiological significance and role of T_4 in fetal development arose also from the finding that T_4 levels in fetal blood are extremely low (100-fold lower than in maternal serum). Studies by Morreale de Escobar and colleagues (92, 96, 97) revealed that, although the fetal serum T_4 concentration is lower than the maternal one, when the proportion of free T_4 (ie, the active form not bound to serum transport proteins) is taken into account, fetal T_4 levels are comparable to adult ones. T_3 increases in the fetal cerebral cortex steadily with gestation to levels comparable to those in adults (2.5 pmol/g), due to local type-2 deiodinase activity, whereas T_3 concentration in the fetal serum remains constant and low. THs are found in embryonic and fetal tissues before the onset of fetal thyroid function (96), and they correlate with maternal hormone concentrations until the fetal thyroid starts functioning and actually secreting THs after maturation of the pituitary portal

Downloaded from https://academic.oup.com/edrv/article/35/1/106/2354709 by guest on 09 April 2024

system (92, 97). Rather than demonstrating that the fetus is insensitive to T_4 until after birth, the phenotype of athyroid children, who are born healthy and develop myxedematous cretinism (a less severe form of growth and mental impairment than neurological cretinism) after birth (91), shows that the maternal input of THs remains significant also after fetal TH is found in cord blood (84, 98). It is widely accepted that maternal subclinical hypothyroidism, defined by mild TSH increase associated with normal TH values (Figure 5A), needs immediate correction. However, it is often overlooked that maternal free T_4 should also be closely monitored and that maternal hypothyroxinemia, without changes in TSH levels (Figure 5B), negatively affects progeny neurodevelopmental markers (Figure 4B).

Of note, ID is the most common cause of maternal hypothyroxinemia (98, 99). The relationship between psychomotor impairment (100) at 10 months of age (101) and other developmental indices at 3 weeks, 1 year, and 2 years of age correlates with maternal free T_4 in the first trimester (102) and not with maternal TSH serum concentration (reviewed in Ref. 10). In fact, increased serum TSH is seldom found in ID, and when it occurs, it is much less pronounced in I^--deficient subjects than in patients with a similar decrease in T_4/T_3 levels arising from other conditions (103–105). These important differences in ID, as compared with hypothyroidism due to illness, result from a thyroid autoregulatory system working in ID that has not been characterized at the molecular level. Immediate effects of thyroid autoregulation in response to ID include increased T_3 over T_4 synthesis (106–108); increased thyroid vascularization, blood flow, and volume; hyperplasia; increased acinar cell height; and increased I^- uptake (97). All these changes occur well before and independently of changes in TSH, as they were also shown to take place in hypophysectomized animals (109, 110). As a result, serum T_3 is not significantly altered, and paradoxically, the body maintains a euthyroid state with low TSH and adequate T_3 levels. Thus, TSH screenings are insufficient predictors in ID populations. However, some tissues, such as brain (111), which rely almost exclusively on local T_3 synthesis by the action of type-2 deiodinase, which converts circulating T_4 to T_3, may be selectively hypothyroid, because lower circulating levels of T_4 preclude reaching normal tissue T_3 concentrations. This phenomenon also occurs in fetal brain, as elegantly demonstrated by Morreale de Escobar and collaborators (326). Dams treated with an organification blocker (to prevent endogenous TH synthesis) were given T_4 or T_3, and the concentration of the hormones was measured in maternal and fetal blood and tissues. Surprisingly, administration of enough T_3 to dams to normalize maternal and fetal serum T_3 levels failed to increase the T_3 concentration in fetal brain. In contrast, T_4 administration rescued fetal brain T_3 to normal values (92, 96).

The lack of distinction between ID- and CH-induced neurological disorders (Figure 4B) had 2 important neg-

Figure 5.

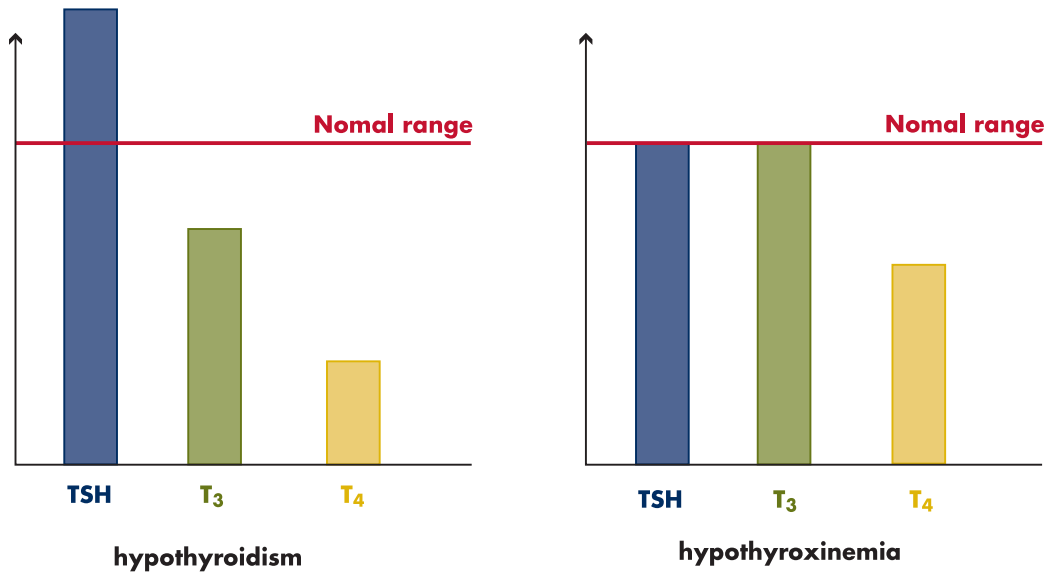

Figure 5. Comparison of hormone levels in hypothyroxinemia and hypothyroidism. Red line indicates normal TSH range. ID is the most common cause of maternal hypothyroxinemia. Maternal serum T_4 is correlated to fetal development. In contrast to hypothyroidism, hypothyroxinemia does not produce significant changes in TSH or T_3 concentrations. Therefore, TSH screenings are not appropriate for the identification of pregnant mothers whose T_4 levels need corrective measures.

Downloaded from https://academic.oup.com/edrv/article/35/1/106/2354709 by guest on 09 April 2024

ative consequences: 1) it was overlooked for a long time that patients with ID needed I^- supplementation as a preventive measure (unlike those with some kinds of CH due to genetic mutations in the fetus, which can be treated after birth with prompt administration of T_4); and 2) pregnant women were screened for TSH, but not T_4. Although TSH levels are extremely effective in identifying CH due to subclinical maternal hypothyroidism, they are not optimal for detecting ID, as discussed above (92).

V. NIS, the Mediator of Active I^- Uptake in the Thyroid and Beyond

A. Molecular identification of NIS

The rat NIS (rNIS) cDNA was cloned in our laboratory by functional expression in *Xenopus laevis* oocytes from a highly functional rat thyroid cell line (FRTL-5 cells) (5). Our group has since extensively characterized the protein (5, 24, 112–118) and generated high-affinity site-directed antibodies (113). NIS relies on the Na^+ electrochemical gradient, maintained by the Na^+/K^+ ATPase, to drive the transport of the second anion substrate (for example I^-) into the cell. By coupling the inward transport of Na^+ down its electrochemical gradient to the translocation of I^- against its electrochemical gradient across the basolateral plasma membrane, NIS avidly concentrates I^- in the thyroid 30- to 60-fold inside thyroid cells (119–121) (Figure 1). The K_m of NIS for I^- transport is 10μM to 30μM, and its K_m for $Na^+$is 40mM to 60mM (122). The experimentally tested secondary structure model of NIS depicts a hydrophobic protein of 618 amino acids with 13 transmembrane segments (TMSs), an extracellularly facing amino terminus, and an intracellular carboxy terminus (114) (Figure 2). NIS is a phosphoprotein, and most phosphorylation occurs on its carboxy terminus. The carboxy terminus is also important for NIS trafficking and its localization at the basolateral plasma membrane (123). NIS is a highly glycosylated protein (114), with 3 N-linked glycosylation sites (1 in the loop between TMS VI and VII and 2 in the loop between TMS XII and XIII) (Figure 2); however, glycosylation is not essential for function, as demonstrated by the high activity and the same K_m for I^- displayed by an NIS mutant protein in which all 3 glycosylated Asn were replaced with Gln (114).

Given the highly significant roles that NIS plays in physiology and medicine, it is imperative that we uncover the protein's substrate translocation pathways. There is novel evidence, derived from the detailed characterization of positions where NIS mutations have been found in patients and from structural homology modeling (see *Section VI*), that TMS III, VII, and IX are key for substrate coordination, coupling, stoichiometry, and translocation (Figure 2).

Using primers derived from the rNIS sequence, the human NIS (hNIS) cDNA was cloned by Jhiang's group (124). hNIS shares 84% amino acid identity and 93% similarity to rNIS. The major differences between the 2 proteins are a 5–amino-acid insertion between the last 2 TMSs and a 2–amino-acid insertion at the carboxy terminus (amino acids 618–637) of hNIS. The hNIS gene is located on chromosome 19p12–13.2 and encodes an integral membrane glycoprotein of 643 amino acids. NIS belongs to solute carrier family 5 (gene name *SLC5A5*); other Na^+-dependent transporters, which share high sequence homology with NIS, belong to the same family, including the Na^+/glucose transporters (SGLT-1 and 2), the Na^+/monocarboxylate transporters (SMCT-1 and -2), the Na^+/multivitamin transporter (SMVT), and the Na^+/myoinositol transporter (SMIT) (125).

B. NIS substrates

1. Anions

In addition to its well-known I^- transport activity, NIS mediates the translocation of other anions (112), according to the following order of maximal transport rates: $I^- \geq$ selenium cyanate ($SeCN^-$) > thiocyanate (SCN^-) > $ClO_3^- > NO_3^-$. The anions Br^-, BF_4^-, IO_4^-, and BrO_3^- are also transported, but to a lesser extent. The geometry of transported substrates varies greatly; whereas I^- is nearly spherical, $SeCN^-$ and SCN^- are nearly linear, ClO_3^- is trigonal pyramidal, and NO_3^- is planar. The NIS K_m for SCN^-, derived from I^- transport inhibition experiments and 2-electrode voltage-clamp studies in *X. laevis* oocytes, is ~30μM to 100μM, with a maximal transport rate of ~80% of that of I^- (112, 126). Pertechnetate (TcO_4^-), which exists only as the metastable nuclear isomer $^{99m}TcO_4^-$, is also a NIS substrate. ^{99m}Tc is widely used in nuclear medicine, because its decay emission energy (140-keV γ-rays) and its short (6 hours) half-life make it extremely useful for imaging and diagnostic procedures.

Two other compounds, perrhenate (ReO_4^-), which is available as $^{188}ReO_4^-$ and has a potentially attractive clinical use in the treatment of tumors expressing NIS endogenously or via gene transfer (*Section IX.E.*), and ClO_4^-, a competitive NIS inhibitor and environmental pollutant, are also NIS substrates (126–129) and will be discussed in more detail below (*Section V.C.*).

2. Cations

The Na^+ specificity of Na^+-dependent transporters is not absolute. In some instances, transport can be driven by cations other than Na^+. For example, H^+ can substitute

Downloaded from https://academic.oup.com/edrv/article/35/1/106/2354709 by guest on 09 April 2024

for Na^+ in SGLT-1 (130) and the serotonin transporter (SERT) (131). SGLT-1 can also use Li^+ as the driving cation. NIS-mediated I^- transport, however, cannot be driven by H^+, and only 10% to 20% of transport activity is observed in the presence of Li^+ (112, 132).

As discussed below, De la Vieja et al (133) have experimentally inferred the location of a Na^+ binding site in NIS. With the recent surge in membrane protein crystal structures, it has now been shown that this site is conserved not only in other Na^+-dependent transporters, such as LeuT (134), the *Vibrio parahaemolyticus* SGLT (vSGLT) (135), and Mhp1 (136), but also in Na^+-independent transporters, where, astoundingly, an amino acid side chain provides the positive charge provided by Na^+ in Na^+-dependent transporters (137–139).

C. New developments concerning NIS stoichiometry: NIS transports I^- electrogenically but ClO_4^- and ReO_4^- electroneutrally

Flux and electrophysiological data have established that NIS-mediated I^- transport is electrogenic, with a 2:1 Na^+ to I^- stoichiometry. NIS-expressing oocytes were held at a membrane potential of −90 mV and perfused with a Na^+- and I^--containing solution, and the evoked positively charged inward current was recorded. Measurements of $^{22}Na^+$ and $^{125}I^-$ transport were made in the same oocyte, revealing a stoichiometry of 2:1 (112). NIS transports most of its substrates, including $SeCN^-$, SCN^-, ClO_3^-, and NO_3^- in an electrogenic fashion. In the initial electrophysiological characterization of NIS transport, our laboratory and others observed that another anion, ClO_4^-, a well-known goitrogenic drug used in the past to treat hyperthyroidism (140, 141) and still in use in Europe in recalcitrant cases (142–144) that, as mentioned above, inhibits I^- transport in a competitive manner, did not elicit currents in *X. laevis* oocytes or Chinese hamster ovary cells (145), but acted as a potent blocker (K_i ~2μM) of I^- transport (112). Indeed, ClO_4^- inhibition is one of the clearest hallmarks of NIS-mediated I^- transport, both in the thyroid and other tissues. It was concluded that ClO_4^- was a strong, nontransported competitive NIS inhibitor. ReO_4^-, an anion with a tetragonal geometry similar to that of ClO_4^-, had been reported to be transported in thyroid cells and NIS-transfected cells (126–128), but in an electrophysiology setting acted as a potent NIS inhibitor (K_i ~3μM) eliciting only minimal currents (112). Another possible explanation for the absence of ClO_4^-- and ReO_4^--induced currents was that these 2 anions were transported at minimal rates that could not be detected by 2-electrode voltage clamp, given that the currents generated were relatively small and limited by the slow turnover rates of cotransporters (37 charges/s for NIS at −50 mV), compared with channels that translocate ions at 10^6 to 10^9 charges/s. In summary, mechanistically, it was uncertain whether ClO_4^- was an NIS blocker or a transported NIS substrate (112, 126, 145–148). Most significantly, as the notion that a transporter would translocate different substrates with different stoichiometries was unprecedented, it was not considered likely that NIS would mediate Na^+/ClO_4^- and Na^+/ReO_4^- symport electroneutrally with a 1:1 stoichiometry. However, in a surprising turn of events, this was precisely what Dohán et al (129) ultimately showed.

To establish whether NIS actually transports ClO_4^- at all and, if so, whether the Na^+/ClO_4^- stoichiometry was electroneutral, Dohán et al (129) had to overcome the impossibility of carrying out direct determinations of ClO_4^- flux experiments given the unavailability of radiolabeled ClO_4^-. Thus, instead, Dohán et al (129) used a bioassay in a bicameral setup (Figure 6A) in which they unequivocally demonstrated NIS-mediated active vectorial ClO_4^- transport in polarized NIS-expressing cells (129). When ClO_4^- alone was added to the apical chamber of polarized Madin-Darby canine kidney (MDCK) cells stably transfected with a NIS construct lacking the last 43 amino acids, which displays the same kinetic properties as wild-type (WT) NIS, and is exclusively expressed apically, ClO_4^- was transported via NIS into the cells; from there, without being metabolized, the anion continued through diffusion to the basolateral chamber, most likely via Cl^- channels. Aliquots from the basolateral chamber inhibited I^- transport in NIS-expressing cells, indicating that the aliquots contained ClO_4^- at concentrations that demonstrated active translocation against the ClO_4^- concentration gradient (Figure 6A).

Because Na^+-dependent ClO_4^- transport is not electrogenic, its kinetic analysis would have to be carried out by direct substrate flux measurements. However, as noted above, such measurements are precluded by the unavailability of $^{36}ClO_4^-$. Thus, the kinetic parameters of NIS-mediated transport of a structurally similar anion, ReO_4^-, were analyzed, taking advantage of the availability of $^{186}ReO_4^-$. The initial rates of NIS-mediated, Na^+-dependent ReO_4^- transport yielded a hyperbolic curve indicative of an electroneutral stoichiometry, strongly suggesting that, most probably, NIS-mediated Na^+/ClO_4^- transport was also electroneutral. This was in stark contrast to the electrogenic 2:1 Na^+/anion stoichiometry observed with most other NIS substrate anions (112). This finding demonstrated that NIS translocates different substrates with different stoichiometries, an unprecedented property for any transporter. Furthermore, a mini systems biology model based on I^- transport data in NIS-transfected polarized MDCK cells in vitro was generated that accurately

Downloaded from https://academic.oup.com/edrv/article/35/1/106/2354709 by guest on 09 April 2024

Figure 6.

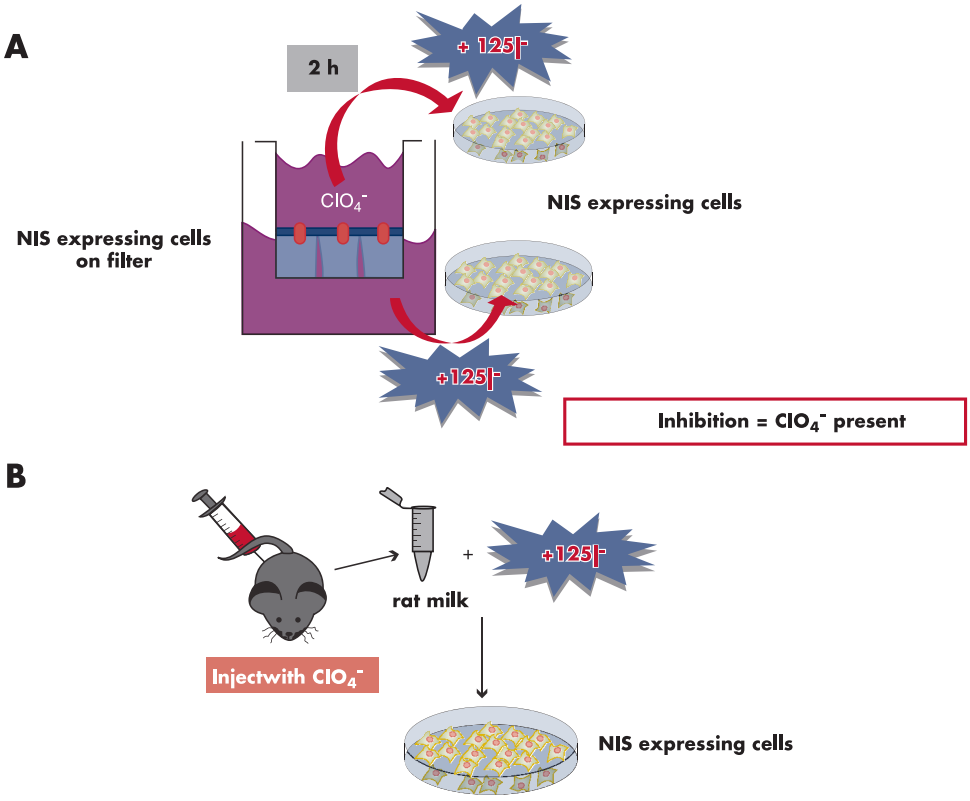

Figure 6. In vitro and in vivo bioassays reveal that perchlorate is a NIS substrate actively transported against its concentration gradient. A, A polarized monolayer of MDCK cells stably transfected with a NIS mutant that is targeted exclusively to the apical surface was exposed to ClO_4^- to allow for vectorial transepithelial transport. After a 2-hour incubation, an aliquot was taken from each compartment to assess its effect on $^{125}I^-$ transport in NIS-expressing cells grown on a plastic dish. The degree of I^- transport inhibition in cells reflects the amount of ClO_4^- present in the aliquot, and can be quantified by serial dilutions and by measuring the inhibition by ClO_4^- of I^- transport in kinetic experiments (129). B, ClO_4^- is actively concentrated in maternal milk. To assess whether NIS transports ClO_4^- into maternal milk in vivo, lactating dams were injected ip with ClO_4^- or saline solution. Pups were separated from their mothers, and lactation was stimulated with oxytocin. Milk collected from the dams was diluted to investigate its effect on $^{125}I^-$ transport in NIS-expressing cells grown on a plastic dish. The degree of inhibition of I^- transport is directly correlated to the amount of ClO_4^- present in the sample, and ClO_4^- concentration can be quantified by serial dilutions and inhibition kinetics. Based on the distribution volume of ClO_4^- and its IC_{50}, it was determined that ClO_4^- is actively concentrated in maternal milk (129).

predicts the degree of competition between ClO_4^- and I^- and the effect of ClO_4^- transport on the rate and extent of I^- accumulation, leading the authors to infer that the maximal velocity (V_{max}) of NIS for ClO_4^- is 3 times lower than that for I^- (129).

Additional studies by 2 other groups support these results. One group used a halide-sensitive yellow fluorescent protein (149), and the other relied on ion chromatography coupled to tandem mass spectrometry (150–152), a technique these authors themselves (ie, Blount and colleagues) optimized to detect ClO_4^- in more complex matrices; both groups showed ClO_4^- accumulation in FRTL-5 cells (149, 153).

Dohán et al (129) also demonstrated that ClO_4^- is actively translocated by NIS in epithelial mammary cells in vivo, resulting in ClO_4^- accumulation in the milk. In that study, they showed that milk samples from ClO_4^--treated rats inhibited I^- uptake in cells stably expressing exogenous NIS (Figure 6B). That NIS actively concentrates ClO_4^- in the milk suggests that exposure to high levels of ClO_4^- may pose a greater environmental health risk than previously acknowledged. Aside from the effects of ClO_4^- on the health of adult women, if a nursing mother is exposed to high levels of ClO_4^-, the anion will not only inhibit I^- accumulation in the milk, which is critical for TH biosynthesis by the newborn, but also will itself be actively concentrated in the milk and thus directly inhibit the newborn's thyroidal I^- uptake. This effect would have potentially serious consequences for the child's mental and physical development.

VI. Recent Advances in Structure/Function of NIS

Major strides in the elucidation of structure/function attributes of NIS have been made in recent years. A par-

Downloaded from https://academic.oup.com/edrv/article/35/1/106/2354709 by guest on 09 April 2024

Figure 7.

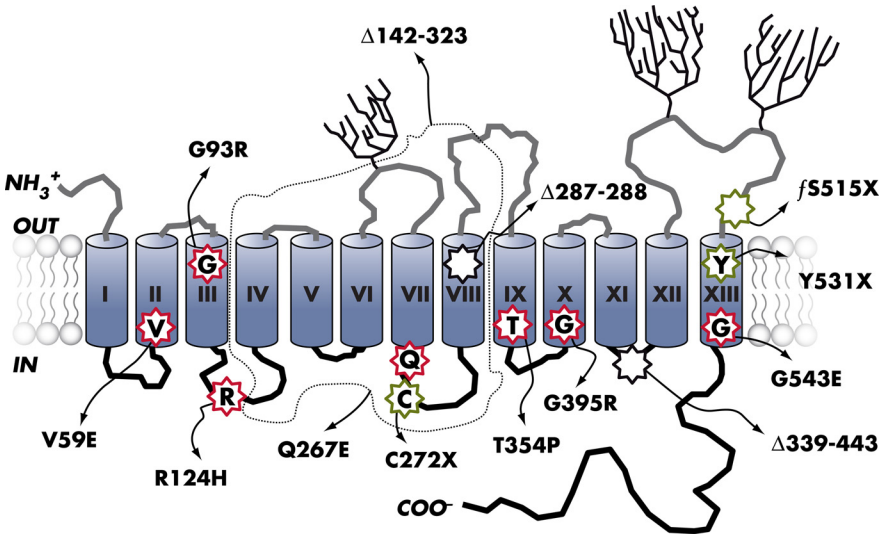

Figure 7. Experimentally tested NIS secondary structure model. Gray cylinders represent TMS; gray lines, extracellular segments; black lines, intracellular segments; and branches, N-linked glycosylation sites (N225, 485, and 497). NIS mutations identified in patients with ITD are indicated using the single-letter amino acid code. Those for which the letters are outlined in red (V59E, R124H, Q276E, T354P, G395R, G543E, and Δ339–443) have been studied at the molecular level, as has the effect of different amino acid substitutions at these positions. Δ indicates deletions, and X terminations.

ticularly rich source for this information has been the investigation of amino acid positions that have been found mutated in patients with CH due to an I^- transport defect (ITD). Another key source of structure/function data has been the determination of the crystal structures of prokaryotic homologs of eukaryotic Na^+-driven transporters as well as homology models based on those structures.

A. CH-causing NIS mutations have been a rich source of structure/function information on NIS

As mentioned earlier, CH results in goiter and impaired physical and mental development when not recognized immediately after birth and left untreated. In CH due to fetal somatic mutations, maternal THs are transferred to the fetus via the placenta, allowing for proper fetal development. The newborn's TH insufficiency manifests itself after birth, when maternal T_4 transfer is interrupted and the newborn's CNS development relies entirely on its own TH biosynthesis. CH occurs in 1 in 2000–4000 live births, and is diagnosed with routine newborn thyroid screening tests (73, 154), which have been implemented for over 2 decades in most developed countries.

Thyroid gland developmental failure (thyroid dysgenesis) is caused by mutations in transcription factors, such as thyroid transcription factor-1, Pax-8, and NK2 homeobox 5 (NKX2.5) (encoded by the *NKX2–1*, *PAX8*, and *NKX2–5* genes, respectively) (155–159). Mutations in any of the genes involved in the TH biosynthesis machinery, in regulating hormonal control of THs synthesis, or in I^- recycling cause CH. Specifically, gene defects disrupting the hypothalamic/pituitary axis cause so-called secondary hypothyroidism. Mutations in the genes encoding for proteins in the TH biosynthetic pathway (Tg, TPO, Duox2, Dehal1, TSH receptor, and NIS) lead to dyshormonogenesis (28, 50, 57, 160–162).

CH resulting from mutations in *SLCA5A*, the gene encoding NIS, is specifically referred to as ITD, because it is a direct result of a nonfunctional NIS molecule and therefore an inability of the thyroid to concentrate I^-. ITD follows an autosomal recessive inheritance pattern and is diagnosed by reduced or absent thyroid I^- uptake and a low saliva-to-plasma I^- ratio (>20 in nonaffected subjects). When untreated, ITD is clinically characterized by hypothyroidism, goiter and mental impairment of varying degrees. Although ITD is a rare autosomal recessive disorder, to date, 13 such mutations have been reported in the NIS coding region (V59E [163], G93R [164], R124H [165], Δ143–323, Q267E [166], C272X, Δ287–288 [167], T354P [133], Δ439–443 [168], G395R [164], G543E [169], 515X, and Y531X) (Figure 7) and 1 in the 5′-untranslated region (−54 C→T transition) (170). In the absence of a crystal structure for NIS, valuable structure/function data on NIS have been obtained from the study of patients who bear mutations in the NIS gene. Molecular characterization of the mutations indicated in Table 1 has provided novel information on the molecular requirements for NIS function at specific amino acid po-

Table 1. Functional NIS Expression

Tissue	Subcellular Localization	Regulation
Thyroid	Basolateral	TSH, I^-, KCNQ1/KCNE2 K^+ channel
Salivary gland	Basolateral	Constitutive
Stomach	Basolateral	Constitutive
Small intestine	Apical	I^-
Lactating mammary gland	Basolateral	β-Estradiol, oxytocin, prolactin

Downloaded from https://academic.oup.com/edrv/article/35/1/106/2354709 by guest on 09 April 2024

Table 2. Molecular Characterization of NIS Mutations Found in ITD Patients

Mutation in Patient	Defect	Location in NIS	Uncovered Information From Studying the Effect of Amino Acid Substitutions at the Indicated Position	
			Side-Chain Requirement	Changes in Kinetic Parameters and/or Stoichiometry
V59E	Nonfunctional protein	TMS I	Neutral, branching at β -carbon	V_{max}
G93R	Nonfunctional protein	TMS III		Anion and Na^+ K_{ms}, stoichiometry substrate selectivity
R124H	Immature; intracellularly retained	Intracellular helix between TMS III and IV	ϵ-NH for H-bonding (R or Q) Located in a region that allows relative movements of TMSs III and IV	
Q267E	Modestly active	Loop between TMS VII and VIII	Neutral or E	V_{max}
T354P	Nonfunctional protein	TMS IX	OH^- at β-carbon Na2 coordination and transport	Na^+ K_m
G395R	Nonfunctional protein	TMS X	Uncharged residue with small side chain	V_{max}
G543E	Immature; intracellularly retained	TMS XIII	Small neutral amino acid	V_{max}
Δ439–443	Intracellularly retained	Intracellular loop between TMS XI and XII	Helix-capping at position 441	V_{max} and K_m

sitions and in neighboring regions. Mutations in many membrane proteins (eg, CFTR Δ508 [171], aquaporin mutations associated with nephrogenic diabetes insipidus [172], and SGLT mutations associated with glucose malabsorption [173]) result in intracellular retention of these proteins. Mutations in NIS, however, do not impair NIS expression at the plasma membrane, for the most part (Table 2).

B. Identification of transmembrane segment IX amino acids key for Na^+ binding and/or translocation

Notably, analysis of the T354P substitution, the first NIS mutant reported (174), revealed that position 354 requires an OH group at the β-carbon (175) and led De la Vieja et al (133) to study other β-OH–containing residues in TMS IX. After substituting all the Ser and Thr in TMS IX, it was determined that 5 of these (S351, S353, T354, S356, and T357) are important for NIS function. When Ala, Cys, or Pro was substituted at these positions, activity was decreased or absent. I^- transport requires an amino acid bearing a β-OH group at these positions. Furthermore, a reduced apparent affinity for Na^+ was noted when the Na^+ dependence of I^- transport was examined, indicating that these amino acids are involved in Na^+ binding/translocation.

In 2005, the structure of LeuT, a bacterial homolog of neurotransmitter transporters, was determined at atomic resolution (134). The LeuT structure was a milestone that greatly advanced the understanding of the structural basis for how eukaryotic Na^+-driven symporters belonging to different families work. Although NIS and LeuT belong to different families and bear no sequence similarity, De la Vieja et al (133) proposed the possible existence of structural homology between the two, based on evidence emerged from the study of an ITD-causing mutation identifying S353 and T354 in NIS TMS IX as critical for Na^+ translocation. These NIS residues correspond to those in TMS VIII of LeuT (T354 and S355) shown to coordinate Na2 (133, 134). Our prediction was confirmed a year later, when the structure of vSGLT, the Na^+/galactose transporter from *V. parahaemolyticus*, revealed the same fold as LeuT (135), even though there is very little sequence homology (<17%) between the 2 proteins. The relevance of the structure of vSGLT for NIS becomes readily apparent when one considers that the 32% identity and 60% similarity of the prokaryotic vSGLT to its own eukaryotic analog SGLT-1 are extremely close to the 27% identity and 57% similarity that exist between vSGLT and NIS, which after all belongs to the same SLC5 family as SGLT1 (135, 176, 177). These considerations provided the basis for us to generate a homology model of NIS (Figure 8) based on the structure of vSGLT (71).

C. A crucial structure/function insight from the analysis of NIS mutants: seemingly unrelated transporters may exhibit a common fold and other shared characteristics

That proteins with unrelated sequences have a common structural fold is clear (177). Within the last few years, 4 structures of bacterial Na^+-driven transporters sharing the same fold have been determined at atomic resolution by x-ray crystallography: LeuT; vSGLT (135), a homolog of the eukaryotic SGLT-1; the benzyl-hydantoin transporter (Mhp1) from *Mycobacterium liquefaciens* (136), a member of the nucleobase cation symport-1 (NCS1) family of transporters; and the Na^+/betaine symporter (BetP) from *Corynebacterium glutamicum*, a member of the betaine/choline/carnitine transporter (BCCT) family (178). Since then, numerous structures of other Na^+-driven and H^+-driven transporters and even antiporters, with no homology to LeuT but exhibiting the LeuT fold have been reported (SGLT [135], Mhp1 [136], BetP [178], ApcT [139], AdiC [137, 138], and CaiT antiporter [179]). The conservation of the structural fold suggests the existence of an evolutionary relationship between them.

Downloaded from https://academic.oup.com/edrv/article/35/1/106/2354709 by guest on 09 April 2024

Figure 8.

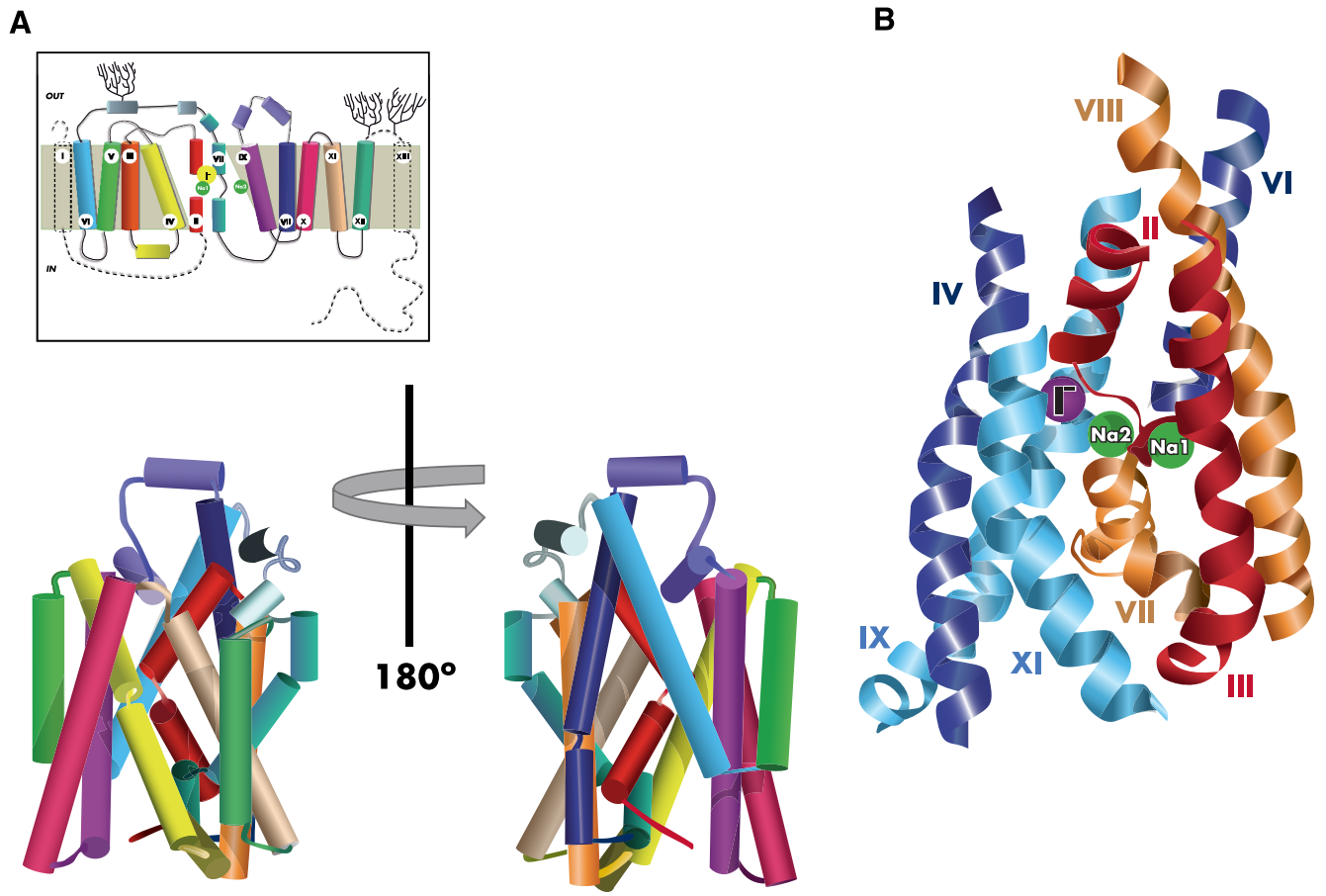

Figure 8. NIS homology model. A, An NIS 3-dimensional homology model was generated by sequence and structural alignment with vSGLT (27% identity and 57% similarity). The homology model was built on manually corrected sequence alignment. The resulting model was then manually adjusted to improve side-chain interactions and energy minimized. The color code used for the TMSs is the same one used for the secondary structure model (inset, and Figure 2). Helices are represented by cylinders. The model is oriented with the extracellular and intracellular milieux on the top and bottom, respectively. The amino and carboxy termini, along with TMSs I and XIII, are not present in the reference 3-dimensional structures and therefore cannot be modeled. B, Helical model depicting the bundle (TMSs II–III from repeat 1 in red, and VII–VIII from repeat 2 in orange), and the scaffold (TMSs III–V from repeat 1 in blue, and VIII–X from repeat 2 in cyan). The remaining helices and loops are omitted for clarity. The 2 Na^+ and the I^- are shown at positions inferred from experimental data and molecular dynamics calculations.

Remarkably, although all 4 structures (LeuT, vSGLT, Mhp1, and BetP) belong to different gene families and lack sequence homology, they share common structural features: inverted topology repeats, unwound helices in regions critical for substrate binding, and a similar way of coordinating Na^+ (134–136, 178). In all cases, 10 helical TMSs containing an internal inverted topology repeat of 5 TM helical bundles are present; the first bundle (TMSs I–V) is related to the second one (TMSs VI–X) by a 2-fold pseudosymmetry axis running parallel to the membrane plane through the center. The high degree of structural homology between these internal repeats (root mean square deviation 3.8–4.5 Å) allows superimpositition of these structures onto one another (176). The helical bundles are arranged in such a way that TMS I, II, III, VI, VII, VIII, and X face the central pore where the substrates reside (176).

Given the diversity of substrates for these transporters, it is not unexpected that the specific interactions required to coordinate each substrate are unique. However, despite the variability of the specific interactions, the inverted repeat topology provides a general scaffold capable of accommodating a wide range of substrates. For instance, the substrate leucine in LeuT is coordinated directly by carbonyl groups of the main-chain atoms (TMSs I and VI). In vSGLT, the OH groups of galactose are coordinated by H-bonds from polar side chains from TMSs I, VI, VII, and X (135). In Mhp1, benzyl-hydantoin resides between 2 tryptophan residues provided by TMSs III and VI and is coordinated by glutamine and asparagines from TMSs I

Downloaded from https://academic.oup.com/edrv/article/35/1/106/2354709 by guest on 09 April 2024

and VIII (136). The betaine in BetP is confined between 3 tryptophans and a tyrosine from TMSs II and VI (178).

For Na^+-driven transporters, the Na^+ to substrate stoichiometry varies. For example, LeuT and BetP transport 2 Na^+ to 1 substrate, whereas vSGLT and Mhp transport 1 Na^+ to 1 substrate. LeuT was the only structure where the Na^+ sites (Na1 and Na2) could be unequivocally identified, owing to the high resolution at which it was determined (1.65 Å). Na1 is coordinated directly by the carboxylate oxygen of the substrate, whereas Na2 is located at the intersection of TMSs I and VIII and is coordinated by the main-chain carbonyl oxygens from the unwound portion of TMS I and the OH^- groups from Ser and Thr from TMS VIII as described above. The Na2 site is conserved in all 4 structures and is located ~8 Å from the substrate binding site.

D. Position 93 is critical for NIS substrate specificity and stoichiometry

The NIS homology model generated using the x-ray structure of vSGLT (20) as a template has provided vital information on the mechanism of NIS, as was clearly shown in connection to the analysis of position 93 (71). The study of the G93R NIS mutant started with the identification of a patient who developed goitrous hypothyroidism due to ITD (180). The patient actually had a compound heterozygous G93R/T354P NIS mutation, having inherited the G93R substitution from his mother and the T354P from his father (181). Paroder-Belenitsky et al (71) undertook a detailed study of the role of position 93 in NIS by carrying out various amino acid substitutions at this position and assessing the effect of the substitutions on the activity and behavior of the protein. They determined that G93R NIS was targeted to the plasma membrane but was inactive and showed that the cause of the lack of activity was not the presence of the positively charged Arg residue, as G93K NIS was not only functional but also accumulated I^- at values comparable to those of WT NIS. They reported that the longer the side chains of substituted neutral residues at this position, the higher the protein's K_m values for I^-. G93N and G93T NIS exhibited >18-fold higher K_m values for I^- than WT NIS, and G93Q NIS had an astonishingly >200-fold higher K_m for I^- (6.1 mM). This was the first time that any NIS mutant had displayed such high K_m values for I^-, after the analysis of dozens of NIS mutants over several years.

Paroder-Belenitsky et al (71) then proceeded to study how their mutants would transport NIS anion substrates other than I^-. They found that the levels of ReO_4^- accumulation by G93T NIS were considerably higher than those of WT NIS, a finding that, in turn, prompted a look into whether the presence of Thr at position 93 had caused a change in the protein's Na^+/ReO_4^- transport stoichiometry as compared with WT NIS. Remarkably, they discovered that it had. As mentioned in *Section V.C.*, WT NIS mediates Na^+/I^- symport with an electrogenic 2:1 stoichiometry and Na^+/ReO_4^- and ClO_4^- symport with an electroneutral 1:1 stoichiometry. In contrast, G93T NIS-mediated Na^+/ReO_4^- symport was electrogenic with a 2:1 stoichiometry, as evidenced by a characteristic sigmoidal Na^+-dependence curve, with a Hill coefficient of 2. This observation led to the extraordinary conclusion that the engineering of a single amino acid substitution, Thr instead of Gly at position 93, converted the electroneutral transport of ReO_4^- by WT NIS (1 Na^+ to 1 ReO_4^- symport) to electrogenic (2 Na^+ to 1 ReO_4^-) by G93T NIS. Consistent with this notion was the observation that ReO_4^- elicited inward currents in *X. laevis* oocytes expressing G93T NIS, in contrast to the absence of currents when WT NIS was expressed. Moreover, the environmental pollutant ClO_4^-, which is structurally similar to ReO_4^-, also elicited currents in oocytes expressing G93T or G93N NIS but, as previously reported, not in those expressing WT NIS (112), a finding consistent with the notion that ClO_4^- is actively translocated by G93T/N NIS and that the process is electrogenic (Table 3). In addition to G93T and -N, G93D, -E, and -Q also transport ReO_4^- and ClO_4^- electrogenically (Figure 9). Finally, whereas G93E and G93Q NIS also transported ReO_4^- and ClO_4^-, their ability to transport I^- was severely impaired, strongly suggesting that each of these 2 amino acids at this position confers to the molecule the ability to discriminate between anion substrates (Table 3). In conclusion, position 93 appears to be a key Na^+/anion coupling link (129) that controls both transport stoichiometry and anion substrate specificity.

Table 3. Substrate Specificity and Stoichiometry

NIS Molecule	Substrate	Stoichiometry	Currents
WT	I^-	2 Na^+ to 1 I^-	Yes
WT	ClO_4^-	1 Na^+ to 1 ClO_4^-	No
WT	ReO_4^-	1 Na^+ to 1 ReO_4^-	No
G93T/N/D	I^-	2 Na^+ to 1 I^-	Yes
G93T/N/D	ClO_4^-	2 Na^+ to 1 ClO_4^-	Yes
G93T/N/D	ReO_4^-	2 Na^+ to 1 ReO_4^-	Yes
G93E/Q	I^- (no transport)	2 Na^+ to 1 I^-	No
G93E/Q	ClO_4^-	2 Na^+ to 1 ClO_4^-	Yes
G93E/Q	ReO_4^-	2 Na^+ to 1 ReO_4^-	Yes

As briefly stated above, a 3-dimensional homology model of NIS was built using as a template the available x-ray structure of vSGLT (135). In the NIS homology model, TMSs III and X are at the edge of the molecule, in

Downloaded from https://academic.oup.com/edrv/article/35/1/106/2354709 by guest on 09 April 2024

Figure 9.

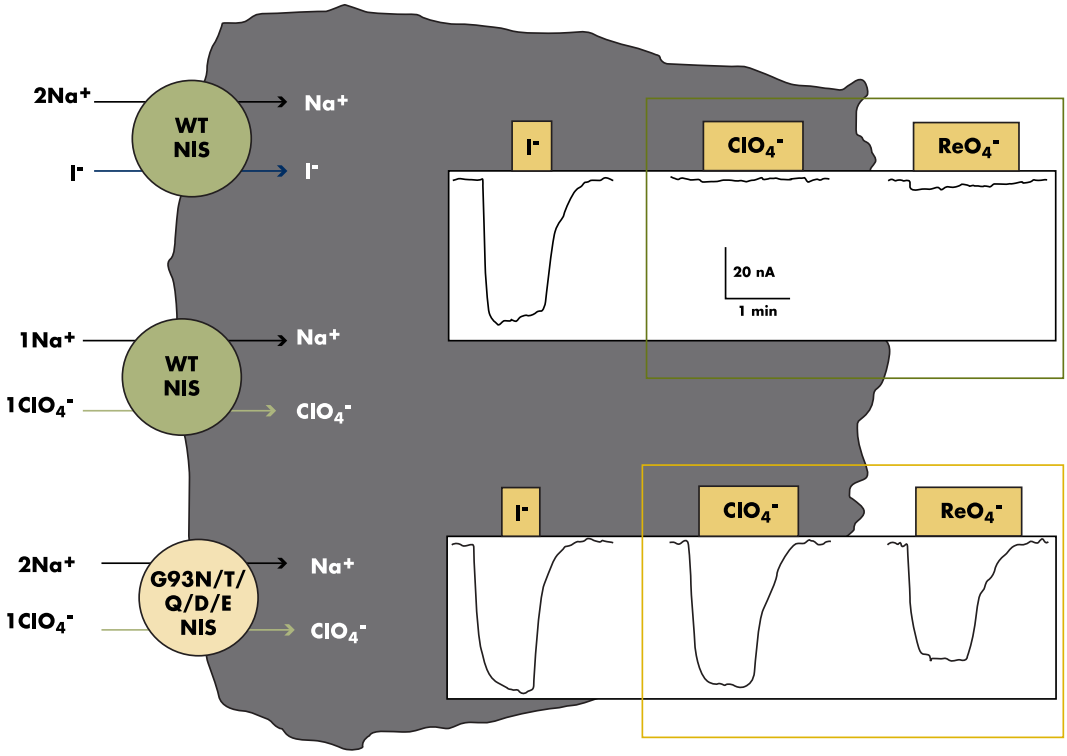

Figure 9. A single amino acid substitution converts NIS-mediated ClO_4^- and ReO_4^- transport from electroneutral to electrogenic. The stoichiometry of WT NIS is 2 Na^+ per I^-. Thus, I^- transport is electrogenic, as 1 net positive charge is translocated, and it elicits inward positive currents in 2-electrode voltage-clamp experiments in *X. laevis* oocytes (upper left current trace). In contrast, ClO_4^- and ReO_4^- do not elicit any current (traces in green box). However, the experiments described in Figure 6 showed that ClO_4^- and ReO_4^- are transported by NIS, with a V_{max} that is only approximately one-third that of I^-, which would have produced currents of recordable magnitude. Therefore, it is concluded that ClO_4^- (and ReO_4^-) transport occurs with a different stoichiometry (1 Na^+ to 1 ClO_4^-/ReO_4^-) than that of I^- transport and that it is electroneutral. Interestingly, it is possible to modify the Na^+/anion transport stoichiometry by replacing a single amino acid in TMS III (Figures 2 and 7); G93N/T/D/Q/E NIS, for example, transports ClO_4^- and ReO_4^- in an electrogenic fashion (yellow rectangle).

contact with the membrane. They define the outer wall of a cavity that in vSGLT contains the galactose substrate (135). The same cavity is present in the NIS homology model. TM VII crosses TMS III at an angle in such a way that G93 and W255 are in close contact, with the Cα of Gly abutting the indole ring of W255. Consistent with the notion that W255 plays an important role during the transport cycle, W255A NIS was inactive even at high concentrations of I^-, whereas W255Y NIS did accumulate I^-, although to a lesser extent than WT NIS. Expression levels and plasma membrane targeting were not responsible for the lack of activity of W255A NIS, as it was equally expressed and properly targeted to the cell surface, as assessed by immunoblot and flow cytometry under nonpermeabilized conditions. The lack of activity was also shown with other substrates, as W255A did not transport ReO_4^- either, even at very high concentrations.

The NIS homology model offers a rationale for the above-described effects of amino acid substitutions at position 93 on NIS activity, substrate specificity, and stoichiometry. The change from the inwardly to the outwardly facing conformations of the protein is best described as a 25° to 30° rotation of the TMS II-III helical hairpin, which, strikingly, pivots around the contact between G93 and the indole ring of W255 (71). Residues 118 to 132, which connect to the helical hairpins, provide a key structural element that permits the rotation of the 2 hairpins with small variations in their respective structures. As the conformational transition changes the distance between the end of TMS III and the beginning of TMS IV, the connecting residues must accommodate this change. Residues 118 to 132 are ideally suited for this task. This region consists of a short helix flanked by 2 short unstructured stretches. The change in distance between the ends of the 2 hairpins is easily accommodated by a rotation of the short helix with small changes in the connecting pieces acting as hinges. The large displacement of the C terminus of TMS III pushes, via the connecting rod, the short helix, resulting in a large displacement of its N-terminal portion, whereas its C terminus acts as a hinge for the rotation of

Downloaded from https://academic.oup.com/edrv/article/35/1/106/2354709 by guest on 09 April 2024

the helix and does not move significantly, allowing TMSs IV and V to remain close to their original positions. TMS VII, in the second half of NIS, which encompasses W255 (the residue against which G93 rests), runs at an angle with respect to TMS IV. As the rotation takes place, TMS VII has to move away as part of the overall conformational change (71). These proposed conformational changes are compatible with previously proposed models (177, 182–184).

Thus, the nature of the side chain at position 93 of NIS may control the extent as well as the final state of the transition between the outwardly and the inwardly open conformations and play a role in the kinetic parameters as well as the stoichiometry of the protein. It is worth pointing out that the significance of position 93 would have remained unknown had it not been for the naturally occurring mutation found in the ITD patient. These findings may have implications for other proteins, as positions equivalent to G93 of NIS in other transporters may have a similar function (71). The discovery that by manipulating position 93, NIS molecules may be engineered to selectively transport some anion substrates and not others may be applicable to NIS-based gene transfer efforts, in which an optimally tailored molecule cold be used in cancer treatment (see *Section IX.E.*).

E. The study of the ITD-causing NIS mutation Δ439–443 provided novel information on helix capping

The study of the ITD-causing NIS mutation Δ439–443 (deletion of amino acids ACNTP) has also shed light on properties of specific amino acid residues. This mutation, first described in an Italian patient with CH, is putatively located in the intracellular loop between TMSs XI and XII (Figure 7) (185). Δ439–443 NIS is retained intracellularly. Engineering 5 Ala at these positions markedly improves membrane targeting and even restores some of its activity. Remarkably, although the recognition of the Δ439–443 mutant by an anti-NIS antibody, directed against a conformational epitope on the last third of the protein, is compromised, reactivity is restored upon introduction of the 5-Ala stretch. This strongly suggests that the Δ439–443 significantly alters NIS tertiary structure. Using the NIS homology model, Li et al (168) determined that the length of the sixth intracellular loop between TMSs XI and XII is ~12 Å, and proposed that the amide hydrogen in the main chain at the beginning of TMS XII is capped by the side chain of N441 (one of the residues missing in this deletion). For the Δ439–443 mutant, this distance is significantly shorter. Bringing the carboxy terminus of TMS XI and the amino terminus of TMS X together requires large changes in the orientation of the 2 helices and the entire protein. These changes produce a NIS molecule that is neither targeted to the plasma membrane nor functional. The 5-Ala mutant may form a helix that increases the distance to 5 to 7 Å, minimally rescuing targeting. Interestingly, in the background of the 5-Ala mutant, both N441 and Q441 yield proteins that behave like WT NIS, completely restoring membrane targeting and activity, suggesting that TMS XII in these mutants is capped. Moving the N just 1 residue over, N440, does not restore WT properties (168). N441 is extremely conserved in the SLC5 family, and its function is likely to be as well.

VII. Functional Expression of NIS in Extrathyroidal Tissues

Extrathyroidal accumulation of I^- has been reported in the salivary glands, gastric mucosa, small intestine, lactating mammary gland, choroid plexus, and the ciliary body of the eye (127, 186). However, in contrast to the thyroid, I^- is not organified and I^- uptake is not regulated by TSH in these tissues (Table 2). Albeit NIS mRNA has been detected in various other tissues, such as colon (187), ovaries (188), uterus (189), and spleen (188) by RT-PCR, functional NIS expression or subcellular localization in these tissues has not been established. Thus, the role and importance of NIS in these tissues is unclear (24, 122, 190, 191). We will focus on tissues where NIS expression has been functionally characterized.

A. Salivary glands

The ability of the salivary glands to concentrate I^- is an important diagnostic tool for the detection of thyroid disorders in newborns through the saliva to plasma I^- ratio. NIS protein expression has been unequivocally shown at the basolateral surface of ductal epithelial cells. The physiological role of I^- secretion in the saliva and gastric juices is a matter of debate. A role in recycling of the body I^- pool has been suggested (192). I^- that has not been taken up by the thyroid or I^- released by the action of deiodinases is secreted into the saliva and gastric juice to be reabsorbed by the small intestine. Given its antioxidant properties, I^- may act as an antimicrobial agent in saliva and gastric juice as well, and in saliva, I^- has been reported to enhance epidermal growth factor levels, which promotes mucosal healing and intestinal growth (193, 194).

A bactericidal/bacteriostatic effect is consistent with the presence of an H_2O_2/peroxidase system in the salivary glands. Interestingly, Duox2 mRNA was detected in salivary glands by in situ hybridization (195). The H_2O_2 generated by this enzyme is used by lactoperoxidase (LPO), a heme-dependent secreted peroxidase produced by the submucosal glands, which is also abundantly secreted in saliva, to oxidize SCN^- (a NIS substrate) to hypothiocyanite ($OSCN^-$), which is present in human saliva at micromolar

Downloaded from https://academic.oup.com/edrv/article/35/1/106/2354709 by guest on 09 April 2024

concentrations (196). I^- is also an LPO substrate, and it has been shown that, in the airways, I^- and $OSCN^-$ produced by the H_2O_2/peroxidase system have different and complementary antimicrobial/antiviral roles (as detailed in *Section VII.G.*).

B. Stomach

NIS is expressed on the basolateral surface of mucin-secreting and parietal cells in the stomach. As NIS is expressed on the basolateral surface of gastric mucosal cells, NIS mediates the active uptake of I^- from the blood into the gastric epithelial cells from where it is secreted into the gastric juice. Therefore, gastric NIS plays no role in the absorption of dietary I^-. Interestingly, gastric NIS expression is downregulated in gastric cancer as well as intestinal metaplasia (197). This observation suggests that the decrease in NIS expression may be a marker for the diagnosis and possibly evaluation of the prognosis of stomach cancer patients.

C. Small intestine

NIS is also present in enterocytes of the small intestine, where dietary I^- is absorbed (198). Using intestinal brush border membrane vesicles, Nicola et al (198) showed that the K_m for Na^+-dependent, ClO_4^--sensitive I^- transport in small intestine is comparable to that of thyroid cells ($\sim$10μM–30μM). Pertechnetate (TcO_4^-), a NIS substrate, is transported by the small intestine in a ClO_4^--sensitive manner in vivo. In contrast to other NIS-expressing tissues, NIS in the small intestine is targeted apically. It is therefore plausible that I^- secreted into the saliva and the gastric juice is reabsorbed and recycled via NIS in the small intestine, together with the dietary I^- pool. Although a contribution from other I^--permeable transporters and channels (eg, Cl^- channels and pendrin) that may be present in the intestine cannot be formally excluded, it must be noted that these transporters have a K_m for I^- transport at least two orders of magnitude higher (in the mM range) than the concentration of I^- in most foods. Recently, SMVT has been reported to transport I^- with a K_m of $\sim$150μM in voltage-clamped oocytes (199). The main characterized function of SMVT in the intestine is biotin transport at the brush border of enterocytes (200). However, the contribution of SMVT to I^- absorption under physiological conditions in vivo remains to be determined.

In addition, intestinal NIS expression is decreased by high I^- in the diet, just as it is in the thyroid. High I^- downregulates NIS protein expression and I^- uptake in the small intestine in a time-dependent manner in vivo, as assessed in brush border membrane vesicles isolated from rats treated with 0.05% KI in their drinking water. After 12 hours of high I^- supplementation, NIS protein levels decreased by $\sim$50% and after 24 hours by $\sim$80% (198). Therefore, it seems that NIS downregulation after high I^- exposure is an autoregulatory mechanism to protect the thyroid or other I^--transporting tissues from the possibly deleterious consequences of I^- overload. It will be interesting to investigate whether this mechanism occurs in other NIS-expressing tissues, including tumors.

D. Lactating breast

NIS expression in normal breast occurs only during pregnancy and lactation, when cell proliferation occurs. I^- secreted into the milk is the sole source of this nutrient for the newborn and is critical for his/her normal thyroid function, as discussed above (122). The electrophoretic mobility of breast NIS (116) is generally higher than that of thyroid NIS as a result of differences in glycosylation. As discussed in *Section IX.C.1.* of this review, NIS expression was also found by Tazebay et al (116) in >80% of human breast cancers as well as in several transgenic animal models of mammary adenocarcinomas. Of note, NIS is not regulated by TSH in the breast. This property has a potential medical impact in the development of a treatment for NIS-expressing breast tumors with radioiodide, as it allows downregulation of NIS in the thyroid but not in the breast, thus protecting the healthy thyroid from the radioisotope (*Section IX.C.*) (201).

E. Kidney

I^- is excreted through the kidneys, and UI is the simplest method to assess ID. However, the mechanism of UI excretion remains a subject of controversy. Full-length NIS mRNA was detected by RT-PCR followed by Southern blot hybridization in human kidney tissue (202). These authors reported NIS immunoreactivity along the full length of the nephron, with the exception of the glomerulus. Basolateral staining was predominant in the proximal tubular cells, whereas cytoplasmic and more diffuse staining was apparent in the distal ones. Immunohistochemical studies by other groups did not reveal NIS expression in the kidney (190, 203). A study performed on high-density tissue microarrays (204) showed NIS expression at the apical surface of the collecting duct. None of these studies described NIS activity in the kidney, with the exception of a human kidney tumor epithelial cell line (G401) derived from Wilms' tumor (202), in which the hallmarks of NIS activity (Na^+-dependent, ClO_4^--sensitive I^- uptake) were demonstrated (202). In summary, the existence of functional expression, localization and regulation of NIS in the kidney is still an open question, which will be interesting to address to better understand the fate of I^- in the body and how the I^- balance and supply to the thyroid are modulated.

Downloaded from https://academic.oup.com/edrv/article/35/1/106/2354709 by guest on 09 April 2024

F. Placenta

Importantly, low levels of NIS expression have been reported by immunohistochemistry in different subtypes of placental cells, where NIS likely mediates transplacental I^- translocation for fetal TH biosynthesis (205–207). However, the level of NIS expression varies dramatically from sample to sample, and neither membrane localization nor activity has yet been shown definitively, although a nonpolarized pattern of expression in the cytotrophoblast has been observed (207).

G. Airway mucosal surface host defense: a new role for NIS?

In addition to being essential for TH biosynthesis, I^- plays a role in innate antimicrobial defense. It has been shown that, when applied to human or porcine primary airway epithelium, I^- inhibits viral infection by both encapsidated and enveloped respiratory viruses (72). The antiviral effect relies on the availability of H_2O_2 (which is produced in the airway epithelium by Duox1) and LPO. LPO, present at a concentration of 3 to 12 μg/mL in airway secretions (208), generates hypoiodite (HOI^-) in the presence of H_2O_2 and I^-. Addition of 5μM I^- to polarized primary human and porcine airway epithelia cultures (AECs) is enough to drastically reduce virus infectivity. However, I^- was provided in this study in the apical chamber or in both chambers. Also, NIS inhibitors were not tested. Therefore, a direct assessment of NIS involvement in the submucosal-to-mucosal I^- transport was not carried out. This is particularly relevant, because in the experiments where I^- was also supplemented in the basolateral chamber, a much higher concentration of I^- might have been available to mediate the antiviral effect as a result of NIS active transport.

I^- concentration in human airway surface liquid (ASL) was detected after administration of a 130-mg KI bolus to human subjects. The ASL to serum I^- ratio exceeded 50-fold, showing that an active transporter is responsible for I^- accumulation in ASL. Without KI administration, I^- concentration was below the technique detection limit, which could not measure concentrations below ~12μM in an undiluted sample. Considering the serum I^- concentration (which ranges between 10nM and 100nM), and the 50-fold accumulation in ASL found by these authors, 0.5μM to 5μM I^- could be present in human ASL. Although this I^- concentration could not be detected, it was enough, as shown in this study, to mediate a biological antiviral effect in in vitro experiments (72). Concurrently with the KI bolus administration, the SCN^- concentration in ASL decreased from ~400μM to ~170μM. These data indicate that 1) active I^-/SCN^- transport exists in human airway epithelia, and 2) I^- and SCN^- compete for the same transport system, in a manner compatible with NIS transport properties (Figure 10).

Interestingly, a higher concentration of SCN^- (500μM, comparable to the ~400μM found in ASL) did not inhibit infection by respiratory viruses (72). However, similar SCN^- concentrations (400μM) were shown to dramatically reduce Gram-positive and Gram-negative bacteria viability after incubation with H_2O_2-producing, LPO-supplemented rat AECs, or cow tracheal explants (containing LPO-secreting submucosal glands) (209). Of note, AECs from CF patients are unable to sustain an antimicrobial activity when 40μM SCN^- is provided in the basolateral chamber and were shown to have decreased transepithelial SCN^- transport from the basolateral to the apical side, suggesting that CFTR is required to transport SCN^- across the apical membrane to the lumen, where SCN^- is oxidized to $OSCN^-$. In contrast, AECs from nonaffected subjects showed a 10-fold higher concentration in the apical chamber after incubation with 40μM SCN^-.

The temporal and causal relationship between lung inflammation and infection has been unclear for a long time; mouse animal models generated in the past do not recapitulate the features of the human disease. However, a defect in the primary mucosal surface host defense system seems to be one of the first pathogenic events in CF, as recently found in $CFTR^{-/-}$ and $CFTR^{-/\Delta 508}$ pigs (210). Lungs of newborn transgenic or KO pigs contain bacteria more often than control pigs and contain a higher number of bacteria, with no signs of inflammation at early stages, indicating a defect in early lung bacterial clearance.

In a study investigating the identity of the basolateral SCN^- transporter in primary human airway cultures (211), the authors found that basolateral-to-apical SCN^- transport is ClO_4^--sensitive, competes with I^-, and is dependent on Na^+, which is highly suggestive of NIS-mediated transport. In addition, the kinetic characteristics for transport of these anions were compatible with those reported for NIS. In support of this notion, immunofluorescence with an anti-NIS antibody revealed a signal in the submucosal glands, probably at the basolateral surface, although there was no immunoblot to confirm the specificity of the antibody signal. In addition, NIS mRNA has been found in lung (189, 203).

Taken together, these results contribute to the elucidation of the role of SCN^-/I^- transport together with LPO/H_2O_2, respectively, in an antibacterial or antiviral host defense system in the lung. They also link a defect in SCN^- or I^- transport with the pathogenesis of lung infections in CF and non-CF patients and indirectly point to active transport at the basolateral surface of the airway epithelium and to a potential role of NIS in host defense at mu-

Downloaded from https://academic.oup.com/edrv/article/35/1/106/2354709 by guest on 09 April 2024

Figure 10.

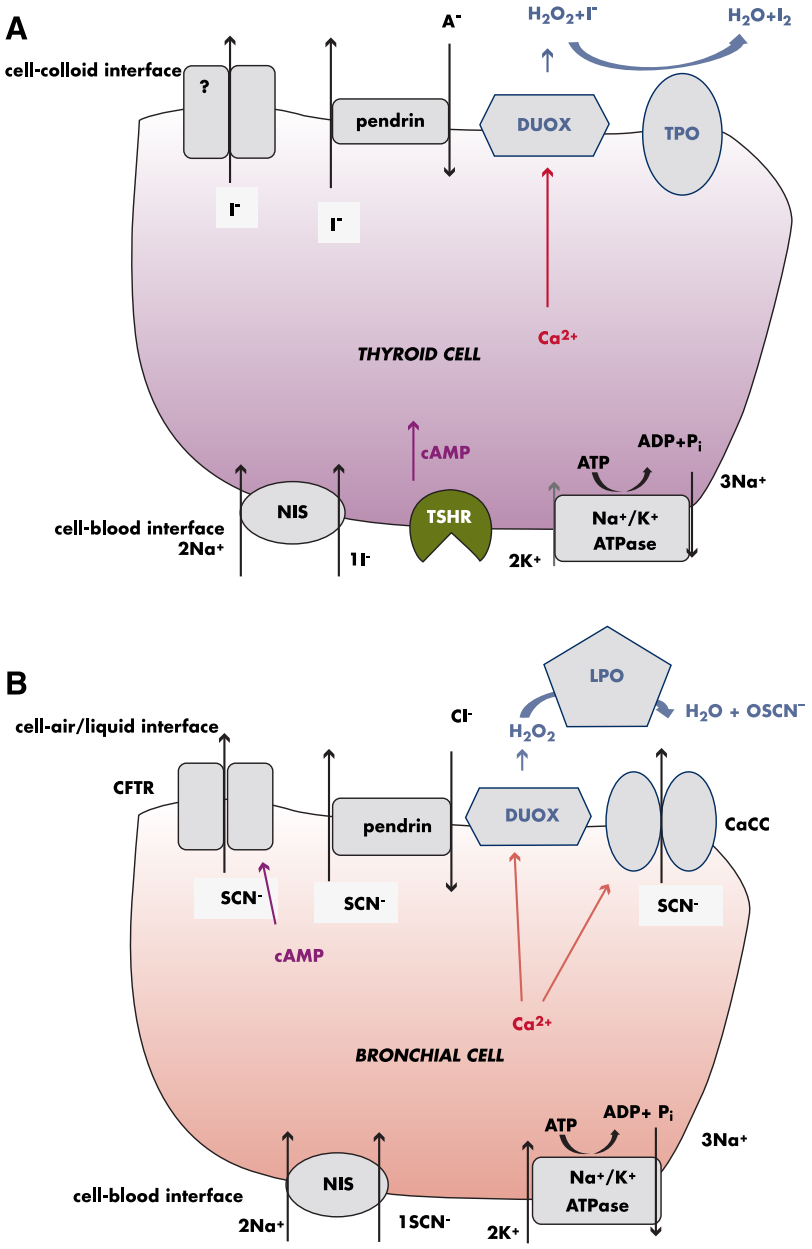

Figure 10. I^- and SCN^- transport and oxidation play an antimicrobial role in airway epithelium. A new function for NIS? A, In thyrocytes, I^- is translocated across the basolateral membrane by NIS, using the Na^+ electrochemical gradient generated by the Na^+/K^+ ATPase. I^- exits the apical surface via an unknown carrier or carriers; pendrin, an anion exchanger, is a candidate for this function. Stimulation of TSH receptor increases the concentration of cAMP and intracellular Ca^{2+}, which activates Duox2-catalyzed H_2O_2 synthesis for TPO-catalyzed oxidation of I^- to iodine. B, Airway epithelial cells share certain features with thyrocytes; SCN^- is actively transported into these cells across the basolateral membrane, likely by NIS. SCN^- is secreted in the ASL at concentrations 50 times those found in blood. CFTR is involved in the apical exit of SCN^- upon intracellular cAMP increase under basal conditions (342). Ca^{2+}-activated Cl^- channels (CaCC), and pendrin, which is also expressed in airway epithelial cells, are also responsible for SCN^- translocation, in particular under conditions that increase their expression (for instance, under the stimulation of IL-4, an anti-inflammatory cytokine) (342). Duox1, which is expressed at the apical surface in airway epithelium, generates H_2O_2, a substrate for the oxidation by LPO of SCN^- to $OSCN^-$, a species that has antibacterial activity. I^- at the cell air/liquid interface has also recently been found to have an analogous and complementary function; it reduces viral infection in the airway epithelia in vitro (336).

cosal surfaces (Figure 10). Whether SCN^- or I^- transport defects account for at least the initial pathogenic events in CF is a fascinating question that must be investigated.

VIII. Regulation of NIS in the Thyroid and Extrathyroidal Tissues

Here we concentrate on NIS regulation by TSH and I^-, by a novel mechanism involving the potassium voltage-gated channel, KQT-like subfamily member 1 (KCNQ) 1/KCNE2 K^+ channel, and by lactogenic hormones. For NIS regulation by Tg, a negative feedback mechanism involving the downregulation of several thyroid-specific transcription factors, the reader is referred to the 2011 review by Suzuki et al (212). For a comprehensive overview of transcriptional regulation of NIS, the reader is referred to a recent review by Kogai and Brent (213).

A. By TSH

The thyroid-pituitary-hypothalamic axis regulates TH production, and its integrity is critical for metabolic homeostasis. TH secretion is activated by TSH, a glycoprotein produced by thyrotrophs in the anterior pituitary and the major regulator of thyroid function. TSH consists of 2 subunits: the α-subunit is identical to that of the other 3 hormones synthesized by the anterior pituitary (LH, FSH, and CG), whereas the β-subunit is unique and confers functional specificity. TSH release is stimulated by TRH, a tripeptide (pyro-Glu-His-Pro-NH_2) produced by the parvocellular neurons in the hypothalamus as a preprohormone (pre-pro-TRH), which, in humans, consists of 6 copies of the TRH sequence that are cleaved to yield mature TRH (43). THs, in turn, act via a negative feedback mechanism to downregulate production of both stimulating hormones. In the absence of a sufficient I^- supply, THs

Downloaded from https://academic.oup.com/edrv/article/35/1/106/2354709 by guest on 09 April 2024

Figure 11.

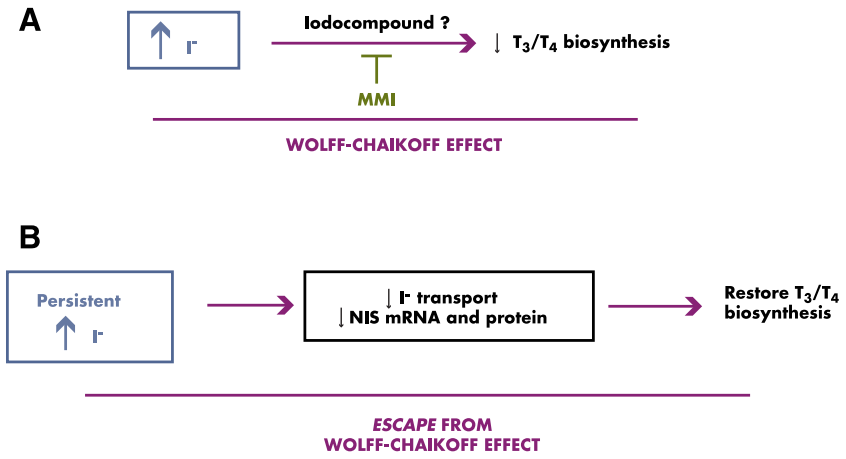

Figure 11. Wolff-Chaikoff effect and the escape therefrom. I^- itself is a major regulator of I^- accumulation in the thyroid. A, High plasma I^- levels decrease TH biosynthesis; this mechanism is known as the Wolff-Chaikoff effect. B, Thyroid cells adapt to persistent high I^- by downregulating NIS and restoring TH production; this process is called the escape from the Wolff-Chaikoff effect.

cannot be synthesized, and continuous stimulation by TSH leads to goiter, an enlargement of the thyroid gland. Thyroid function is mainly regulated by TSH, which acts via the TSH receptor. This receptor is a 7-TMS protein at the basolateral surface of thyrocytes, coupled to a heterotrimeric G protein. cAMP, produced from the $G_{s\alpha}$-mediated activation of adenylate cyclase, stimulates NIS transcription (214, 215). In addition to NIS, TSH also upregulates expression of TPO and Tg as well as iodinated Tg endocytosis. Levy et al (113) have shown that thyroid NIS protein expression is upregulated by TSH in vivo.

A TSH-mediated increase in NIS expression and I^- accumulation was demonstrated in FRTL-5 cells and human thyroid primary cultures (214, 216, 217). Withdrawal of TSH from FRTL-5 cell media results in reduction of both cAMP levels and I^- transport activity (24, 118, 121, 218). Interestingly, persistent I^- uptake activity is observed in membrane vesicles from non-I^-–transporting FRTL-5 cells cultured under conditions of prolonged TSH deprivation, suggesting that mechanisms other than transcription may be involved in regulating NIS activity in response to TSH (121). NIS can be detected in FRTL-5 cells up to 10 days after TSH withdrawal and NIS de novo synthesis is TSH-dependent (118). This observation is consistent with the extremely long half-life of NIS (5 days in the presence of TSH and 3 days without TSH in FRTL-5 cells), as established by metabolic labeling and immunoprecipitation experiments (118). In addition to transcription, TSH regulates the subcellular localization of NIS and is required for NIS targeting to, and/or retention at, the plasma membrane (118). The intracellular localization of active NIS molecules in the absence of TSH explains the above-described persistence of I^- transport in membrane vesicles observed by Kaminsky et al (121). In thyroid cells, NIS is phosphorylated, mainly on its carboxy terminus, and TSH increases NIS carboxy terminus phosphorylation, which occurs on Ser residues (118).

B. By I^-

In addition to TSH, I^- itself is a major regulator of I^- accumulation in the thyroid. The ability to block thyroid function with high I^- was described by Plummer (219) as early as 1923. In 1948, Wolff and Chaikoff (220) reported that high plasma I^- levels blocked I^- organification in rat thyroid in vivo. The ability of high doses of I^- to decrease thyroid function became known as the Wolff-Chaikoff effect (Figure 11A). However, this inhibitory effect of I^- lasts ~2 days in the presence of high plasma I^-, after which TH biosynthesis is restored (221). This adaptation to persistent high I^- was termed the escape from the Wolff-Chaikoff effect (Figure 11B). Significantly, adapted thyroids accumulated less I^- than nonadapted thyroids, which rescued thyroid function. This led Braverman and Ingbar (222) to suggest that the escape from the Wolff-Chaikoff effect was mediated by a reduction in I^- transport (Figure 11B), which would alleviate the high intracellular I^- concentrations and restore TH biosynthesis.

What is the mechanism for the escape/decrease in I^- transport? In 1986, it was reported that I^- preincubation suppressed I^- uptake in FRTL-5 cells in a time- and dose-dependent manner, an effect preventable with methimazole (MMI), which inhibits I^- organification (223). Inhibition by MMI suggested that the Wolff-Chaikoff effect was mediated by an intracellular iodinated compound. Consistent with the observed reduction in I^- transport, later studies demonstrated an I^--induced reduction in NIS and TPO mRNA in dog thyroid (224) and NIS mRNA and I^- transport in FRTL-5 cells (225). A decrease in NIS mRNA and protein as well was demonstrated 24 hours after incubation with high I^-, but no correlation was made with NIS activity (226).

Thus, the Wolff-Chaikoff effect and its escape constitute an intrinsic autoregulatory mechanism to protect the thyroid gland from the deleterious effects of I^- overload. The escape from the Wolff-Chaikoff effect is unquestion-

Downloaded from https://academic.oup.com/edrv/article/35/1/106/2354709 by guest on 09 April 2024

ably mediated by inhibition of I^- transport. Recent data are consistent with the hypothesis that the NIS mRNA half-life is reduced by a posttranscriptional mechanism at least at short time points, rather than a change in NIS promoter activity (227). In addition, I^- excess was also found to trigger an increase in ROS production and in the expression and activity of ROS-scavenging selenoenzymes (228). The results described above point to both a posttranscriptional and a posttranslational component to the escape mechanism and suggest that the presence of high I^-, which is oxidized intracellularly through an unknown mechanism, inhibits thyroid function. However, various possibilities exist that could explain the reduction in NIS-mediated I^- accumulation. As indicated by these authors (228), although an attractive hypothesis, it remains to be determined whether the redox state of thyroid cells and its potential effect on amino acid modifications or oligomeric state directly modulate NIS activity. Another question open to investigation is whether, in addition to effects on NIS mRNA, high I^- concentrations also modulate NIS protein biogenesis, subcellular localization, and degradation.

Significantly, it was recently demonstrated that I^--induced NIS downregulation is not a thyroid-specific phenomenon, because it occurs also in small intestine enterocytes (198) (*Section VII.C.*).

High concentrations of I^-, presumably in the form of iodolipids, inhibit the generation of H_2O_2 (229–231). Interestingly, iodolipids have been found in rat, horse, dog, and human thyroid. These iodolipids inhibit Duox and adenylyl cyclase, suggesting that they are involved in regulatory actions of I^- in the thyroid (232, 233).

C. By a novel mechanism involving a K^+ channel

Roepke et al (234) have demonstrated for the first time that an ion channel plays a key role in thyroid function. Specifically, these authors reported that the β-subunit (KCNE2) of the voltage-gated potassium channel KCNQ1/KCNE2 is required for TH biosynthesis. This channel is a complex comprising 4 large KCNQ1 subunits, which traverse the membrane 6 times each, and 2 small KCNE2 subunits, which traverse the membrane only once each (235). KCNQ1/KCNE2 K^+ channels participate in the repolarization of the cardiac ventricles (235). The regulation of NIS by this channel was uncovered when mice in which the *Kcne2* gene had been genetically deleted (*Kcne2*$^{-/-}$ mice) presented not only cardiac symptoms (cardiomegaly, hypertrophy, and impaired contractility) but also several other, unexpected symptoms including alopecia, a 50% embryonic death rate, and growth retardation resulting in dwarfism. These findings led Roepke et al (234) to determine the thyroid status of these mice; they were hypothyroid. Hypothyroidism in these animals is due to decreased I^- accumulation in the thyroid gland, as evaluated by quantitative micro–positron emission tomography (PET) imaging with $^{124}I^-$, and most symptoms were alleviated by TH administration or, remarkably, by having the *Kcne2*$^{-/-}$ pups be fed by WT dams, which provide their pups with an abundant supply of THs through their milk (234). Of note, *Kcnq1*$^{-/-}$ mice are also hypothyroid (236), indicating that both subunits of KCNQ1/KCNE2 are required for adequate thyroid function.

As a first step to elucidate the basis for the decrease in I^- accumulation observed in *Kcne2*$^{-/-}$ mice, Purtell et al (237) investigated whether the effect of the absence of KCNE2 was on I^- uptake or iodine organification. A standard test of I^- organification is the ClO_4^- discharge assay. When ClO_4^- is given to a patient whose organification is impaired, a discharge of I^- is observed because, as I^- is not covalently incorporated into Tg and NIS-mediated I^- uptake is being blocked by ClO_4^-, free I^- that is released from the gland is not taken back in. In contrast, when organification is intact, only a very small amount of I^- is released upon the addition of ClO_4^-. Purtell et al (237) monitored NIS-mediated I^- uptake in WT and *Kcne2*$^{-/-}$ mice after injecting them with ClO_4^- and recorded no difference in I^- release between them, indicating that organification is not impaired in *Kcne2*$^{-/-}$ mice.

To analyze I^- uptake at steady state, ie, in the absence of I^- organification, these authors used $^{124}I^-$ PET imaging in MMI-treated WT mice. They recapitulated the phenotype of *Kcne2*$^{-/-}$ mice by pharmacologically blocking KCNQ1/KCNE2 with (−)-[3R,4S]-chromanol 293B (C293B), an enantiomer of chromanol 293B (1) that selectively inhibits KCNQ1/KCNE2. In the absence of organification, NIS-mediated I^- uptake was markedly decreased in C293B-treated animals, supporting the notion that *Kcne2*$^{-/-}$ mice exhibit defective NIS-mediated thyroid I^- uptake but intact I^- organification.

Consistent with their in vivo results, Purtell et al (237) showed in vitro that C293B decreased NIS-mediated I^- uptake but not nicotinate transport mediated by another Na^+-dependent transporter, SMCT, in FRTL-5 cells. C293B did not have any effect on I^- uptake when NIS was expressed in COS cells, which do not express endogenous KCNQ1/KCNE2 K^+ channels.

The localization of KCNE2, like that of NIS, varies with tissue type. Thus, although KCNE2 is basolaterally targeted in thyrocytes, it is apically expressed in the gastric parietal cells (238). That NIS is regulated by KCNQ1/KCNE2 has potential relevance to human cardiac function, given that cardiac manifestations observed in patients with mutations in *KCNQ1* or *KCNE2* may have an

Downloaded from https://academic.oup.com/edrv/article/35/1/106/2354709 by guest on 09 April 2024

endocrine component. Clearly, one question that emerges is how KCNQ1/KCNE2 regulates NIS function. One possibility is that the activity of this channel is critical for maintaining the membrane potential in thyroid cells. If this is so, then alteration of KCNQ1/KCNE2 by either genetic or pharmacological means will decrease the membrane potential. Because this potential is part of the driving force for NIS-mediated I^- uptake (which is electrogenic), such a decrease would impair NIS activity. The molecular mechanism involved in the regulation of NIS by KCNQ1/KCNE2 will likely be elucidated by a combination of genetic, pharmacological, biochemical, and biophysical approaches.

D. By lactogenic hormones

Although absent in nubile rats, NIS expression in the mammary gland progressively increases toward the end of gestation and is most prominent during lactation. Hormonal regulation of rat mammary gland NIS has been studied both in vitro and in vivo. NIS expression is reversibly regulated by suckling during lactation. In vivo studies in ovariectomized mice revealed that the combination of β-estradiol, oxytocin, and prolactin results in the highest level of NIS expression in the mammary gland (116).

IX. Clinical Applications of NIS

A. Hyperthyroid states

Radioiodide therapy has been successfully used in the treatment of hyperactive thyroid states such as Graves' disease and toxic nodular goiter for over 60 years. Its use in these benign thyroid diseases is thoroughly reviewed by Bonnema and Hegedüs (239). Briefly, although $^{131}I^-$ is still used to treat Graves' disease, antithyroid drugs have replaced it as the preferred treatment, largely because $^{131}I^-$ can cause hypothyroidism. It has been reported that although hyperthyroidism is cured in 50% to 90% of those treated within 3 to 12 months of $^{131}I^-$ treatment, hypothyroidism is observed with an incidence of 5% to 50% within the first year of treatment in those patients (239). Patients with toxic nodular or multinodular goiters also benefit from $^{131}I^-$ ablation and exhibit lower rates of hypothyroidism. Some European countries currently preferentially use $^{131}I^-$ to treat patients with benign nontoxic goiter (239).

B. Thyroid cancer

Over 44 000 people in the United States are estimated to have been diagnosed with thyroid cancer in 2010 (240), an incidence that has more than doubled since the 1970s. Thyroid cancer is the fastest rising among malignancies and accounts for 5% of newly diagnosed cancers among women. The follicular or papillary variants of differentiated thyroid cancer are the most common endocrine malignancies. Mutations in proteins along the MAPK signaling pathway are also found in thyroid cancer. Altogether, mutations in *RET*, all 3 *RAS* isoforms, and *BRAF* are found in ~70% of all thyroid cancers (241, 242). Constitutive activation of these proteins stimulates the MAPK signaling pathway, inhibiting the expression of proteins involved in the TH biosynthetic pathway, including NIS. Tellingly, *BRAF* mutations are commonly found in sporadic papillary thyroid cancer (PTC), but not in radiation-induced, RET/PTC-positive PTC, indicating that RET/PTC and BRAF very likely reside in the same signaling pathway (243). Mutations in upstream proteins lead to activation of other signaling pathways, whereas *BRAF* mutations (~45% of PTCs) result in the activation of the 2 known effectors, MAPK kinase 1 (MEK1) and MEK2. In contrast to melanoma, where the correlation between *BRAF* mutations and poor prognosis and survival is controversial (although there is a clear association with invasiveness), in thyroid cancer, there is a well-recognized association between *BRAF* mutations and a less favorable prognosis (invasiveness, cancer recurrence, lymph node metastases, and advanced stage at presentation) (244). Virtually all *BRAF* mutations in PTC result in the production of a constitutively active $BRAF^{V600E}$. $BRAF^{V600E}$ is thought to be involved in promoting cell survival and proliferation by hyperphosphorylation of retinoblastoma protein (Rb) (which promotes the cell cycle transition from G1 to S phase by releasing the inhibition of elongation factor 2 [E2F]-dependent transcription) (244). Interestingly, in many cases, oncogenic *BRAF* mutations alone are not enough to drive transformation in vivo and in vitro: in fact, most micro-PTCs (precursors of PTC) and benign nevi (precursors of melanomas) carry oncogenic *BRAF*. Expression of physiological levels of $BRAF^{V600E}$ in a lung mouse model induced adenocarcinomas when mice were crossed with mice carrying inactivating mutations of p53 or p16/Ink4a, suggesting that a second, senescence-bypassing mutation is required. Overexpression of mutated Harvey rat sarcoma viral oncogene homologue (H-Ras) in thyroid cells is also not enough to promote cell transformation. In PTC, however, mutations in p16 or p53 are virtually never found (although they are common in anaplastic thyroid cancer). However, thyroid knock-in of $BRAF^{V600E}$ in mice results in short-latency, invasive PTC (244). It has been suggested that because activated BRAF decreases TH biosynthesis, the resulting high blood concentration of TSH may play a role in tumor development. This suggestion is consistent with the well-established clinical observation that TSH and tumor develop-

Downloaded from https://academic.oup.com/edrv/article/35/1/106/2354709 by guest on 09 April 2024

ment are associated (an association, however, whose molecular underpinnings are not known in detail).

Notably, PTCs harboring $BRAF^{V600E}$ have absent or decreased NIS-mediated $^{131}I^-$ uptake. Conditional exogenous expression of RET/PTC3, which induces activation of MAPK signaling, decreases NIS protein expression in rat thyroid cells (PCCL3), an effect prevented by silencing RNA knockdown of *BRAF*, but not other *RAF* isoforms (244, 245). Doxycycline-induced $BRAF^{V600E}$ expression in PCCL3 cells induces mistargeting and lower expression of NIS, an effect that is reversed by removal of doxycycline or treatment with MEK inhibitors. Interestingly, NIS plasma membrane expression is also restored in vivo in animals harboring doxycycline-inducible, thyroid-specific knock-in $BRAF^{V600E}$ upon administration of MEK inhibitors or specific $BRAF^{V600E}$ inhibitors or by switching off $BRAF^{V600E}$ expression by doxycycline removal. Importantly, restoration of I^- uptake has been shown by micro-PET and quantitative dosimetry as well as an increase in apoptosis and DNA damage upon $^{131}I^-$ administration (246). The availability of thyroid cancer mouse models recapitulating the characteristics of the human disease has been crucial in unveiling signaling pathways that are key in tumor initiation and progression and will undoubtedly help in identifying novel drug molecular targets.

Clinical trials are currently ongoing to determine whether MEK inhibitors increase $^{131}I^-$ uptake (247–252). Most recently, a clinically significant increase in radioiodide uptake and retention was reported in a trial with selumetinib, a selective allosteric MEK1 and MEK2 inhibitor, in patients with thyroid cancer refractory to radioiodide. Twelve of 20 patients treated for 4 weeks with selumetinib, including those carrying *BRAF* and *NRAS* mutations, showed increased $^{124}I^-$ uptake. Eight of these 12 were treated with $^{131}I^-$ because they had reached the dosimetry threshold (>2000 cGy). Strikingly, of these 8 patients, 5 had confirmed partial responses and 3 stable disease (253). $^{131}I^-$ therapy after treatment with selumetinib was especially efficacious in patients whose tumors had a mutated *NRAS* gene (5 of 5) (253).

The ability of differentiated thyroid cancer to accumulate I^- via NIS is exploited in the treatment of thyroid cancer and its metastases with $^{131}I^-$, in the diagnosis of metastases, and in follow-up studies with $^{123}I^-$, which has a shorter half-life and superior imaging characteristics. Before radioiodide administration, totally or nearly totally thyroidectomized patients under T_4 supplementation are withdrawn from therapy for 4 to 5 weeks to achieve high serum TSH concentrations (up to 30 μIU/mL) (254) or receive stimulation with two im injections of human recombinant TSH within 48 hours in a low-I^- diet regimen (255). Radioiodide remnant ablation (RRA) with 30 to 150 mCi $^{131}I^-$ after total removal of the thyroid is administered to patients to destroy cancer remnants and residual thyroid tissue. RRA also has the advantage of allowing for an easier follow-up by measurement of serum Tg, which in a thyroidectomized, radioablated patient is detected only in case of thyroid cancer recurrences or metastases. Although the use of RRA in patients with low-risk thyroid cancer variants (tumors ≤1 cm without metastases or capsule invasion or without more aggressive histological morphologies) is controversial, adjuvant RRA is widely recommended with very few exceptions (256). Radioiodide therapy (RIT) after T_4 withdrawal or stimulation with human recombinant TSH is also used as an alternative treatment in nonresectable lymph node, lung, soft-tissue (in these cases, and also in recurrent disease, when $^{131}I^-$ is administered as long as there is tumor uptake, or until remission), and bone metastases to eradicate or decelerate tumor progression (256). RIT is also sometimes administered in patients with negative whole-body scans, as residual $^{131}I^-$ activity may be present that cannot be visualized on a whole-body scan but can still induce tumor regression, measured by lower Tg levels in the blood. With the same purpose, RIT is also used in some anaplastic cancer cases, where a part of the tumor retains a certain degree of differentiation or when serum Tg can be measured, with the rationale that the $^{131}I^-$-accumulating part of the tumor can be destroyed and the surrounding undifferentiated tissue can be reached by a β-particle cross-fire effect (256).

Side effects are common but generally mild: nausea, posttreatment neck pain, sialadenitis, taste alteration, and pulmonary fibrosis (in the repeated treatment of lung metastases). Increased risk of radiation-induced leukemia is controversial and probably associated with extremely high doses that were more commonly administered in the past (254).

Patients with thyroid carcinoma have an overall 97% 5-year survival rate (257), and in numerous retrospective studies on large numbers of patients, radioiodide therapy was found to be the most powerful indicator for disease-free survival (258) and to decrease recurrence rates and tumor-specific deaths (254, 256, 259). In addition, radioiodide uptake in distant metastases was found to increase survival rate at 10 years from 10% to 56% (259).

C. Emerging roles of NIS in extrathyroidal pathologies: endogenous NIS expression and exogenous NIS expression by gene transfer

1. Breast cancer

In 2000, NIS expression was demonstrated in >80% of human breast cancers and in several transgenic animal

Downloaded from https://academic.oup.com/edrv/article/35/1/106/2354709 by guest on 09 April 2024

models of mammary adenocarcinomas (116). Significantly, NIS is functionally expressed in human breast cancer metastases, as assessed by scintigraphy (201). NIS is also expressed in triple-negative (estrogen receptor-, progesterone receptor-, and Her2-negative) breast cancers (65% of cases), for which the therapeutic choices are limited to chemotherapeutic agents (260). These observations suggest that $^{131}I^-$ may prove to be a useful tool in breast cancer therapy.

A recent study analyzed NIS expression in breast cancer brain metastases. Brain metastases constitute a therapeutic challenge because of the impermeability of the blood-brain barrier to most chemotherapeutic agents, which limits the therapy to surgery and external radiation. As a result, the prognosis of breast cancer brain metastasis patients is poor (2.3- to 7.1-month median survival). It has been reported that 75% of total cases and 80% of $HER2^+$ metastases expressed NIS. Although NIS expression was largely intracellular, plasma membrane expression was detected in 24% of NIS-positive samples (261). Although these observations are promising, whether the degree of $^{131}I^-$ accumulation by breast tumors and their metastases will be sufficient for successful therapy needs to be thoroughly evaluated.

Various factors must be considered in applying $^{131}I^-$ therapy to breast cancer. As different tumor types may have different sensitivity to radiation, the clinical outcome of a similar dose could differ between thyroid and breast cancer, and a smaller radiation dose might be sufficient to elicit a therapeutic effect in breast cancer cells. Second, it has been noted that tumor NIS positivity changes over time (201, 260) as a result of disease progression and/or treatments. Therefore, it is of interest to study tumor-specific radioiodide accumulation in breast cancer patients who have not undergone extensive treatment and in primary tumors. In addition, the use of another NIS substrate, $^{188}ReO_4^-$, could also increase the radiation dose delivered to the tumor (discussed in *Section IX.E*).

Liu et al (262) have reported NIS expression in cholangiocarcinoma, only the second extrathyroidal cancer, after breast cancer, to be found to express the protein endogenously. Considering that currently available therapies for cholangiocarcinoma are not effective (the 5-year survival rate for cholangiocarcinoma patients is only 2%), this discovery raises the notion that NIS-mediated radioiodide therapy should be investigated as a potential new treatment.

The upregulation and mislocalization of NIS in various tumor types has sparked interest in the role that these phenomena play in carcinogenesis. Recent studies by Lacoste et al (263) have suggested that the expression of NIS, and not its translocation of ions, is involved in upregulating cell migration and invasion via binding to leukemia-associated RhoA guanine exchange factor and activation of the small GTPase RhoA. It will be extremely interesting to investigate how wide a variety of tumors display upregulation of cell migration and invasion by NIS.

2. NIS as a reporter gene

PET-based imaging using reporter genes is a powerful technique that allows monitoring of gene delivery and adoptive-cell therapies (ie, T cell and stem cell transfers) (264). For gene transfer, reporters enable quantitative monitoring of the location of viral vectors and the extent and duration of transgene expression, whereas for cell therapy, they permit monitoring of the targeting and location of the transplanted cells. For a complete review of the advances in using NIS as a reporter gene, please refer to Penheiter et al (265). Here we discuss some highlights.

NIS is an extremely useful human reporter gene, whose use as an imaging modality is more than promising. Unlike receptors, which can bind ligands with only a 1:1 stoichiometry, NIS, being an active transporter, accumulates its radiolabeled substrates and concentrates the signal. This is highly desirable; otherwise, weak transgene expression would be difficult to detect. Furthermore, radiotracers already approved for clinical use in both PET ($^{124}I^-$ and $^{94m}TcO_4^-$) and γ-camera imaging ($^{123}I^-$, $^{131}I^-$, and $^{99m}TcO_4^-$) are available NIS substrates (264). NIS can be used to monitor not only its own delivery but also that of other genes, and potentially the size of the tumor, given that once NIS is expressed in the target tissue/tumor, diagnostic scintigraphic imaging can be performed (266–268).

Several reports in recent years highlight the feasibility and potential of this strategy (269–273), particularly in oncology. NIS may prove to be a useful reporter in the arena of pulmonary gene therapy. In 2005, Niu et al (274) used adenoviral (Ad)-hNIS delivered intranasally into the lungs of Cotton rats and were able to detect $^{124}I^-$ PET signal up to 17 days after administration of the vector. Thus, NIS may potentially be helpful in monitoring the delivery of therapeutic genes for lung disease such as *CFTR* for CF. However, intranasal administration of any foreign substance in human subjects may prove to not be trivial, because induction of anaphylaxis can be a fatal complication. The feasibility of using NIS for cardiac gene expression imaging has also been demonstrated in animal models (275–279). Safety for myocardial injection was evaluated by echocardiography, serial creatine kinase measurements, and a histologic examination in rats.

Reporter genes are useful for tracing the localization of transplanted cells. In 2008, Terrovitis et al (280) demonstrated for the first time the use of NIS, introduced in a

Downloaded from https://academic.oup.com/edrv/article/35/1/106/2354709 by guest on 09 April 2024

lentiviral vector, as a reporter gene for transplanted rat cardiac-derived stem cells via single-photon emission computed tomography (or PET) imaging using $^{99m}TcO_4^-$ (or $^{124}I^-$) (280). Given the nonimmunogenic nature of NIS and the current routine use of single-photon emission computed tomography $^{99m}TcO_4^-$ and PET scans, this in vivo tracking system may be a candidate for clinical translation into transplant procedures aimed at regenerating ischemia-damaged myocardium. In a follow-up study, Lautamäki et al (281) evaluated the effect of perfusion defect size on engraftment and retention of intramyocardially injected NIS-transduced CDCs after acute myocardial infarction. Along similar lines, Higuchi et al (282) have demonstrated that it is possible to use $^{124}I^-$ and PET to monitor cell engraftment and survival of NIS-expressing human endothelial progenitor cells isolated from umbilical cord blood and retrovirally transduced with NIS after transplantation into the rat heart.

Seo et al (283) demonstrated the feasibility of PET imaging with $^{124}I^-$, using NIS as a reporter, for studying recruitment of macrophages to sites of inflammation induced in vivo in a preclinical model. Macrophages have been shown to be critical players in various pathological processes, ranging from inflammatory disease to tumor growth. Thus, an effective way of visualizing these cells in vivo would be highly valuable for studies of the mechanisms underlying these processes. NIS expression in lentivirally transduced RAW264.7 macrophages, a nonepithelial system, was well tolerated and did not affect cell proliferation, cytokine production, or phagocytic activity (283). However, although avid I^- transport was observed in vitro, with >70 times more I^- accumulation in NIS-transduced than in nontransduced cells, the percentage of the injected dose of $^{124}I^-$ per gram in the region of interest at the inflammation site in vivo was only 2-fold higher in mice injected with NIS-transduced cells than in controls. Furthermore, very rapid I^- efflux (half-life = 5 minutes) was reported in this study (283). Both these factors underscore the importance of developing methods of increasing NIS expression and membrane targeting, as well as I^- retention, to make it possible to most effectively use NIS as a reporter gene in vivo.

3. NIS as a therapeutic gene

Although the reporter properties of NIS have been explored, most studies have focused on the protein's therapeutic potential in a variety of cancers in animal models. Here we highlight some of the exciting results that have been obtained in the field. For a more comprehensive summary on the topic, the reader is referred to recent reviews (213).

Radioisotopes are used clinically in 2 forms, as sealed and unsealed sources. A sealed source is one that is surrounded by an inert cover and is delivered to either the surface or inside of a tumor and is used to administer brachytherapy. After treatment, the radioactive source is removed from the patient. In this case, the patient never comes into direct contact with the source and remains cold. In contrast, unsealed sources are not encapsulated. They are administered through ingestion or injection and do come into direct contact with the patient. Thus far, the use of unsealed sources is limited to a few malignancies, including thyroid cancer ($^{131}I^-$), prostate cancer (^{89}Sr and ^{223}Ra) (284, 285), neuroblastoma/pheochromocytoma ([^{131}I]meta-iodobenzyl-guanidine) (286), and lymphomas (^{90}Y-labeled anti-CD20 monoclonal antibodies) (287, 288).

A way to augment NIS expression in tumors that already express NIS or induce expression in those that do not is via gene transfer. Gene transfer advances have opened up a new avenue for the development of a novel therapeutic strategy for cancer through targeted expression of functional NIS to malignant cells. The first report on the restoration of I^- transport activity in malignantly transformed thyroid cells (FRTL-Tc, which do not transport I^-) after NIS cDNA transfection appeared shortly after the cloning of NIS. However, $^{131}I^-$ treatment of these xenotransplants in rats did not significantly reduce tumor growth as compared with xenografts from nontransfected cells, perhaps owing to the short effective half-life of $^{131}I^-$ in the tumor (6 hours) (289). Since then, more efficient ways to deliver NIS using viral vectors have been exploited and promising results obtained.

The potential and feasibility of NIS in gene therapy has been extensively evaluated in numerous preclinical studies. Introduction of NIS via gene transfer has been undertaken by several groups to render tumors susceptible to $^{131}I^-$ treatment. Success with this approach has been reported both in vitro and in vivo in liver, prostate, colon, ovarian, pancreatic, and cervical carcinomas and in melanoma, glioma, and multiple myeloma (24, 25, 122, 269–273, 290–306).

Particularly interesting results have been obtained with hepatocarcinoma, prostate cancer, and multiple myeloma. NIS gene transfer has been used in an aggressive model of hepatocarcinoma induced by diethylnitrosamine in immunocompetent rats. Injection of an adenoviral vector expressing NIS under the cytomegalovirus (CMV) promoter (Ad-CMV-NIS) into the portal vein of hepatocarcinoma-bearing rats followed by $^{131}I^-$ therapy resulted in a strong inhibition of tumor growth and prolonged survival (270, 304). Although rapid efflux was reported in vitro, sustained uptake was observed for >11 days in vivo. The authors attributed this to the recycling of effluxed I^- through the portal circulation. Notably, despite the use of

Downloaded from https://academic.oup.com/edrv/article/35/1/106/2354709 by guest on 09 April 2024

the ubiquitous CMV promoter, the inherent tropism of adenovirus for the liver and the intraportal route of injection allowed for a rather targeted delivery.

The success of NIS gene transfer therapy depends on efficient delivery of the NIS gene into the target tissue and proper NIS expression at the plasma membrane, a requirement for $^{131}I^-$ uptake and tumor destruction. Tissue-specific promoters provide a way to target NIS selectively to malignant cells, maximizing tissue-specific cytotoxicity and minimizing toxic side effects in nonmalignant cells. Tissue-specific NIS expression resulting in NIS-mediated I^- uptake was first demonstrated in 1999 in an androgen-sensitive human prostate cancer cell line (LNCaP) using the prostate-specific promoter prostate-specific antigen (267, 307, 308). These authors subsequently established xenografts in nude mice from a NIS-expressing human prostate cancer cell line that actively accumulated as much as 25% to 30% of administered I^- in vivo. Strikingly, the size of xenograft tumors in these mice was significantly reduced after a single ip injection of a therapeutic dose of $^{131}I^-$. In preparation for a phase I clinical trial of Ad-mediated NIS gene therapy for prostate cancer, Dwyer et al (309) injected the Ad-NIS intraprostatically in dogs, which then received a therapeutic dose of $^{131}I^-$. The study demonstrated the successful introduction of localized functional NIS expression to the prostate without radiation damage or vector-related toxicity to other cells or organs. At the time of writing, a clinical trial using Ad-NIS for prostate cancer is ongoing at the Mayo Clinic, indicating the potential of the NIS gene transfer approach.

A self-inactivating lentiviral vector with NIS under the Ig promoter has been used by Dingli et al (269) to selectively target multiple myeloma cells. Strikingly, in this study, tumor xenografts expressing NIS were completely destroyed by a single dose of $^{131}I^-$ (1 mCi) and sustained complete tumor regression up to 5 months after treatment, the longest follow-up reported to date. This group also evaluated the bystander effect of $^{131}I^-$ therapy by injecting tumor xenografts consisting of a mixed population of NIS-expressing and non–NIS-expressing cells (50:50 and 10:90). Remarkably, the xenografts that expressed NIS in only 50% of cells completely resolved, whereas those that expressed NIS in only 10% still displayed slower growth than those not expressing NIS. This is an extremely important observation, because the efficiency of viral transduction in vivo is far from 100%. These results demonstrate the potential of NIS as a transgene, as the bystander effect of NIS-mediated $^{131}I^-$ therapy can potentially overcome the hurdle of low transduction efficiency. The radiosensitive nature of multiple myeloma could be a major contributing factor to the success of radiotherapy in this case, and although NIS may become a new avenue for therapy of this currently incurable cancer, more extensive studies are certainly warranted.

More recently, a significant regression of pancreatic carcinoma transduced in vivo with a replication-defective adenoviral construct containing NIS under the MUC1 promoter (Ad-MUC1-NIS) in mice was reported after iv $^{131}I^-$ treatment. In this study, no isotope was detected in the liver, in contrast to the hepatotoxicity induced by nonspecific promoters such as CMV (291). Many studies using tissue-specific promoters have followed.

Another tumor-specific approach not limited to a particular tumor type is the use of tumor-specific promoters to drive expression of a therapeutic transgene into tumor cells. One example is the use of telomerase. Aberrant telomerase gene expression in cancer remains an area of continued interest for development of anticancer therapeutics (310, 311). Recombinant adenoviruses have been used to introduce NIS into ovarian and pancreatic carcinoma xenografts. Using NIS as a reporter gene, the activities of the telomerase promoters have been monitored by PET with $^{124}I^-$. Most recently, the possibility of using these constructs therapeutically has been investigated. Using the promoters of the 2 subunits of telomerase, the RNA subunit (hTR) and the reverse transcriptase subunit (hTERT), to transcriptionally target NIS in colon and melanoma xenograft models, delayed tumor progression was demonstrated after a 1-mCi therapeutic dose of $^{131}I^-$ administered ip (312).

Although most of the work on NIS gene transfer has been done using adenoviral vectors, some effort has been made to use the oncolytic measles virus (MV). Recombinant replication-competent viruses based on the Edmonston strain of MV (MV-Edm) have been shown to be highly effective oncolytic viruses that can potentially be used to treat a broad range of tumors (313–316). MV recognizes CD46 on the surface of target cells. Upon infection, it induces syncytium formation and lysis. For replication-competent viruses, it is crucial to monitor the viral distribution, adjust dosing, and assess outcome. Thus, MV-NIS was engineered to retain the oncolytic capacity of the parent virus, allowing noninvasive detection of its distribution and expression with $^{123}I^-$ over time. Additionally, an enhancement of the therapeutic effect can be achieved by $^{131}I^-$ administration. MV-NIS has been approved by the Recombinant DNA Advisory Committee for a phase I study in patients with advanced or refractory multiple myeloma (317–320). After pharmacological and toxicological studies of MV-NIS in mice and squirrel monkeys (316), a clinical trial using iv MV-NIS to treat multiple myeloma with or without cyclophosphamide in patients with recurrent or refractory multiple myeloma is ongoing at the Mayo Clinic at the time of writing. The

Downloaded from https://academic.oup.com/edrv/article/35/1/106/2354709 by guest on 09 April 2024

purpose of administering cyclophosphamide in this trial is to suppress the immune response elicited by MV, because the use of MV-NIS may be hindered by immune clearance. Because children are routinely vaccinated against measles, most of the population has antibodies against it; therefore, iv-administered MV-NIS is rapidly neutralized and cleared by antiviral antibodies. To address this problem experimentally, different modes of viral delivery have been explored. Given their natural bone marrow tropism, myeloma cells themselves were used to carry MV-NIS to sites of disease deposits in mice. By infecting myeloma cells ex vivo and infusing them back into mice with disseminated disease, the authors showed that the antitumor activity of MV-NIS was evident even in previously immunized mice. Thus, the problem of immune clearance could perhaps be circumvented by systemically delivering cells infected with MV-NIS, rather than iv injecting MV-NIS (321). Whether this can be translated to humans should be investigated, as it may provide a new treatment modality for this disease.

Additionally, although MV has been used for its oncolytic properties, highly specific tumor targeting remains a problem. MV recognizes CD46 and signaling lymphocytic activation molecule (SLAM) receptors on target cells (322, 323). Although the WT virus enters cells more efficiently through SLAM, CD46 is preferentially used by the attenuated MV-Edm strain. CD46 functions to protect tumor cells against complement-mediated lysis and is overexpressed in tumor cells (324); these molecules are present in all nucleated primate cells, and so methods to enhance tumor tropism would be extremely desirable. Engineering molecules capable of targeting MV to cancer cells is being actively explored (321, 325).

In numerous preclinical evaluations of NIS-mediated radiotherapy, the responses observed, although impressive, were not sustained, thus leading to resumption of tumor growth. Given that the overall response to radiotherapy is highly dependent on the vulnerability of the endothelial cells (ECs) (327) and that radiotherapy itself activates angiogenesis (328), in a thorough study, Schlumberger's group (329) evaluated the tumoricidal effect of NIS-mediated $^{131}I^-$ radiotherapy in conjunction with canstatin (with both NIS and castatin delivered through intratumoral Ad virus injection) in the MDA 231 human metastatic breast cancer xenograft model and the transgenic retinal pigmented epithelium spontaneous tumor model. Canstatin is a 24-kDa human basement membrane-derived fragment of human collagen that has been shown to inhibit angiogenesis and tumor growth by inducing EC apoptosis, reducing EC migration and tube formation in mice (330). It has been shown to bind to the $\alpha_v\beta_3$ and the $\alpha_v\beta_3$-integrin receptors and promote mitochondrial apoptosis in both ECs and tumor cells (330–332). Interestingly, contrary to the emphasized role of hypoxia inducible factor-1α (HIF-1α) as a contributing factor to radioresistance, this study showed that it also plays a pivotal role in inducing apoptosis by forcing both the tumor and ECs into aberrant mitoses. This particular combination therapy is able to overcome the prosurvival mechanisms induced by activation of HIF-1α in response to radiotherapy, and further highlights the complexity of HIF-1α signaling in tumors.

To our knowledge, this is the only time that radioiodide therapy has been combined with an antiangiogenic agent. Magnon et al (329) observed as much as an 86% sustained growth reduction of MDA 231 xenografts and a 70% reduction in the intraocular tumor model after a single dose of $^{131}I^-$ during a relatively long follow-up period of 30 days. Furthermore, these authors used a single therapeutic dose of only 300 μCi (as compared with 1–3 mCi administered in most mice and up to 18 mCi in rat studies), making the point that the doses for which a therapeutic effect is seen in xenografts are far too high to be useful in a clinical setting.

As alternatives to virus-based delivery systems, several synthetic vectors for efficient systemic delivery of NIS have been developed (333–335). The greatest benefit that NIS-mediated radionuclide therapy could confer would be an enhancement of our ability to treat metastatic disease, as opposed to primary tumors. The last several years have seen some development of non–virus-based methods for systemic delivery of the NIS gene, such as the use of synthetic polyamine vectors with high tumor affinity to deliver CMV-NIS pcDNA3 to neuroblastoma cells, which resulted in a 51-fold increase in ClO_4^--sensitive I^- uptake in vitro. After iv administration of NIS-containing polyplexes, 8% to 13% of each injected dose of $^{123}I^-$ was accumulated per gram of tissue, as observed by scintigraphy and ex vivo γ-counting in mouse neuroblastomas, and critically, tumor growth was significantly delayed, and survival improved (334). A follow-up study used different polyplexes based on linear polyethylamine, polyethylene glycol, and a synthetic peptide GE11 (an epidermal growth factor receptor-specific ligand) to target NIS to tumoral sites in a hepatocellular carcinoma xenograft mouse model. This too resulted in delayed tumor growth and longer survival after radioiodide ablation (333). Another study by the same group evaluated the potential of biodegradable nanoparticle vectors based on pseudodendritic oligoamines, with similar results (333). Clearly, synthetic vectors may offer a novel, efficient, and promising approach to NIS gene transfer.

Downloaded from https://academic.oup.com/edrv/article/35/1/106/2354709 by guest on 09 April 2024

D. Downregulation of thyroid function is required for NIS-mediated $^{131}I^-$ therapy for extrathyroidal tumors

In using NIS-mediated radioiodide therapy to destroy extrathyroidal tumors, whether they endogenously express NIS (ie, >80% of breast cancers) or NIS expression is induced via gene transfer, it is important to prevent healthy thyroid cells from taking up administered $^{131}I^-$. Owing to its ability to organify I^-, the thyroid acts as a sink for the isotope, consequently destroying the gland and limiting the amount of isotope available to NIS-expressing tumors that are incapable of organification. For these reasons, it is key to selectively downregulate NIS expression in the thyroid before initiation of therapy. Our group has shown that thyroidal NIS can be efficiently and selectively downregulated with T_3 in combination with MMI to inhibit organification in humans (201). T_3 and T_4 negatively regulate TSH production by the adenohypophysis. Given that TSH induces NIS biosynthesis and plasma membrane targeting, a reduction in TSH results in a reduction in NIS expression and thus in I^- accumulation in the thyroid.

TH therapy is not the only way to downregulate NIS. The Wolff-Chaikoff effect and its escape (*Section VIII.B.*) can be exploited for this purpose as well. High doses of I^-, via the escape from the Wolff-Chaikoff effect (Figure 11), will also downregulate NIS expression. High doses of I^- (Lugol's solution) are often administered before thyroid surgery to reduce thyroid gland size, vascularity, and function. Two NIS mutants discussed in *Section VI.D.* may prove to be particularly useful for NIS-mediated gene therapy, as they display an extremely low affinity for I^- but transport ReO_4^-. It is unknown whether I^--mediated NIS-downregulation occurs in tumors. If it does, expressing mutant NIS in these tumors, as opposed to WT NIS, would make them less susceptible to NIS downregulation by I^- pretreatment to reduce thyroidal NIS expression while still allowing them to concentrate the therapeutic isotope $^{188}ReO_4^-$ (71).

E. Another NIS substrate potentially useful for therapy: $^{188}ReO_4^-$

Some challenges remain in NIS gene transfer, namely methods to increase radioisotope uptake and its cytotoxicity. It has been proposed that a NIS substrate with a shorter half-life and superior decay properties to $^{131}I^-$ may provide a better therapeutic option (337, 338). Although its main physiological role is I^- transport, NIS has been shown to transport other anions as well, including ReO_4^- (126). As $^{188}ReO_4^-$ satisfies both aforementioned requirements, many consider it a promising therapeutic substrate, with encouraging preliminary results in breast and prostate xenografts (338, 339). ^{188}Re has a half-life of only 16.7 hours and emits higher-energy β-particles than $^{131}I^-$ (268). These are effective over a greater range, sufficient to eradicate larger tumors by a crossfire effect, whereas the lower-energy γ-photons (155 keV) are suitable for imaging (268, 340). It has been estimated that the number of atoms of radioisotope per gram tumor needed to produce a cure probability of 90% at the optimal range is 12-fold higher for $^{131}I^-$ than for ^{188}Re (340). This clearly shows that ^{188}Re has the potential to deliver larger doses of radiation to tumors expressing NIS than $^{131}I^-$, although NIS-mediated $^{188}ReO_4^-$ uptake is lower than that of $^{131}I^-$ (129). This, together with its convenient availability from the $^{188}W/^{188}Re$ generators, make $^{188}ReO_4^-$ a potentially valuable candidate for radiotherapy via NIS (337).

Recently, as a follow-up to their earlier study assessing the therapeutic efficacy of $^{131}I^-$ in a hepatocarcinoma model with HepG2 cells stably transfected with hNIS cDNA under the α-fetoprotein (AFP) promoter (303), Spitzweg's group (341) compared tumor ablation with $^{131}I^-$ and $^{188}ReO_4^-$ in this model. Although a significant reduction in tumor volume and delay in tumor growth was observed with either radionuclide in the HepG2 xenografts after intratumoral injection of Ad-AFP-NIS, no significant difference was observed with $^{188}ReO_4^-$ as compared with $^{131}I^-$. Promoter specificity was shown by contrasting iv administration of Ad-CMV-NIS to that of the AFP construct. The tumor accumulated a substantial amount of radioisotope (~15% injected dose per gram of tumor tissue). The tumor-absorbed dose of $^{188}ReO_4^-$ was only 1.7 times higher than that of $^{131}I^-$, a lower factor than those previously reported. Importantly, no adverse effects of weight loss, lethargy, or respiratory failure were observed in any animals after radiotherapy. Additionally, the authors pointed out that the similar behavior of $^{188}ReO_4^-$ and $^{131}I^-$ might be due to small tumor volumes, as the cross-fire effect of ^{188}Re would be more evident in larger tumors, supporting the view that ^{188}Re may in fact have therapeutic potential in certain cases.

The discovery that the G93E/Q NIS mutants selectively transport ReO_4^- and $^{99m}TcO_4^-$ but not I^- (see *Section VI.D.*) is extremely relevant for the possibility of using $^{188}ReO_4^-$ instead of $^{131}I^-$ as a therapeutic radioisotope to treat cancers that express NIS exogenously by NIS transfer (71). Clearly, any patient undergoing $^{131}I^-$ therapy for an extrathyroidal malignancy would require that his/her thyroid be protected from the radioisotope. As indicated in the previous section, one way to accomplish this objective is to downregulate NIS expression by administering T_4 (201). T_4 must be administered for 1 week before the onset of therapy, as a result of the long half-life of NIS. Although this approach is effective, it has a negative effect on the patient's well-being, and patients may not comply. In

Downloaded from https://academic.oup.com/edrv/article/35/1/106/2354709 by guest on 09 April 2024

addition, this treatment is not suitable for patients with heart conditions. One potential way to overcome these hurdles would be to express G93E or -Q NIS in the malignant cells, instead of WT NIS, by gene transfer. If this were done, and $^{188}ReO_4^-$ were administered instead of $^{131}I^-$, the thyroid could be downregulated with high doses of cold I^- ($^{127}I^-$) without interfering with the therapeutic effect of $^{188}ReO_4^-$ on the extrathyroidal tumor. In addition, the tumor could be imaged with $^{99m}TcO_4^-$, again without any adverse effects on the thyroid.

F. Additional considerations pertaining to NIS gene transfer

The extremely high dose of radioisotope administered in some preclinical studies will likely not be translatable to humans. Thus, it may not be possible to achieve the effective lethal dose per body weight equivalent. Treatment regimens described in mice range from 500 μCi to 3 mCi and up to 18 mCi in rats (262). Therefore, it seems crucial to validate that lower doses of radioiodide would still produce a therapeutic effect.

Although there exist concerns that the lack of iodide organification in extrathyroidal tissues would limit retention of radioiodide and thus produce no therapeutic benefit, it is clear from results in the literature that NIS-mediated radioiodide treatment is effective in the absence of organification (267, 270, 307, 308) and thus could be useful in extrathyroidal tumors.

Although most studies focus on reduction in tumor volume or delay in tumor growth as a readout of the effectiveness of treatment, this alone may not be an accurate portrayal of human disease. Therapeutic efficacy is not illustrated by tumor volume alone, particularly on the short time scale that murine tumor studies are conducted. Thus, it would be useful to not only examine the size, weight, and volume of the tumor mass but also combine it with analysis of various markers of proliferation, apoptosis, and even angiogenesis. Although the obstacle to cancer therapy remains metastatic disease rather than elimination of the primary tumor in most cases, introduction of viral vectors should focus on systemic delivery rather than direct intratumoral injection.

X. Concluding Remarks

The relatively young field of NIS research at the molecular level, born with the cloning of the protein in 1996, seems to be reaching a certain maturity, and doing so by delivering a healthy dose of surprises and novel potential applications. Previous reviews of NIS research accurately predicted that the study of NIS would lead to new insights into the structure/function of plasma membrane proteins and into the mechanisms of NIS activity and of the differential regulation of NIS in different tissues, and it has. The exciting and highly promising search for ways of extending the benefits of NIS-mediated radioiodide treatment of thyroid cancer to other malignancies has continued with considerable success, and some of the latter studies have reached the stage of clinical trials. Still, no one could have foreseen that NIS would be found to transport different anion substrates with different stoichiometries, that amino acid substitutions at a single position in NIS would suffice to switch the transport of some anion substrates from electroneutral to electrogenic (and back), that NIS molecules would be engineered to selectively transport only a desired anion and thus optimized for gene transfer, or that NIS would be shown to be regulated in the thyroid by a K^+ channel. It would have been difficult to anticipate that NIS would be demonstrated to actively translocate ClO_4^-, thus thrusting NIS to the center of the debate on the public health effects of ClO_4^- contamination of food and water. The recent x-ray resolution of the structures of the bacterial transporters LeuT, vSGLT, Mhp1, and BetP; the new notion that proteins without sequence homology between them may nevertheless share a similar fold; and the generation of a new homology model for NIS have all had a strong impact on the continued elucidation of structure/function information on the symporter.

To conclude, the future of basic NIS research, in addition to continuing the trends discussed in this review, will also ultimately aim at the determination of the protein's 3-dimensional crystal structure, a feat that has yet to be achieved for any mammalian symporter. On the other hand, given the unique properties of NIS as an easily monitored therapeutic and reporter molecule, its clinical applications in the diagnosis and treatment of extrathyroidal cancers, and possibly other medical conditions, can only be expected to grow in number and scope.

Acknowledgments

Address requests for reprints to: Nancy Carrasco, 333 Cedar Street, Sterling Hall of Medicine, B-Wing BE60, New Haven, CT 06510. E-mail: nancy.carrasco@yale.edu.

This work was supported by National Institutes of Health Grants 5T32GM002788 (to M.P.B.) and DK 41544 (to N.C.).

Present address for C.P.: European Molecular Biology Laboratory (EMBL), 00015 Monterotondo, Rome, Italy.

Present address for M.P.-B.: Department of Pathology, Columbia University Medical Center, New York, NY 10032.

Disclosure Summary: The authors have nothing to disclose.

References

1. **Baumann E.** Uber den Jodgehalt der Schilddrusen von Menchen und tieren. *Hoppe Seylers Z Physiol Chem*. 1986; 22:1–17.

Downloaded from https://academic.oup.com/edrv/article/35/1/106/2354709 by guest on 09 April 2024

2. **Baumann E.** Uber das Thyrojodin. *Munch Med Wschr*. 1896;43:309–312.
3. **Seidlin SM, Marinelli LD, Oshry E.** Radioactive iodine therapy: effect on functioning of metastases of adenocarcinomas of the thyroid. J Am Med Assoc. 1946;132:838–847.
4. **Dai G, Levy O, Amzel LM, Carrasco N.**The mediator of thyroidal iodide accumulation: the sodium/iodide symporter. In: Konings WN, Kaback HR, Lolkema JS, eds. *Handbook of Biological Physics*; *Vol. II, Transport Processes in Eukaryotic and Prokaryotic Organisms*. Amsterdam, The Netherlands: Elsevier Science BV; 1996;343–367.
5. **Dai G, Levy O, Carrasco N.** Cloning and characterization of the thyroid iodide transporter. *Nature*. 1996;379:458–460.
6. **Vescia FG, Basso L.** Goiters in the Renaissance. *Vesalius*. 1997;3:23–32.
7. **Delange F, Bürgi H, Chen ZP, Dunn JT.** World status of monitoring iodine deficiency disorders control programs. *Thyroid*. 2002;12:915–924.
8. **Pharoah PO, Buttfield IH, Hetzel BS.** Neurological damage to the fetus resulting from severe iodine deficiency during pregnancy. *Lancet*. 1971;1:308–310.
9. **Dunn JT, Delange F.** Damaged reproduction: the most important consequence of iodine deficiency. *J Clin Endocrinol Metab*. 2001;86:2360–2363.
10. **Morreale de Escobar G, Obregón MJ, Escobar del Rey F.** Is neuropsychological development related to maternal hypothyroidism or to maternal hypothyroxinemia? *J Clin Endocrinol Metab*. 2000;85:3975–3987.
11. **Bleichrodt N, Born MP.** A meta-analysis of research on iodine and its relationship to cognitive development. In: Stanbury JB, ed. *The Damaged Brain of Iodine Deficiency*. New York, NY: Cognizant Communication; 1994;195–200.
12. **Vitti P RT, Aghini-Lombardi F, Chiovato L, Ferretti G, Pinchera A.** Neuropsychological assessment in humans living in mild to moderate iodine deficiency. In: Morreale de Escobar G, de Vijlder JJM, Butz S, Hostalek U, eds. *The Thyroid and Brain. Merck European Thyroid Symposium, Seville 2002. May 30–June 2*. Stuttgart, Germany Schattauer; 2003:57–63.
13. **Santiago-Fernandez P, Torres-Barahona R, Muela-Martínez JA, et al.** Intelligence quotient and iodine intake: a cross-sectional study in children. *J Clin Endocrinol Metab*. 2004;89:3851–3857.
14. **Caldwell KL, Makhmudov A, Ely E, Jones RL, Wang RY.** Iodine status of the U.S. population, National Health and Nutrition Examination Survey, 2005–2006 and 2007–2008. *Thyroid*. 2011;21:419–427.
15. **Glinoer D.** Iodine nutrition requirements during pregnancy. *Thyroid*. 2006;16:947–948.
16. **de Benoist B, McLean E, Andersson M, Rogers L.** Iodine deficiency in 2007: global progress since 2003. *Food Nutr Bull*. 2008;29:195–202.
17. **Li M, Eastman CJ.** The changing epidemiology of iodine deficiency. *Nat Rev Endocrinol*. 2012;8:434–440.
18. **Towery BT.** The physiology of iodine. *Bull World Health Organ*. 1953;9:175–182.
19. **Mazzaferri EL.** 2000 Thyroid diseases: tumors. Radioiodine and other treatment and outcomes. In: Braverman LE, Utiger, R.D. ed. *Werner, Ingbar's The Thyroid*. 8th ed. Lipincott Williams, Wilkins; 2000:904–930.
20. **Mazzaferri EL.** Long-term outcome of patients with differentiated thyroid carcinoma: effect of therapy. *Endocr Pract*. 2000;6:469–476.
21. **Carrasco N.** Iodide transport in the thyroid gland. *Biochim Biophys Acta*. 1993;1154:65–82.
22. **Vilkki P.** An iodide-complexing phospholipid. *Arch Biochem Biophys*. 1962;97:425–427.
23. **Schneider PB, Wolff J.** Thyroidal iodide transport. VI. On a possible role for iodide-binding phospholipids. *Biochim Biophys Acta*. 1965;94:114–123.
24. **De La Vieja A, Dohan O, Levy O, Carrasco N.** Molecular analysis of the sodium/iodide symporter: impact on thyroid and extrathyroid pathophysiology. *Physiol Rev*. 2000;80:1083–1105.
25. **Dohán O, Carrasco N.** Advances in Na^+/I^- symporter (NIS) research in the thyroid and beyond. *Mol Cell Endocrinol*. 2003;213:59–70.
26. **Bernal J.** Thyroid hormones and brain development. *Vitam Horm*. 2005;71:95–122.
27. **Saber-Lichtenberg Y, Brix K, Schmitz A, et al.** Covalent cross-linking of secreted bovine thyroglobulin by transglutaminase. *FASEB J*. 2000;14:1005–1014.
28. **Bizhanova A, Kopp P.** Genetics and phenomics of Pendred syndrome. *Mol Cell Endocrinol*. 2010;322:83–90.
29. **Everett LA, Glaser B, Beck JC, et al.** Pendred syndrome is caused by mutations in a putative sulphate transporter gene (PDS). *Nat Genet*. 1997;17:411–422.
30. **Everett LA, Belyantseva IA, Noben-Trauth K, et al.** Targeted disruption of mouse Pds provides insight about the inner-ear defects encountered in Pendred syndrome. *Hum Mol Genet*. 2001;10:153–161.
31. **Calebiro D, Porazzi P, Bonomi M, et al.** Absence of primary hypothyroidism and goiter in $Slc26a4^{-/-}$ mice fed on a low iodine diet. *J Endocrinol Invest*. 2011;34:593–598.
32. **Li H, Ganta S, Fong P.** Altered ion transport by thyroid epithelia from $CFTR^{-/-}$ pigs suggests mechanisms for hypothyroidism in cystic fibrosis. *Exp Physiol*. 2010;95:1132–1144.
33. **De Luca F, Trimarchi F, Sferlazzas C, et al.** Thyroid function in children with cystic fibrosis. *Eur J Pediatr*. 1982;138:327–330.
34. **Segall-Blank M, Vagenakis AG, Shwachman H, Ingbar SH, Braverman LE.** Thyroid gland function and pituitary TSH reserve in patients with cystic fibrosis. *J Pediatr*. 1981;98:218–222.
35. **Steinmeyer K, Schwappach B, Bens M, Vandewalle A, Jentsch TJ.** Cloning and functional expression of rat CLC-5, a chloride channel related to kidney disease. *J Biol Chem*. 1995;270:31172–31177.
36. **van den Hove MF, Croizet-Berger K, Jouret F, et al.** The loss of the chloride channel, ClC-5, delays apical iodide efflux and induces a euthyroid goiter in the mouse thyroid gland. *Endocrinology*. 2006;147:1287–1296.
37. **Rodriguez AM, Perron B, Lacroix L, et al.** Identification and characterization of a putative human iodide transporter located at the apical membrane of thyrocytes. *J Clin Endocrinol Metab*. 2002;87:3500–3503.
38. **Coady MJ, Chang MH, Charron FM, et al.** The human

Downloaded from https://academic.oup.com/edrv/article/35/1/106/2354709 by guest on 09 April 2024

tumour suppressor gene SLC5A8 expresses a Na^+-monocarboxylate cotransporter. *J Physiol*. 2004;557:719–731.
39. **Li H, Myeroff L, Smiraglia D, et al.** SLC5A8, a sodium transporter, is a tumor suppressor gene silenced by methylation in human colon aberrant crypt foci and cancers. *Proc Natl Acad Sci U S A*. 2003;100:8412–8417.
40. **Paroder V, Spencer SR, Paroder M, et al.** Na^+/monocarboxylate transport (SMCT) protein expression correlates with survival in colon cancer: molecular characterization of SMCT. *Proc Natl Acad Sci U S A*. 2006;103:7270–7275.
41. **Frank H, Gröger N, Diener M, Becker C, Braun T, Boettger T.** Lactaturia and loss of sodium-dependent lactate uptake in the colon of SLC5A8-deficient mice. *J Biol Chem*. 2008;283:24729–24737.
42. **Gavaret JM, Cahnmann HJ, Nunez J.** Thyroid hormone synthesis in thyroglobulin. The mechanism of the coupling reaction. *J Biol Chem*. 1981;256:9167–9173.
43. **Braverman LE, Utiger RD.** Thyroid hormone synthesis. In: *Werner and Ingbar's The Thyroid*. 9th ed. Philadelphia, PA: Lippincott Williams and Wilkins; 2004:309–328.
44. **Bedard K, Lardy B, Krause KH.** NOX family NADPH oxidases: not just in mammals. *Biochimie*. 2007;89:1107–1112.
45. **Donkó A, Péterfi Z, Sum A, Leto T, Geiszt M.** Dual oxidases. *Philos Trans R Soc Lond B Biol Sci*. 2005;360:2301–2308.
46. **Ris-Stalpers C.** Physiology and pathophysiology of the DUOXes. *Antioxid Redox Signal*. 2006;8:1563–1572.
47. **Dupuy C, Pomerance M, Ohayon R, et al.** Thyroid oxidase (THOX2) gene expression in the rat thyroid cell line FRTL-5. *Biochem Biophys Res Commun*. 2000;277:287–292.
48. **Morand S, Dos Santos OF, Ohayon R, et al.** Identification of a truncated dual oxidase 2 (DUOX2) messenger ribonucleic acid (mRNA) in two rat thyroid cell lines. Insulin and forskolin regulation of DUOX2 mRNA levels in FRTL-5 cells and porcine thyrocytes. *Endocrinology*. 2003;144:567–574.
49. **Milenkovic M, De Deken X, Jin L, et al.** Duox expression and related H_2O_2 measurement in mouse thyroid: onset in embryonic development and regulation by TSH in adult. *J Endocrinol*. 2007;192:615–626.
50. **Moreno JC, Bikker H, Kempers MJ, et al.** Inactivating mutations in the gene for thyroid oxidase 2 (THOX2) and congenital hypothyroidism. *N Engl J Med*. 2002;347:95–102.
51. **Zamproni I, Grasberger H, Cortinovis F, et al.** Biallelic inactivation of the dual oxidase maturation factor 2 (DUOXA2) gene as a novel cause of congenital hypothyroidism. *J Clin Endocrinol Metab*. 2008;93:605–610.
52. **Moreno JC, Visser TJ.** Genetics and phenomics of hypothyroidism and goiter due to iodotyrosine deiodinase (DEHAL1) gene mutations. *Mol Cell Endocrinol*. 2010;322:91–98.
53. **Hoste C, Rigutto S, Van Vliet G, Miot F, De Deken X.** Compound heterozygosity for a novel hemizygous missense mutation and a partial deletion affecting the catalytic core of the H_2O_2-generating enzyme DUOX2 associated with transient congenital hypothyroidism. *Hum Mutat*. 2010;31:E1304–E1319.
54. **Stanbury JB, Litvak J.** The metabolism of iodotyrosines. IV. Metabolism of L-diiodotyrosine in patients with hypothyroidism. *J Clin Endocrinol Metab*. 1957;17:654–657.
55. **Stanbury JB, Morris ML.** Deiodination of diiodotyrosine by cell-free systems. *J Biol Chem*. 1958;233:106–108.
56. **Rosenberg IN, Goswami A.** Purification and characterization of a flavoprotein from bovine thyroid with iodotyrosine deiodinase activity. *J Biol Chem*. 1979;254:12318–12325.
57. **Moreno JC, van Toor H, Pinto G, et al.** Mutations in the iodotyrosine deiodinase gene and hypothyroidism. *N Engl J Med*. 2008;358:1811–1818.
58. **DeGroot LJ.** Kinetic analysis of iodine metabolism. *J Clin Endocrinol Metab*. 1966;26:149–173.
59. **Stanbury JB, Kassenaar AA, Meijer JW, Terpstra J.** The occurrence of mono- and di-iodotyrosine in the blood of a patient with congenital goiter. *J Clin Endocrinol Metab*. 1955;15:1216–1227.
60. **Paris M, Hillenweck A, Bertrand S.** Active metabolism of thyroid hormone during metamorphosis of amphioxus. *Integr Comp Biol*. 2010;50:63–74.
61. **Paris M, Brunet F, Markov GV, Schubert M, Laudet V.** The amphioxus genome enlightens the evolution of the thyroid hormone signaling pathway. *Dev Genes Evol*. 2008;218:667–680.
62. **Eales JG.** Iodine metabolism and thyroid-related functions in organisms lacking thyroid follicles: are thyroid hormones also vitamins? *Proc Soc Exp Biol Med*. 1997;214:302–317.
63. **Saito M, Seki M, Amemiya S, Yamasu K, Suyemitsu T, Ishihara K.** Induction of metamorphosis in the sand dollar *Peronella japonica* by thyroid hormones. *Dev Growth Differ*. 1998;40:307–312.
64. **Heyland A, Reitzel AM, Price DA, Moroz LL.** Endogenous thyroid hormone synthesis in facultative planktotrophic larvae of the sand dollar *Clypeaster rosaceus*: implications for the evolutionary loss of larval feeding. *Evol Dev*. 2006;8:568–579.
65. **Heyland A, Reitzel AM, Hodin J.** Thyroid hormones determine developmental mode in sand dollars (Echinodermata: Echinoidea). *Evol Dev*. 2004;6:382–392.
66. **Miller AE, Heyland A.** Endocrine interactions between plants and animals: implications of exogenous hormone sources for the evolution of hormone signaling. *Gen Comp Endocrinol*. 2010;166:455–461.
67. **Heyland A, Moroz LL.** Cross-kingdom hormonal signaling: an insight from thyroid hormone functions in marine larvae. *J Exp Biol*. 2005;208:4355–4361.
68. **Chino Y, Saito M, Yamasu K, Suyemitsu T, Ishihara K.** Formation of the adult rudiment of sea urchins is influenced by thyroid hormones. *Dev Biol*. 1994;161:1–11.
69. **Küpper FC, Carpenter LJ, McFiggans GB, et al.** Iodide accumulation provides kelp with an inorganic antioxidant impacting atmospheric chemistry. *Proc Natl Acad Sci U S A*. 2008;105:6954–6958.
70. **Dehal P, Satou Y, Campbell RK, et al.** The draft genome of *Ciona intestinalis*: insights into chordate and vertebrate origins. *Science*. 2002;298:2157–2167.
71. **Paroder-Belenitsky M, Maestas MJ, Dohán O, et al.** Mechanism of anion selectivity and stoichiometry of the Na^+/I^-

Downloaded from https://academic.oup.com/edrv/article/35/1/106/2354709 by guest on 09 April 2024

symporter (NIS). *Proc Natl Acad Sci U S A*. 2011;108: 17933–17938.
72. **Fischer AJ, Lennemann NJ, Krishnamurthy S, et al.** Enhancement of respiratory mucosal anti-viral defenses by iodide oxidation. *Am J Respir Cell Mol Biol*. 2011;45: 874–881.
73. **Park SM, Chatterjee VK.** Genetics of congenital hypothyroidism. *J Med Genet*. 2005;42:379–389.
74. **Szinnai G, Lacroix L, Carré A, et al.** Sodium/iodide symporter (NIS) gene expression is the limiting step for the onset of thyroid function in the human fetus. *J Clin Endocrinol Metab*. 2007;92:70–76.
75. **Portella AC, Carvalho F, Faustino L, Wondisford FE, Ortiga-Carvalho TM, Gomes FC.** Thyroid hormone receptor β mutation causes severe impairment of cerebellar development. *Mol Cell Neurosci*. 2010;44:68–77.
76. **Morte B, Ceballos A, Diez D, et al.** Thyroid hormone-regulated mouse cerebral cortex genes are differentially dependent on the source of the hormone: a study in monocarboxylate transporter-8- and deiodinase-2-deficient mice. *Endocrinology*. 2010;151:2381–2387.
77. **Morte B, Díez D, Ausó E, et al.** Thyroid hormone regulation of gene expression in the developing rat fetal cerebral cortex: prominent role of the Ca2+/calmodulin-dependent protein kinase IV pathway. *Endocrinology*. 2010;151: 810–820.
78. **Westerholz S, de Lima AD, Voigt T.** Regulation of early spontaneous network activity and GABAergic neurons development by thyroid hormone. *Neuroscience*. 2010;168: 573–589.
79. **Tan XJ, Fan XT, Kim HJ, et al.** Liver X receptor β and thyroid hormone receptor α in brain cortical layering. *Proc Natl Acad Sci U S A*. 2010;107:12305–12310.
80. **Horn S, Heuer H.** Thyroid hormone action during brain development: more questions than answers. *Mol Cell Endocrinol*. 2010;315:19–26.
81. **Melse-Boonstra A, Jaiswal N.** Iodine deficiency in pregnancy, infancy and childhood and its consequences for brain development. *Best Pract Res Clin Endocrinol Metab*. 2010;24:29–38.
82. **de Escobar GM, Ares S, Berbel P, Obregón MJ, del Rey FE.** The changing role of maternal thyroid hormone in fetal brain development. *Semin Perinatol*. 2008;32:380–386.
83. **Opazo MC, Gianini A, Pancetti F, et al.** Maternal hypothyroxinemia impairs spatial learning and synaptic nature and function in the offspring. *Endocrinology*. 2008;149: 5097–5106.
84. **Vulsma T, Gons MH, de Vijlder JJ.** Maternal-fetal transfer of thyroxine in congenital hypothyroidism due to a total organification defect or thyroid agenesis. *N Engl J Med*. 1989;321:13–16.
85. **Mitchell ML, Klein RZ.** The sequelae of untreated maternal hypothyroidism. *Eur J Endocrinol*. 2004;151(Suppl 3): U45–U48.
86. **Arturi F, Presta I, Scarpelli D, et al.** Stimulation of iodide uptake by human chorionic gonadotropin in FRTL-5 cells: effects on sodium/iodide symporter gene and protein expression. *Eur J Endocrinol*. 2002;147:655–661.
87. **Hershman JM, Lee HY, Sugawara M, et al.** Human chorionic gonadotropin stimulates iodide uptake, adenylate cyclase, and deoxyribonucleic acid synthesis in cultured rat thyroid cells. *J Clin Endocrinol Metab*. 1988;67:74–79.
88. **Davies TF, Platzer M.** hCG-induced TSH receptor activation and growth acceleration in FRTL-5 thyroid cells. *Endocrinology*. 1986;118:2149–2151.
89. **World Health Organization.** Technical consultation for the prevention and control of iodine deficiency in pregnant and lactating women and in children less than two years old. Geneva, Switzerland: World Health Organization; 2007.
90. **Berbel P, Obregón MJ, Bernal J, Escobar del Rey F, Morreale de Escobar G.** Iodine supplementation during pregnancy: a public health challenge. *Trends Endocrinol Metab*. 2007;18:338–343.
91. **Stanbury J.** *The Damaged Brain of Iodine Deficiency. Cognitive, Behavioral, Neuromotor, Educative Aspects*. New York, NY: Cognizant Communication; 1994.
92. **de Escobar GM, Obregón MJ, del Rey FE.** Maternal thyroid hormones early in pregnancy and fetal brain development. *Best Pract Res Clin Endocrinol Metab*. 2004;18: 225–248.
93. **Goodwin TM, Montoro M, Mestman JH, Pekary AE, Hershman JM.** The role of chorionic gonadotropin in transient hyperthyroidism of hyperemesis gravidarum. *J Clin Endocrinol Metab*. 1992;75:1333–1337.
94. **Glinoer D.** The regulation of thyroid function in pregnancy: pathways of endocrine adaptation from physiology to pathology. *Endocr Rev*. 1997;18:404–433.
95. **Hetzel BS.** Iodine and neuropsychological development. *J Nutr*. 2000;130:493S–495S.
96. **Calvo RM, Jauniaux E, Gulbis B, et al.** Fetal tissues are exposed to biologically relevant free thyroxine concentrations during early phases of development. *J Clin Endocrinol Metab*. 2002;87:1768–1777.
97. **Morreale de Escobar G, Obregon MJ, Escobar del Rey F.** Role of thyroid hormone during early brain development. *Eur J Endocrinol*. 2004;151(Suppl 3):U25–U37.
98. **Glinoer D, Delange F.** The potential repercussions of maternal, fetal, and neonatal hypothyroxinemia on the progeny. *Thyroid*. 2000;10:871–887.
99. **Utiger RD.** Maternal hypothyroidism and fetal development. *N Engl J Med*. 1999;341:601–602.
100. **Smit BJ, Kok JH, Vulsma T, Briët JM, Boer K, Wiersinga WM.** Neurologic development of the newborn and young child in relation to maternal thyroid function. *Acta Paediatr*. 2000;89:291–295.
101. **Pop VJ, Kuijpens JL, van Baar AL, et al.** Low maternal free thyroxine concentrations during early pregnancy are associated with impaired psychomotor development in infancy. *Clin Endocrinol (Oxf)*. 1999;50:149–155.
102. **Pop VJ, Brouwers EP, Vader HL, de Vijlder J, Vulsma T.** 2000 Maternal thyroid function during early pregnancy and neurodevelopment of the offspring. Proceedings from the 82nd Annual Meeting of The Endocrine Society, Toronto, Canada, 2000;163.
103. **Vagenakis AG, Koutras DA, Burger A, Malamos B, Ingbar SH, Braverman LE.** STudies of serum triiodothyronine, thyroxine and thyrotropin concentrations in endemic goiter in Greece. *J Clin Endocrinol Metab*. 1973;37:485–488.
104. **Patel YC, Pharoah PO, Hornabrook RW, Hetzel BS.** Serum triiodothyronine, thyroxine and thyroid-stimulating

Downloaded from https://academic.oup.com/edrv/article/35/1/106/2354709 by guest on 09 April 2024

hormone in endemic goiter: a comparison of goitrous and nongoitrous subjects in New Guinea. *J Clin Endocrinol Metab*. 1973;37:783–789.
105. **Pharaoh PO, Lawton NF, Ellis SM, Williams ES, Ekins RP.** The role of triiodothyronine (T_3) in the maintenance of euthyroidism in endemic goitre. *Clin Endocrinol (Oxf)*. 1973;2:193–199.
106. **Abrams GM, Larsen PR.** Triiodothyronine and thyroxine in the serum and thyroid glands of iodine-deficient rats. *J Clin Invest*. 1973;52:2522–2531.
107. **Riesco G, Taurog A, Larsen PR.** Variations in the response of the thyroid gland of the rat to different low-iodine diets: correlation with iodine content of diet. *Endocrinology*. 1976;99:270–280.
108. **Santisteban P, Obregon MJ, Rodriguez-Peña A, Lamas L, Del Rey FE, De Escobar GM.** Are iodine-deficient rats euthyroid? *Endocrinology*. 1982;110:1780–1789.
109. **Chapman A.** The relation of the thyroid and the pituitary glands to iodine metabolism. *Endocrinology*. 1941;29: 680–681.
110. **Halmi NS, Spirtos BN.** Analysis of the modifying effect of dietary iodine levels on the thyroidal response of hypophysectomized rats to thyrotrophin. *Endocrinology*. 1955; 56:157–160.
111. **Pedraza PE, Obregon MJ, Escobar-Morreale HF, del Rey FE, de Escobar GM.** Mechanisms of adaptation to iodine deficiency in rats: thyroid status is tissue specific. Its relevance for man. *Endocrinology*. 2006;147:2098–2108.
112. **-Eskandari S, Loo DD, Dai G, Levy O, Wright EM, Carrasco N.** Thyroid Na^+/I^- symporter. Mechanism, stoichiometry, and specificity. *J Biol Chem*. 1997;272: 27230–27238.
113. **Levy O, Dai G, Riedel C, et al.** Characterization of the thyroid Na^+/I^- symporter with an anti-COOH terminus antibody. *Proc Natl Acad Sci U S A*. 1997;94:5568–5573.
114. **Levy O, De la Vieja A, Ginter CS, Riedel C, Dai G, Carrasco N.** N-linked glycosylation of the thyroid Na^+/I^- symporter (NIS). Implications for its secondary structure model. *J Biol Chem*. 1998;273:22657–22663.
115. **Dohan O, De la Vieja A, Carrasco N.** Molecular study of the sodium-iodide symporter (NIS): a new field in thyroidology. *Trends Endocrinol Metab*. 2000;11:99–105.
116. **Tazebay UH, Wapnir IL, Levy O, et al.** The mammary gland iodide transporter is expressed during lactation and in breast cancer. *Nat Med*. 2000;6:871–878.
117. **Dohán O, Baloch Z, Bánrévi Z, Livolsi V, Carrasco N.** Rapid communication: predominant intracellular overexpression of the Na^+/I^- symporter (NIS) in a large sampling of thyroid cancer cases. *J Clin Endocrinol Metab*. 2001; 86:2697–2700.
118. **Riedel C, Levy O, Carrasco N.** Post-transcriptional regulation of the sodium/iodide symporter by thyrotropin. *J Biol Chem*. 2001;276:21458–21463.
119. **Weiss SJ, Philp NJ, Grollman EF.** Iodide transport in a continuous line of cultured cells from rat thyroid. *Endocrinology*. 1984;114:1090–1098.
120. **Rhoden KJ, Cianchetta S, Duchi S, Romeo G.** Fluorescence quantitation of thyrocyte iodide accumulation with the yellow fluorescent protein variant YFP-H148Q/I152L. *Anal Biochem*. 2008;373:239–246.
121. **Kaminsky SM, Levy O, Salvador C, Dai G, Carrasco N.** Na^+-I^- symport activity is present in membrane vesicles from thyrotropin-deprived non-I^--transporting cultured thyroid cells. *Proc Natl Acad Sci U S A*. 1994;91:3789–3793.
122. **Dohán O, De la Vieja A, Paroder V, et al.** The sodium/iodide symporter (NIS): characterization, regulation, and medical significance. *Endocr Rev*. 2003;24:48–77.
123. **Dohan O, Portulano C, Ginter C, Carrasco N.** Polarized plasma membrane targeting of the Na^+/I^- symporter (NIS) is regulated by its carboxy terminus. In: *European Congress of Endocrinology 2007*. Budapest, Hungary: BioScientifica; 2007.
124. **Smanik PA, Liu Q, Furminger TL, et al.** Cloning of the human sodium lodide symporter. *Biochem Biophys Res Commun*. 1996;226:339–345.
125. **Wright EM, Turk E.** The sodium/glucose cotransport family SLC5. *Pflugers Arch*. 2004;447:510–518.
126. **Van Sande J, Massart C, Beauwens R, et al.** Anion selectivity by the sodium iodide symporter. *Endocrinology*. 2003;144:247–252.
127. **Wolff J.** Transport of iodide and other anions in the thyroid gland. *Physiol Rev*. 1964;44:45–90.
128. **Zuckier LS, Dohan O, Li Y, Chang CJ, Carrasco N, Dadachova E.** Kinetics of perrhenate uptake and comparative biodistribution of perrhenate, pertechnetate, and iodide by NaI symporter-expressing tissues in vivo. *J Nucl Med*. 2004;45:500–507.
129. **Dohán O, Portulano C, Basquin C, Reyna-Neyra A, Amzel LM, Carrasco N.** The Na^+/I symporter (NIS) mediates electroneutral active transport of the environmental pollutant perchlorate. *Proc Natl Acad Sci U S A*. 2007;104: 20250–20255.
130. **Hirayama BA, Loo DD, Wright EM.** Protons drive sugar transport through the Na^+/glucose cotransporter (SGLT1). *J Biol Chem*. 1994;269:21407–21410.
131. **Cao Y, Mager S, Lester HA.** H^+ permeation and pH regulation at a mammalian serotonin transporter. *J Neurosci*. 1997;17:2257–2266.
132. **O'Neill B, Magnolato D, Semenza G.** The electrogenic, *Na+-dependent I- transport system in plasma membrane vesicles from thyroid glands. Biochim Biophys Acta*. 1987; 896:263–274.
133. **De la Vieja A, Reed MD, Ginter CS, Carrasco N.** Amino acid residues in transmembrane segment IX of the Na^+/I^- symporter play a role in its Na+ dependence and are critical for transport activity. *J Biol Chem*. 2007;282:25290–25298.
134. **Yamashita A, Singh SK, Kawate T, Jin Y, Gouaux E.** Crystal structure of a bacterial homologue of Na^+/Cl^--dependent neurotransmitter transporters. *Nature*. 2005;437: 215–223.
135. **Faham S, Watanabe A, Besserer GM, et al.** The crystal structure of a sodium galactose transporter reveals mechanistic insights into Na^+/sugar symport. *Science*. 2008; 321:810–814.
136. **Weyand S, Shimamura T, Yajima S, et al.** Structure and molecular mechanism of a nucleobase-cation-symport-1 family transporter. *Science*. 2008;322:709–713.
137. **Fang Y, Jayaram H, Shane T, et al.** Structure of a prokaryotic virtual proton pump at 3.2 A resolution. *Nature*. 2009; 460:1040–1043.

Downloaded from https://academic.oup.com/edrv/article/35/1/106/2354709 by guest on 09 April 2024

138. **Gao X, Lu F, Zhou L, et al.** Structure and mechanism of an amino acid antiporter. *Science*. 2009;324:1565–1568.
139. **Shaffer PL, Goehring A, Shankaranarayanan A, Gouaux E.** Structure and mechanism of a Na^+-independent amino acid transporter. *Science*. 2009;325:1010–1014.
140. **Godley AF, Stanbury JB.** Preliminary experience in the treatment of hyperthyroidism with potassium perchlorate. *J Clin Endocrinol Metab*. 1954;14:70–78.
141. **Crooks J, Wayne EJ.** A comparison of potassium perchlorate, methylthiouracil, and carbimazole in the treatment of thyrotoxicosis. *Lancet*. 1960;1:401–404.
142. **Wenzel KW, Lente JR.** Similar effects of thionamide drugs and perchlorate on thyroid-stimulating immunoglobulins in Graves' disease: evidence against an immunosuppressive action of thionamide drugs. *J Clin Endocrinol Metab*. 1984;58:62–69.
143. **Reichert LJ, de Rooy HA.** Treatment of amiodarone induced hyperthyroidism with potassium perchlorate and methimazole during amiodarone treatment. *BMJ*. 1989; 298:1547–1548.
144. **Martino E, Aghini-Lombardi F, Mariotti S, et al.** Treatment of amiodarone associated thyrotoxicosis by simultaneous administration of potassium perchlorate and methimazole. *J Endocrinol Invest*. 1986;9:201–207.
145. **Yoshida A, Sasaki N, Mori A, et al.** Differences in the electrophysiological response to I- and the inhibitory anions SCN- and ClO-4, studied in FRTL-5 cells. *Biochim Biophys Acta*. 1998;1414:231–237.
146. **Goldman SJ, Stanbury JB.** The metabolism of perchlorate in the rat. *Endocrinology*. 1973;92:1536–1538.
147. **Chow SY, Woodbury DM.** Kinetics of distribution of radioactive perchlorate in rat and guinea-pig thyroid glands. *J Endocrinol*. 1970;47:207–218.
148. **Yoshida A, Sasaki N, Mori A, et al.** Different electrophysiological character of I-, ClO4-, and SCN- in the transport by Na^+/I^- symporter. *Biochem Biophys Res Commun*. 1997;231:731–734.
149. **Cianchetta S, di Bernardo J, Romeo G, Rhoden KJ.** Perchlorate transport and inhibition of the sodium iodide symporter measured with the yellow fluorescent protein variant YFP-H148Q/I152L. *Toxicol Appl Pharmacol*. 2010; 243:372–380.
150. **Valentín-Blasini L, Mauldin JP, Maple D, Blount BC.** Analysis of perchlorate in human urine using ion chromatography and electrospray tandem mass spectrometry. *Anal Chem*. 2005;77:2475–2481.
151. **Capuco AV, Rice CP, Baldwin RL 6th, et al.** Fate of dietary perchlorate in lactating dairy cows: Relevance to animal health and levels in the milk supply. *Proc Natl Acad Sci U S A*. 2005;102:16152–16157.
152. **Kirk AB, Martinelango PK, Tian K, Dutta A, Smith EE, Dasgupta PK.** Perchlorate and iodide in dairy and breast milk. *Environ Sci Technol*. 2005;39:2011–2017.
153. **Tran N, Valentín-Blasini L, Blount BC, et al.** Thyroid-stimulating hormone increases active transport of perchlorate into thyroid cells. *Am J Physiol Endocrinol Metab*. 2008;294:E802–E806.
154. **American Academy of Pediatrics, Rose SR, Section on Endocrinology and Committee on Genetics, American Thyroid Association, et al.** Update of newborn screening and therapy for congenital hypothyroidism. *Pediatrics*. 2006; 117:2290–2303.
155. **Clifton-Bligh RJ, Wentworth JM, Heinz P, et al.** Mutation of the gene encoding human TTF-2 associated with thyroid agenesis, cleft palate and choanal atresia. *Nat Genet*. 1998; 19:399–401.
156. **Pohlenz J, Dumitrescu A, Zundel D, et al.** Partial deficiency of thyroid transcription factor 1 produces predominantly neurological defects in humans and mice. *J Clin Invest*. 2002;109:469–473.
157. **Macchia PE, Lapi P, Krude H, et al.** PAX8 mutations associated with congenital hypothyroidism caused by thyroid dysgenesis. *Nat Genet*. 1998;19:83–86.
158. **Krude H, Schütz B, Biebermann H, et al.** Choreoathetosis, hypothyroidism, and pulmonary alterations due to human NKX2-1 haploinsufficiency. *J Clin Invest*. 2002;109:475–480.
159. **Dentice M, Cordeddu V, Rosica A, et al.** Missense mutation in the transcription factor NKX2–5: a novel molecular event in the pathogenesis of thyroid dysgenesis. *J Clin Endocrinol Metab*. 2006;91:1428–1433.
160. **Pohlenz J, Refetoff S.** Mutations in the sodium/iodide symporter (NIS) gene as a cause for iodide transport defects and congenital hypothyroidism. *Biochimie*. 1999;81:469–476.
161. **Gutnisky VJ, Moya CM, Rivolta CM, et al.** Two distinct compound heterozygous constellations (R277X/IVS34–1G>C and R277X/R1511X) in the thyroglobulin (TG) gene in affected individuals of a Brazilian kindred with congenital goiter and defective TG synthesis. *J Clin Endocrinol Metab*. 2004;89:646–657.
162. **Avbelj M, Tahirovic H, Debeljak M, et al.** High prevalence of thyroid peroxidase gene mutations in patients with thyroid dyshormonogenesis. *Eur J Endocrinol*. 2007;156: 511–519.
163. **Reed-Tsur MD, De la Vieja A, Ginter CS, Carrasco N.** Molecular characterization of V59E NIS, a Na^+/I^- symporter (NIS) mutant that causes congenital I- transport defect (ITD). *Endocrinology*. 2008;149(6):3077–3084.
164. **Dohán O, Gavrielides MV, Ginter C, Amzel LM, Carrasco N.** Na^+/I^- symporter activity requires a small and uncharged amino acid residue at position 395. *Mol Endocrinol*. 2002;16:1893–1902.
165. **Paroder V, Nicola JP, Ginter CS, Carrasco N.** The iodide transport defect-causing mutation R124H: a delta-amino group at position 124 is critical for maturation and trafficking of the Na^+/I^- symporter (NIS). *J Cell Sci*. 2013; 126(Pt 15):3305–3313.
166. **De La Vieja A, Ginter CS, Carrasco N.** The Q267E mutation in the sodium/iodide symporter (NIS) causes congenital iodide transport defect (ITD) by decreasing the NIS turnover number. *J Cell Sci*. 2004;117:677–687.
167. **Montanelli L, Agretti P, Marco G, et al.** Congenital hypothyroidism and late-onset goiter: identification and characterization of a novel mutation in the sodium/iodide symporter of the proband and family members. *Thyroid*. 2009; 19:1419–1425.
168. **Li W, Nicola JP, Amzel LM, Carrasco N.** Asn441 plays a key role in folding and function of the Na^+/I^- symporter (NIS). *FASEB J*. 2013;27:3229–3238.
169. **De la Vieja A, Ginter CS, Carrasco N.** Molecular analysis

Downloaded from https://academic.oup.com/edrv/article/35/1/106/2354709 by guest on 09 April 2024

of a congenital iodide transport defect: G543E impairs maturation and trafficking of the Na^+/I^- symporter. *Mol Endocrinol*. 2005;19:2847–2858.
170. **Nicola JP, Nazar M, Serrano-Nascimento C, et al.** Iodide transport defect: functional characterization of a novel mutation in the Na^+/I^- symporter 5′-untranslated region in a patient with congenital hypothyroidism. *J Clin Endocrinol Metab*. 2011;96:E1100–E1107.
171. **Sato S, Ward CL, Krouse ME, Wine JJ, Kopito RR.** Glycerol reverses the misfolding phenotype of the most common cystic fibrosis mutation. *J Biol Chem*. 1996;271:635–638.
172. **Tamarappoo BK, Verkman AS.** Defective aquaporin-2 trafficking in nephrogenic diabetes insipidus and correction by chemical chaperones. *J Clin Invest*. 1998;101:2257–2267.
173. **Wright EM, Loo DD, Hirayama BA.** Biology of human sodium glucose transporters. *Physiol Rev*. 2011;91:733–794.
174. **Fujiwara H.** Congenital hypothyroidism caused by a mutation in the Na^+/I^- symporter. *Nat Genet*. 1997;17:122.
175. **Levy O, Ginter CS, De la Vieja A, Levy D, Carrasco N.** Identification of a structural requirement for thyroid Na^+/I^- symporter (NIS) function from analysis of a mutation that causes human congenital hypothyroidism. *FEBS Lett*. 1998;429:36–40.
176. **Abramson J, Wright EM.** Structure and function of Na^+-symporters with inverted repeats. *Curr Opin Struct Biol*. 2009;19:425–432.
177. **Krishnamurthy H, Piscitelli CL, Gouaux E.** Unlocking the molecular secrets of sodium-coupled transporters. *Nature*. 2009;459:347–355.
178. **Ressl S, Terwisscha van Scheltinga AC, Vonrhein C, Ott V, Ziegler C.** Molecular basis of transport and regulation in the Na^+/betaine symporter BetP. *Nature*. 2009;458:47–52.
179. **Schulze S, Köster S, Geldmacher U, Terwisscha van Scheltinga AC, Kühlbrandt W.** Structural basis of Na^+-independent and cooperative substrate/product antiport in CaiT. *Nature*. 2010;467:233–236.
180. **Saito K, Yamamoto K, Yoshida S, et al.** Goitrous hypothyroidism due to iodide-trapping defect. *J Clin Endocrinol Metab*. 1981;53:1267–1272.
181. **Kosugi S, Inoue S, Matsuda A, Jhiang SM.** Novel, missense and loss-of-function mutations in the sodium/iodide symporter gene causing iodide transport defect in three Japanese patients. *J Clin Endocrinol Metab*. 1998;83:3373–3376.
182. **Singh SK, Piscitelli CL, Yamashita A, Gouaux E.** A competitive inhibitor traps LeuT in an open-to-out conformation. *Science*. 2008;322:1655–1661.
183. **Singh SK, Yamashita A, Gouaux E.** Antidepressant binding site in a bacterial homologue of neurotransmitter transporters. *Nature*. 2007;448:952–956.
184. **Forrest LR, Zhang YW, Jacobs MT, Gesmonde J, Xie L, Honig BH, Rudnick G.** Mechanism for alternating access in neurotransmitter transporters. *Proc Natl Acad Sci U S A*. 2008;105:10338–10343.
185. **Tonacchera M, Agretti P, de Marco G, et al.** Congenital hypothyroidism due to a new deletion in the sodium/iodide symporter protein. *Clin Endocrinol (Oxf)*. 2003;59:500–506.
186. **Wright EM.** Active transport of iodide and other anions across the choroid plexus. *J Physiol*. 1974;240:535–566.
187. **Smanik PA, Ryu KY, Theil KS, Mazzaferri EL, Jhiang SM.** Expression, exon-intron organization, and chromosome mapping of the human sodium iodide symporter. *Endocrinology*. 1997;138:3555–3558.
188. **Perron B, Rodriguez AM, Leblanc G, Pourcher T.** Cloning of the mouse sodium iodide symporter and its expression in the mammary gland and other tissues. *J Endocrinol*. 2001;170:185–196.
189. **Spitzweg C, Joba W, Eisenmenger W, Heufelder AE.** Analysis of human sodium iodide symporter gene expression in extrathyroidal tissues and cloning of its complementary deoxyribonucleic acids from salivary gland, mammary gland, and gastric mucosa. *J Clin Endocrinol Metab*. 1998;83:1746–1751.
190. **Vayre L, Sabourin JC, Caillou B, Ducreux M, Schlumberger M, Bidart JM.** Immunohistochemical analysis of Na^+/I^- symporter distribution in human extra-thyroidal tissues. *Eur J Endocrinol*. 1999;141:382–386.
191. **Jhiang SM, Cho JY, Ryu KY, et al.** An immunohistochemical study of Na^+/I^- symporter in human thyroid tissues and salivary gland tissues. *Endocrinology*. 1998;139:4416–4419.
192. **Venturi S, Venturi M.** Iodine in evolution of salivary glands and in oral health. *Nutr Health*. 2009;20:119–134.
193. **Gupta A, Lakhoo K, Pritchard N, Herbert M.** Epidermal growth factor in neonatal saliva. *Eur J Pediatr Surg*. 2008;18:245–248.
194. **Dagogo-Jack S.** Dietary iodine affects epidermal growth factor levels in mouse thyroid and submaxillary glands. *Endocr Res*. 1994;20:247–257.
195. **Geiszt M, Witta J, Baffi J, Lekstrom K, Leto TL.** Dual oxidases represent novel hydrogen peroxide sources supporting mucosal surface host defense. *FASEB J*. 2003;17:1502–1504.
196. **Thomas EL, Bates KP, Jefferson MM.** Hypothiocyanite ion: detection of the antimicrobial agent in human saliva. *J Dent Res*. 1980;59:1466–1472.
197. **Altorjay A, Dohan O, Szilagyi A, Paroder M, Wapnir IL, Carrasco N.** Expression of the Na^+/I^- symporter (NIS) is markedly decreased or absent in gastric cancer and intestinal metaplastic mucosa of Barrett esophagus. *BMC Cancer*. 2007;7:5.
198. **Nicola JP, Basquin C, Portulano C, Reyna-Neyra A, Paroder M, Carrasco N.** The Na^+/I^- symporter mediates active iodide uptake in the intestine. *Am J Physiol Cell Physiol*. 2009;296:C654–C662.
199. **de Carvalho FD, Quick M.** Surprising substrate versatility in SLC5A6: Na^+-coupled I- transport by the human Na^+/multivitamin transporter (hSMVT). *J Biol Chem*. 2011;286:131–137.
200. **Said HM.** Cell and molecular aspects of human intestinal biotin absorption. *J Nutr*. 2009;139:158–162.
201. **Wapnir IL, Goris M, Yudd A, Dohan O, Adelman D, Nowels K, Carrasco N.** The Na^+/I^- symporter mediates iodide uptake in breast cancer metastases and can be selectively down-regulated in the thyroid. *Clin Cancer Res*. 2004;10:4294–4302.

Downloaded from https://academic.oup.com/edrv/article/35/1/106/2354709 by guest on 09 April 2024

202. **Spitzweg C, Dutton CM, Castro MR, et al.** Expression of the sodium iodide symporter in human kidney. *Kidney Int*. 2001;59:1013–1023.
203. **Lacroix L, Mian C, Caillou B, et al.** Na^+/I^- symporter and Pendred syndrome gene and protein expressions in human extra-thyroidal tissues. *Eur J Endocrinol*. 2001;144:297–302.
204. **Wapnir IL, van de Rijn M, Nowels K, et al.** Immunohistochemical profile of the sodium/iodide symporter in thyroid, breast, and other carcinomas using high density tissue microarrays and conventional sections. *J Clin Endocrinol Metab*. 2003;88:1880–1888.
205. **Di Cosmo C, Fanelli G, Tonacchera M, et al.** The sodium-iodide symporter expression in placental tissue at different gestational age: an immunohistochemical study. *Clin Endocrinol (Oxf)*. 2006;65:544–548.
206. **Mitchell AM, Manley SW, Morris JC, Powell KA, Bergert ER, Mortimer RH.** Sodium iodide symporter (NIS) gene expression in human placenta. *Placenta*. 2001;22:256–258.
207. **Bidart JM, Lacroix L, Evain-Brion D, et al.** Expression of Na^+/I^- symporter and Pendred syndrome genes in trophoblast cells. *J Clin Endocrinol Metab*. 2000;85:4367–4372.
208. **Wijkstrom-Frei C, El-Chemaly S, Ali-Rachedi R, et al.** Lactoperoxidase and human airway host defense. *Am J Respir Cell Mol Biol*. 2003;29:206–212.
209. **Moskwa P, Lorentzen D, Excoffon KJ, et al.** A novel host defense system of airways is defective in cystic fibrosis. *Am J Respir Crit Care Med*. 2007;175:174–183.
210. **Stoltz DA, Meyerholz DK, Pezzulo AA, et al.** Cystic fibrosis pigs develop lung disease and exhibit defective bacterial eradication at birth. *Sci Transl Med*. 2:29ra31.
211. **Fragoso MA, Fernandez V, Forteza R, Randell SH, Salathe M, Conner GE.** Transcellular thiocyanate transport by human airway epithelia. *J Physiol*. 2004;561:183–194.
212. **Suzuki K, Kawashima A, Yoshihara A, et al.** Role of thyroglobulin on negative feedback autoregulation of thyroid follicular function and growth. *J Endocrinol*. 2011;209:169–174.
213. **Kogai T, Brent GA.** The sodium iodide symporter (NIS): regulation and approaches to targeting for cancer therapeutics. *Pharmacol Ther*. 2012;135:355–370.
214. **Kogai T, Endo T, Saito T, Miyazaki A, Kawaguchi A, Onaya T.** Regulation by thyroid-stimulating hormone of sodium/iodide symporter gene expression and protein levels in FRTL-5 cells. *Endocrinology*. 1997;138:2227–2232.
215. **Ohno M, Zannini M, Levy O, Carrasco N, di Lauro R.** The paired-domain transcription factor Pax8 binds to the upstream enhancer of the rat sodium/iodide symporter gene and participates in both thyroid-specific and cyclic-AMP-dependent transcription. *Mol Cell Biol*. 1999;19:2051–2060.
216. **Saito T, Endo T, Kawaguchi A, et al.** Increased expression of the Na^+/I^- symporter in cultured human thyroid cells exposed to thyrotropin and in Graves' thyroid tissue. *J Clin Endocrinol Metab*. 1997;82:3331–3336.
217. **Kogai T, Curcio F, Hyman S, Cornford EM, Brent GA, Hershman JM.** Induction of follicle formation in long-term cultured normal human thyroid cells treated with thyrotropin stimulates iodide uptake but not sodium/iodide symporter messenger RNA and protein expression. *J Endocrinol*. 2000;167:125–135.
218. **Weiss SJ, Philp NJ, Ambesi-Impiombato FS, Grollman EF.** Thyrotropin-stimulated iodide transport mediated by adenosine 3′,5′-monophosphate and dependent on protein synthesis. *Endocrinology*. 1984;114:1099–1107.
219. **Plummer HS.** Results of administering iodine to patients having exophthalmic goiter. *JAMA*. 1923;80:1955.
220. **Wolff J, Chaikoff IL.** Plasma inorganic iodide as a homeostatic regulator of thyroid function. *J Biol Chem*. 1948;174:555–564.
221. **Wolff J, Chaikoff IL, Goldberg RC, Meier JR.** The temporary nature of the inhibitory action of excess iodide on organic iodide synthesis in the normal thyroid. *Endocrinology*. 1949;45:504–513.
222. **Braverman LE, Ingbar SH.** Changes in thyroidal function during adaptation to large doses of iodide. *J Clin Invest*. 1963;42:1216–1231.
223. **Grollman EF, Smolar A, Ommaya A, Tombaccini D, Santisteban P.** Iodine suppression of iodide uptake in FRTL-5 thyroid cells. *Endocrinology*. 1986;118:2477–2482.
224. **Uyttersprot N, Pelgrims N, Carrasco N, et al.** Moderate doses of iodide in vivo inhibit cell proliferation and the expression of thyroperoxidase and Na^+/I^- symporter mRNAs in dog thyroid. *Mol Cell Endocrinol*. 1997;131:195–203.
225. **Spitzweg C, Joba W, Morris JC, Heufelder AE.** Regulation of sodium iodide symporter gene expression in FRTL-5 rat thyroid cells. *Thyroid*. 1999;9:821–830.
226. **Eng PH, Cardona GR, Fang SL, et al.** Escape from the acute Wolff-Chaikoff effect is associated with a decrease in thyroid sodium/iodide symporter messenger ribonucleic acid and protein. *Endocrinology*. 1999;140:3404–3410.
227. **Serrano-Nascimento C, Calil-Silveira J, Nunes MT.** Post-transcriptional regulation of sodium-iodide symporter mRNA expression in the rat thyroid gland by acute iodide administration. *Am J Physiol Cell Physiol*. 2010;298:C893–C899.
228. **Leoni SG, Kimura ET, Santisteban P, De la Vieja A.** Regulation of thyroid oxidative state by thioredoxin reductase has a crucial role in thyroid responses to iodide excess. *Mol Endocrinol*. 2011;25:1924–1935.
229. **Song Y, Driessens N, Costa M, et al.** Roles of hydrogen peroxide in thyroid physiology and disease. *J Clin Endocrinol Metab*. 2007;92:3764–3773.
230. **Corvilain B, Van Sande J, Dumont JE.** Inhibition by iodide of iodide binding to proteins: the "Wolff-Chaikoff" effect is caused by inhibition of H_2O_2 generation. *Biochem Biophys Res Commun*. 1988;154:1287–1292.
231. **Panneels V, Van Sande J, Van den Bergen H, et al.** Inhibition of human thyroid adenylyl cyclase by 2-iodoaldehydes. *Mol Cell Endocrinol*. 1994;106:41–50.
232. **Pereira A, Braekman JC, Dumont JE, Boeynaems JM.** Identification of a major iodolipid from the horse thyroid gland as 2-iodohexadecanal. *J Biol Chem*. 1990;265:17018–17025.
233. **Panneels V, Macours P, Van den Bergen H, Braekman JC, Van Sande J, Boeynaems JM.** Biosynthesis and metabolism of 2-iodohexadecanal in cultured dog thyroid cells. *J Biol Chem*. 1996;271:23006–23014.
234. **Roepke TK, King EC, Reyna-Neyra A, et al.** Kcne2 dele-

Downloaded from https://academic.oup.com/edrv/article/35/1/106/2354709 by guest on 09 April 2024

tion uncovers its crucial role in thyroid hormone biosynthesis. *Nat Med*. 2009;15:1186–1194.
235. **Jespersen T, Grunnet M, Olesen SP.** The KCNQ1 potassium channel: from gene to physiological function. *Physiology*. 2005;20:408–416.
236. **Fröhlich H, Boini KM, Seebohm G, et al.** Hypothyroidism of gene-targeted mice lacking Kcnq1. *Pflugers Arch*. 2011; 461:45–52.
237. **Purtell K, Paroder-Belenitsky M, Reyna-Neyra A, et al.** The KCNQ1-KCNE2 K^+ channel is required for adequate thyroid I^- uptake. *FASEB J*. 2012;26:3252–3259.
238. **Roepke TK, Anantharam A, Kirchhoff P, et al.** The KCNE2 potassium channel ancillary subunit is essential for gastric acid secretion. *J Biol Chem*. 2006;281:23740–23747.
239. **Bonnema SJ, Hegedüs L.** Radioiodine therapy in benign thyroid diseases: effects, side effects, and factors affecting therapeutic outcome. *Endocr Rev*. 2012;33:920–980.
240. **Jemal A, Siegel R, Xu J, Ward E.** Cancer statistics, 2010. *CA Cancer J Clin*. 2010;60:277–300.
241. **Kimura ET, Nikiforova MN, Zhu Z, Knauf JA, Nikiforov YE, Fagin JA.** High prevalence of BRAF mutations in thyroid cancer: genetic evidence for constitutive activation of the RET/PTC-RAS-BRAF signaling pathway in papillary thyroid carcinoma. *Cancer Res*. 2003;63:1454–1457.
242. **Groussin L, Fagin JA.** Significance of BRAF mutations in papillary thyroid carcinoma: prognostic and therapeutic implications. *Nat Clin Pract Endocrinol Metab*. 2006;2: 180–181.
243. **Nikiforova MN, Ciampi R, Salvatore G, et al.** Low prevalence of BRAF mutations in radiation-induced thyroid tumors in contrast to sporadic papillary carcinomas. *Cancer Lett*. 2004;209:1–6.
244. **Knauf JA, Fagin JA.** Role of MAPK pathway oncoproteins in thyroid cancer pathogenesis and as drug targets. *Curr Opin Cell Biol*. 2009;21:296–303.
245. **Mitsutake N, Miyagishi M, Mitsutake S, et al.** BRAF mediates RET/PTC-induced mitogen-activated protein kinase activation in thyroid cells: functional support for requirement of the RET/PTC-RAS-BRAF pathway in papillary thyroid carcinogenesis. *Endocrinology*. 2006;147:1014–1019.
246. **Chakravarty D, Santos E, Ryder M, et al.** Small-molecule MAPK inhibitors restore radioiodine incorporation in mouse thyroid cancers with conditional BRAF activation. *J Clin Invest*. 2010;121:4700–4711.
247. **Riesco-Eizaguirre G, Gutiérrez-Martínez P, García-Cabezas MA, Nistal M, Santisteban P.** The oncogene BRAF V600E is associated with a high risk of recurrence and less differentiated papillary thyroid carcinoma due to the impairment of Na^+/I^- targeting to the membrane. *Endocr Relat Cancer*. 2006;13:257–269.
248. **Riesco-Eizaguirre G, Santisteban P.** A perspective view of sodium iodide symporter research and its clinical implications. *Eur J Endocrinol*. 2006;155:495–512.
249. **Mitsutake N, Knauf JA, Mitsutake S, Mesa C Jr, Zhang L, Fagin JA.** Conditional BRAFV600E expression induces DNA synthesis, apoptosis, dedifferentiation, and chromosomal instability in thyroid PCCL3 cells. *Cancer Res*. 2005;65:2465–2473.
250. **Liu D, Hu S, Hou P, Jiang D, Condouris S, Xing M.** Suppression of BRAF/MEK/MAP kinase pathway restores expression of iodide-metabolizing genes in thyroid cells expressing the V600E BRAF mutant. *Clin Cancer Res*. 2007; 13:1341–1349.
251. **Liu D, Liu Z, Condouris S, Xing M.** BRAF V600E maintains proliferation, transformation, and tumorigenicity of BRAF-mutant papillary thyroid cancer cells. *J Clin Endocrinol Metab*. 2007;92:2264–2271.
252. **Durante C, Puxeddu E, Ferretti E, et al.** BRAF mutations in papillary thyroid carcinomas inhibit genes involved in iodine metabolism. *J Clin Endocrinol Metab*. 2007;92: 2840–2843.
253. **Ho AL, Grewal RK, Leboeuf R, et al.** Selumetinib-enhanced radioiodine uptake in advanced thyroid cancer. *N Engl J Med*. 2013;368:623–632.
254. **Woodrum DT, Gauger PG.** Role of 131I in the treatment of well differentiated thyroid cancer. *J Surg Oncol*. 2005; 89:114–121.
255. **Schlumberger M, Lacroix L, Russo D, Filetti S, Bidart JM.** Defects in iodide metabolism in thyroid cancer and implications for the follow-up and treatment of patients. *Nat Clin Pract Endocrinol Metab*. 2007;3:260–269.
256. **Middendorp M, Grünwald F.** Update on recent developments in the therapy of differentiated thyroid cancer. *Semin Nucl Med*. 2010;40:145–152.
257. **National Cancer Institute.** Surveillance epidemiology and end results. National Cancer Institute website. http://seer.cancer.gov/statfacts/html/thyro.html. Accessed August 12, 2013.
258. **Mazzaferri EL.** Thyroid remnant ^{131}I ablation for papillary and follicular thyroid carcinoma. *Thyroid*. 1997;7: 265–271.
259. **Durante C, Haddy N, Baudin E, et al.** Long-term outcome of 444 patients with distant metastases from papillary and follicular thyroid carcinoma: benefits and limits of radioiodine therapy. *J Clin Endocrinol Metab*. 2006;91:2892–2899.
260. **Renier C, Yao C, Goris M, et al.** Endogenous NIS expression in triple-negative breast cancers. *Ann Surg Oncol*. 2009;16:962–968.
261. **Renier C, Vogel H, Offor O, Yao C, Wapnir I.** Breast cancer brain metastases express the sodium iodide symporter. *J Neurooncol*. 2010;96:331–336.
262. **Liu B, Hervé J, Bioulac-Sage P, et al.** Sodium iodide symporter is expressed at the preneoplastic stages of liver carcinogenesis and in human cholangiocarcinoma. *Gastroenterology*. 2007;132:1495–1503.
263. **Lacoste C, Hervé J, Bou Nader M, et al.** Iodide transporter NIS regulates cancer cell motility and invasiveness by interacting with the Rho guanine nucleotide exchange factor LARG. *Cancer Res*. 2012;72:5505–5515.
264. **Serganova I, Ponomarev V, Blasberg R.** Human reporter genes: potential use in clinical studies. *Nucl Med Biol*. 2007;34:791–807.
265. **Penheiter AR, Russell SJ, Carlson SK.** The sodium iodide symporter (NIS) as an imaging reporter for gene, viral, and cell-based therapies. *Curr Gene Ther*. 2012;12:33–47.
266. **Cho JY, Xing S, Liu X, et al.** Expression and activity of human Na^+/I^- symporter in human glioma cells by adenovirus-mediated gene delivery. *Gene Ther*. 2000;7:740–749.

Downloaded from https://academic.oup.com/edrv/article/35/1/106/2354709 by guest on 09 April 2024

267. **Spitzweg C, Zhang S, Bergert ER, et al.** Prostate-specific antigen (PSA) promoter-driven androgen-inducible expression of sodium iodide symporter in prostate cancer cell lines. *Cancer Res*. 1999;59:2136–2141.
268. **Dadachova E, Carrasco N.** The Na/I symporter (NIS): imaging and therapeutic applications. *Semin Nucl Med*. 2004;34:23–31.
269. **Dingli D, Diaz RM, Bergert ER, O'Connor MK, Morris JC, Russell SJ.** Genetically targeted radiotherapy for multiple myeloma. *Blood*. 2003;102:489–496.
270. **Faivre J, Clerc J, Gérolami R, et al.** Long-term radioiodine retention and regression of liver cancer after sodium iodide symporter gene transfer in Wistar rats. *Cancer Res*. 2004; 64:8045–8051.
271. **Shen DH, Marsee DK, Schaap J, et al.** Effects of dose, intervention time, and radionuclide on sodium iodide symporter (NIS)-targeted radionuclide therapy. *Gene Ther*. 2004;11:161–169.
272. **Boland A, Ricard M, Opolon P, et al.** Adenovirus-mediated transfer of the thyroid sodium/iodide symporter gene into tumors for a targeted radiotherapy. *Cancer Res*. 2000; 60:3484–3492.
273. **Mandell RB, Mandell LZ, Link CJ Jr.** Radioisotope concentrator gene therapy using the sodium/iodide symporter gene. *Cancer Res*. 1999;59:661–668.
274. **Niu G, Krager KJ, Graham MM, Hichwa RD, Domann FE.** Noninvasive radiological imaging of pulmonary gene transfer and expression using the human sodium iodide symporter. *Eur J Nucl Med Mol Imaging*. 2005;32:534–540.
275. **Miyagawa M, Anton M, Wagner B, et al.** Non-invasive imaging of cardiac transgene expression with PET: comparison of the human sodium/iodide symporter gene and HSV1-tk as the reporter gene. *Eur J Nucl Med Mol Imaging*. 2005;32:1108–1114.
276. **Miyagawa M, Beyer M, Wagner B, et al.** Cardiac reporter gene imaging using the human sodium/iodide symporter gene. *Cardiovasc Res*. 2005;65:195–202.
277. **Lee KH, Kim HK, Paik JY, et al.** Accuracy of myocardial sodium/iodide symporter gene expression imaging with radioiodide: evaluation with a dual-gene adenovirus vector. *J Nucl Med*. 2005;46:652–657.
278. **Rao VP, Miyagi N, Ricci D, et al.** Sodium iodide symporter (hNIS) permits molecular imaging of gene transduction in cardiac transplantation. *Transplantation*. 2007;84:1662–1666.
279. **Ricci D, Mennander AA, Pham LD, et al.** Non-invasive radioiodine imaging for accurate quantitation of NIS reporter gene expression in transplanted hearts. *Eur J Cardiothorac Surg*. 2008;33:32–39.
280. **Terrovitis J, Kwok KF, Lautamaki R, et al.** Ectopic expression of the sodium-iodide symporter enables imaging of transplanted cardiac stem cells in vivo by single-photon emission computed tomography or positron emission tomography. *J Am Coll Cardiol*. 2008;52:1652–1660.
281. **Lautamäki R, Terrovitis J, Bonios M, et al.** Perfusion defect size predicts engraftment but not early retention of intra-myocardially injected cardiosphere-derived cells after acute myocardial infarction. *Basic Res Cardiol*. 2011; 106:1379–1386.
282. **Higuchi T, Anton M, Dumler K, et al.** Combined reporter gene PET and iron oxide MRI for monitoring survival and localization of transplanted cells in the rat heart. *J Nucl Med*. 2009;50:1088–1094.
283. **Seo JH, Jeon YH, Lee YJ, et al.** Trafficking macrophage migration using reporter gene imaging with human sodium iodide symporter in animal models of inflammation. *J Nucl Med*. 2010;51:1637–1643.
284. **Liepe K, Kotzerke J.** A comparative study of 188Re-HEDP, 186Re-HEDP, 153Sm-EDTMP and 89Sr in the treatment of painful skeletal metastases. *Nucl Med Commun*. 2007; 28:623–630.
285. **Shelley MD, Mason MD.** Radium-223 for men with hormone-refractory prostate cancer and bone metastases. *Lancet Oncol*. 2007;8:564–565.
286. **Taggart D, Dubois S, Matthay KK.** Radiolabeled metaiodobenzylguanidine for imaging and therapy of neuroblastoma. *Q J Nucl Med Mol Imaging*. 2008;52:403–418.
287. **Illidge TM, Bayne MC.** Antibody therapy of lymphoma. *Expert Opin Pharmacother*. 2001;2:953–961.
288. **Hingorani M, White CL, Zaidi S, et al.** Therapeutic effect of sodium iodide symporter gene therapy combined with external beam radiotherapy and targeted drugs that inhibit DNA repair. *Mol Ther*. 2010;18:1599–1605.
289. **Shimura H, Haraguchi K, Miyazaki A, Endo T, Onaya T.** Iodide uptake and experimental 131I therapy in transplanted undifferentiated thyroid cancer cells expressing the Na^+/I^- symporter gene. *Endocrinology*. 1997;138:4493–4496.
290. **Chen RF, Li ZH, Pan QH, et al.** In vivo radioiodide imaging and treatment of pancreatic cancer xenografts after MUC1 promoter-driven expression of the human sodium-iodide symporter. *Pancreatology*. 2007;7:505–513.
291. **Dwyer RM, Bergert ER, O'Connor MK, Gendler SJ, Morris JC.** Adenovirus-mediated and targeted expression of the sodium-iodide symporter permits in vivo radioiodide imaging and therapy of pancreatic tumors. *Hum Gene Ther*. 2006;17:661–668.
292. **Dwyer RM, Bergert ER, O'Connor MK, Gendler SJ, Morris JC.** Sodium iodide symporter-mediated radioiodide imaging and therapy of ovarian tumor xenografts in mice. *Gene Ther*. 2006;13:60–66.
293. **Scholz IV, Cengic N, Baker CH, et al.** Radioiodine therapy of colon cancer following tissue-specific sodium iodide symporter gene transfer. *Gene Ther*. 2005;12:272–280.
294. **Spitzweg C, Baker CH, Bergert ER, O'Connor MK, Morris JC.** Image-guided radioiodide therapy of medullary thyroid cancer after carcinoembryonic antigen promoter-targeted sodium iodide symporter gene expression. *Hum Gene Ther*. 2007;18:916–924.
295. **Levy O, De la Vieja A, Carrasco N.** The Na^+/I^- symporter (NIS): recent advances. *J Bioenerg Biomembr*. 1998;30: 195–206.
296. **Riedel C, Dohán O, De la Vieja A, Ginter CS, Carrasco N.** Journey of the iodide transporter NIS: from its molecular identification to its clinical role in cancer. *Trends Biochem Sci*. 2001;26:490–496.
297. **Filetti S, Bidart JM, Arturi F, Caillou B, Russo D, Schlumberger M.** Sodium/iodide symporter: a key transport system in thyroid cancer cell metabolism. *Eur J Endocrinol*. 1999;141:443–457.

Downloaded from https://academic.oup.com/edrv/article/35/1/106/2354709 by guest on 09 April 2024

298. **Chung JK.** Sodium iodide symporter: its role in nuclear medicine. *J Nucl Med*. 2002;43:1188–1200.
299. **Spitzweg C, Morris JC.** The sodium iodide symporter: its pathophysiological and therapeutic implications. *Clin Endocrinol (Oxf)*. 2002;57:559–574.
300. **Baker CH, Morris JC.** The sodium-iodide symporter. *Curr Drug Targets Immune Endocr Metabol Disord*. 2004;4:167–174.
301. **Chung JK, Kang JH.** Translational research using the sodium/iodide symporter in imaging and therapy. *Eur J Nucl Med Mol Imaging*. 2004;31:799–802.
302. **Kakinuma H, Bergert ER, Spitzweg C, Cheville JC, Lieber MM, Morris JC.** Probasin promoter (ARR(2)PB)-driven, prostate-specific expression of the human sodium iodide symporter (h-NIS) for targeted radioiodine therapy of prostate cancer. *Cancer Res*. 2003;63:7840–7844.
303. **Willhauck MJ, Sharif Samani BR, et al.** α-Fetoprotein promoter-targeted sodium iodide symporter gene therapy of hepatocellular carcinoma. *Gene Ther*. 2008;15:214–223.
304. **Hervé J, Cunha AS, Liu B, et al.** Internal radiotherapy of liver cancer with rat hepatocarcinoma-intestine-pancreas gene as a liver tumor-specific promoter. *Hum Gene Ther*. 2008;19:915–926.
305. **Jin YN, Chung HK, Kang JH, et al.** Radioiodine gene therapy of hepatocellular carcinoma targeted human α-fetoprotein. *Cancer Biother Radiopharm*. 2008;23:551–560.
306. **Kim SH, Chung HK, Kang JH, et al.** Tumor-targeted radionuclide imaging and therapy using human sodium iodide symporter gene driven by a modified telomerase reverse transcriptase promoter. *Hum Gene Ther*. 2008;19:951–957.
307. **Spitzweg C, O'Connor MK, Bergert ER, Tindall DJ, Young CY, Morris JC.** Treatment of prostate cancer by radioiodine therapy after tissue-specific expression of the sodium iodide symporter. *Cancer Res*. 2000;60:6526–6530.
308. **Spitzweg C, Dietz AB, O'Connor MK, et al.** In vivo sodium iodide symporter gene therapy of prostate cancer. *Gene Ther*. 2001;8:1524–1531.
309. **Dwyer RM, Schatz SM, Bergert ER, et al.** A preclinical large animal model of adenovirus-mediated expression of the sodium-iodide symporter for radioiodide imaging and therapy of locally recurrent prostate cancer. *Mol Ther*. 2005;12:835–841.
310. **Ouellette MM, Wright WE, Shay JW.** Targeting telomerase-expressing cancer cells. *J Cell Mol Med*. 2011;15:1433–1442.
311. **Shay JW, Wright WE.** Telomerase therapeutics for cancer: challenges and new directions. *Nat Rev Drug Discov*. 2006;5:577–584.
312. **Riesco-Eizaguirre G, De la Vieja A, Rodríguez I, et al.** Telomerase-driven expression of the sodium iodide symporter (NIS) for in vivo radioiodide treatment of cancer: a new broad-spectrum NIS-mediated antitumor approach. *J Clin Endocrinol Metab*. 2011;96:E1435–E1443.
313. **Blechacz B, Splinter PL, Greiner S, et al.** Engineered measles virus as a novel oncolytic viral therapy system for hepatocellular carcinoma. *Hepatology*. 2006;44:1465–1477.
314. **Peng KW, Ahmann GJ, Pham L, Greipp PR, Cattaneo R, Russell SJ.** Systemic therapy of myeloma xenografts by an attenuated measles virus. *Blood*. 2001;98:2002–2007.
315. **Nakamura T, Russell SJ.** Oncolytic measles viruses for cancer therapy. *Expert Opin Biol Ther*. 2004;4:1685–1692.
316. **Myers RM, Greiner SM, Harvey ME, et al.** Preclinical pharmacology and toxicology of intravenous MV-NIS, an oncolytic measles virus administered with or without cyclophosphamide. *Clin Pharmacol Ther*. 2007;82:700–710.
317. **Dingli D, Peng KW, Harvey ME, et al.** Image-guided radiovirotherapy for multiple myeloma using a recombinant measles virus expressing the thyroidal sodium iodide symporter. *Blood*. 2004;103:1641–1646.
318. **Dingli D, Peng KW, Harvey ME, et al.** Interaction of measles virus vectors with Auger electron emitting radioisotopes. *Biochem Biophys Res Commun*. 2005;337:22–29.
319. **Dingli D, Bergert ER, Bajzer Z, O'Connor MK, Russell SJ, Morris JC.** Dynamic iodide trapping by tumor cells expressing the thyroidal sodium iodide symporter. *Biochem Biophys Res Commun*. 2004;325:157–166.
320. Clinical trial (NCT00450814): vaccine therapy with or without cyclophosphamide in treating patients with recurrent or refractory multiple myeloma phase I trial of systemic administration of Edmonston strain of measles virus, genetically engineered to express NIS, with or without cyclophosphamide, in patients with recurrent or refractory multiple myeloma. http://clinicaltrials.gov/show/NCT00450814%20MC038C%20P30CA015083%20MC038C%2006-005263%20NCI-2009-01194%20NCT00450814. Accessed August 12, 2013.
321. **Liu C, Russell SJ, Peng KW.** Systemic therapy of disseminated myeloma in passively immunized mice using measles virus-infected cell carriers. *Mol Ther*. 2010;18:1155–1164.
322. **Tatsuo H, Ono N, Tanaka K, Yanagi Y.** SLAM (CDw150) is a cellular receptor for measles virus. *Nature*. 2000;406:893–897.
323. **Dörig RE, Marcil A, Chopra A, Richardson CD.** The human CD46 molecule is a receptor for measles virus (Edmonston strain). *Cell*. 1993;75:295–305.
324. **Msaouel P, Dispenzieri A, Galanis E.** Clinical testing of engineered oncolytic measles virus strains in the treatment of cancer: an overview. *Curr Opin Mol Ther*. 2009;11:43–53.
325. **Hummel HD, Kuntz G, Russell SJ, et al.** Genetically engineered attenuated measles virus specifically infects and kills primary multiple myeloma cells. *J Gen Virol*. 2009;90:693–701.
326. **Calvo R, Obregon MJ, Ruiz de Ona C, Escobar del Rey F, Morreale de Escobar G.** Congenital hypothyroidism, as studied in rats: crucial role of maternal thyroxine but not of 3,5,3′- triiodothyronine in the protection of the fetal brain. *J Clin Invest*. 1990;86:889–899.
327. **Garcia-Barros M, Paris F, Cordon-Cardo C, et al.** Tumor response to radiotherapy regulated by endothelial cell apoptosis. *Science*. 2003;300:1155–1159.
328. **Moeller BJ, Cao Y, Li CY, Dewhirst MW.** Radiation activates HIF-1 to regulate vascular radiosensitivity in tumors: role of reoxygenation, free radicals, and stress granules. *Cancer Cell*. 2004;5:429–441.
329. **Magnon C, Opolon P, Ricard M, et al.** Radiation and inhibition of angiogenesis by canstatin synergize to induce

Downloaded from https://academic.oup.com/edrv/article/35/1/106/2354709 by guest on 09 April 2024

HIF-1α-mediated tumor apoptotic switch. *J Clin Invest*. 2007;117:1844–1855.
330. **Kamphaus GD, Colorado PC, Panka DJ, et al.** Canstatin, a novel matrix-derived inhibitor of angiogenesis and tumor growth. *J Biol Chem*. 2000;275:1209–1215.
331. **Friedlander M, Brooks PC, Shaffer RW, Kincaid CM, Varner JA, Cheresh DA.** Definition of two angiogenic pathways by distinct αv integrins. *Science*. 1995;270:1500–1502.
332. **Magnon C, Galaup A, Mullan B, et al.** Canstatin acts on endothelial and tumor cells via mitochondrial damage initiated through interaction with αvβ3 and αvβ5 integrins. *Cancer Res*. 2005;65:4353–4361.
333. **Klutz K, Willhauck MJ, Dohmen C, et al.** Image-guided tumor-selective radioiodine therapy of liver cancer after systemic nonviral delivery of the sodium iodide symporter gene. *Hum Gene Ther*. 2011;22:1563–1574.
334. **Klutz K, Russ V, Willhauck MJ, et al.** Targeted radioiodine therapy of neuroblastoma tumors following systemic nonviral delivery of the sodium iodide symporter gene. *Clin Cancer Res*. 2009;15:6079–6086.
335. **Chisholm EJ, Vassaux G, Martin-Duque P, et al.** Cancer-specific transgene expression mediated by systemic injection of nanoparticles. *Cancer Res*. 2009;69:2655–2662.
336. **Fischer AJ, Lennemann NJ, Krishnamurthy S, et al.** Enhancement of respiratory mucosal antiviral defenses by the oxidation of iodide. *Am J Respir Cell Mol Biol*. 2011;45:874–881.
337. **Dadachova E, Nguyen A, Lin EY, Gnatovskiy L, Lu P, Pollard JW.** Treatment with rhenium-188-perrhenate and iodine-131 of NIS-expressing mammary cancer in a mouse model remarkably inhibited tumor growth. *Nucl Med Biol*. 2005;32:695–700.
338. **Willhauck MJ, Sharif Samani BR, et al.** Application of 188rhenium as an alternative radionuclide for treatment of prostate cancer after tumor-specific sodium iodide symporter gene expression. *J Clin Endocrinol Metab*. 2007;92:4451–4458.
339. **Dadachova E, Bouzahzah B, Zuckier LS, Pestell RG.** Rhenium-188 as an alternative to Iodine-131 for treatment of breast tumors expressing the sodium/iodide symporter (NIS). *Nucl Med Biol*. 2002;29:13–18.
340. **O'Donoghue JA, Bardiès M, Wheldon TE.** Relationships between tumor size and curability for uniformly targeted therapy with β-emitting radionuclides. *J Nucl Med*. 1995;36:1902–1909.
341. **Klutz K, Willhauck MJ, Wunderlich N, et al.** Sodium iodide symporter (NIS)-mediated radionuclide (^{131}I, ^{188}Re) therapy of liver cancer after transcriptionally targeted intratumoral in vivo NIS gene delivery. *Hum Gene Ther*. 2011;22:1403–1412.
342. **Pedemonte N, Caci E, Sondo E, et al.** Thiocyanate transport in resting and IL-4-stimulated human bronchial epithelial cells: role of pendrin and anion channels. *J Immunol*. 2007;178:5144–5153.

Downloaded from https://academic.oup.com/edrv/article/35/1/106/2354709 by guest on 09 April 2024

ENDOCRINE SOCIETY

Mark Your Calendar for Clinical Endocrinology Update
September 4-6, 2014, San Francisco, California
www.endocrine.org/CEU